

**MAPPING OF RADIOFREQUENCY EXPOSURE AND  
ASSESSMENT OF POTENTIAL HEALTH HAZARD  
FROM BASE TRANSCIVING STATIONS AND  
COMMON MOBILE PHONES IN SELECTED CITIES  
IN NIGERIA**

---

**BOLAJI OMOGBEMIGA AYINMODE**

**MAPPING OF RADIOFREQUENCY EXPOSURE AND ASSESSMENT  
OF POTENTIAL HEALTH HAZARD FROM BASE TRANSCIVING  
STATIONS AND COMMON MOBILE PHONES IN SELECTED CITIES  
IN NIGERIA**

BY

BOLAJI OMOGBEMIGA AYINMODE

B.Tech. Pure and Applied Physics (LAUTECH), M.Sc. Physics (Ibadan)

Matric No: 147633

A Thesis in the Department of Physics, Submitted to the Faculty of Science in  
partial fulfilment of the requirements for the Degree of

DOCTOR OF PHILOSOPHY

of the

UNIVERSITY OF IBADAN

JULY, 2019

## **DEDICATION**

This work is dedicated to Almighty God for the life of Chief Samuel Adejuwon Ayinmode (1930 – 2017) and Chief (Mrs)Janet Ibidun Abereoran (1934 – 2017) both who were outstanding parents and for the grace and strength given to Professor Idowu Peter Farai to mentor excellent scientists, some of who are now professors in the field of radiation and health physics.

## **CERTIFICATION**

I certify that this work was carried out by Mr B.O. Ayinmode in the Department of  
Physics, University of Ibadan

.....  
Supervisor

I.P. Farai, B.Sc. (Nig), M.Sc., Ph.D. (Ibadan)

Professor, Department of Physics, University of Ibadan, Nigeria

## ACKNOWLEDGEMENTS

My sincere appreciation goes to my supervisor Professor I.P.Farai, who has given me his unreserved support and guidance throughout this work. I appreciate the opportunity he gave me to work on radiofrequency radiation since my MSc. Programme. I acknowledge the support of Professor (Mrs) J.A. Ademola (head of the Department) and other members of the radiation and health research group of the department of Physics University of Ibadan. I acknowledge the sincere support and encouragement of Professor N.N. Jibiri. I express my gratitude to Professor O.E. Awe for his support throughout my stay as a student in the department.

I am indebted to Mr and Mrs Laja Abereoran for being wonderful foster parents and the major sponsors of this work. I appreciate the support of my lovely mother Mrs Omotewa Ayinmode. I also appreciate the love and support of my brothers Dr. Tunde Ayinmode and Mr Ayodele Ayinmode, my sisters Mrs Titilayo Fagbemi, Mrs Adeshola Ajetomobi and Mrs Monishola Olorunmaiye.

Special thanks to my brother and a good friend Dr. Kunle Ayinmode for his tremendous support throughout my stay in the University of Ibadan. I appreciate the love and support shown to me by Mrs Victoria Ayinmode and her children: Goodness, Mercy and Grace. Finally, special thanks to my amazing wife Yewande, who has selflessly contributed to the success of this study and to the upbringing of our children Oreoluwa and Iyanuoluwa.

## LIST OF ABBREVIATIONS

<b>2G</b>	Second Generation
<b>3G</b>	Third Generation
<b>AM</b>	Amplitude Modulation
<b>BTS</b>	Base Transceiver Station
<b>CDMA</b>	Code Division Multiple Access
<b>dB</b>	Decibel
<b>DC</b>	Direct Current
<b>DCS1800</b>	Digital Cellular System at 1800MHz
<b>DNA</b>	Deoxyribonucleic Acid
<b>E</b>	Electric field intensity
<b>EDGE</b>	Enhanced Data for Global Evolution
<b>EM</b>	Electromagnetic
<b>EMF</b>	Electromagnetic Field
<b>EMR</b>	Electromagnetic Radiation
<b>FCC</b>	Federal Communications Commission
<b>FDMA</b>	Frequency Division Multiple Access
<b>FFT</b>	Fast Fourier Transform
<b>FM</b>	Frequency Modulation
<b>FNBW</b>	First Null Beam width
<b>GPS</b>	Geographic Positioning System
<b>GSM</b>	Global System of Mobile communication
<b>H</b>	Magnetic field intensity
<b>HPBW</b>	Half Power Beam width
<b>HRP</b>	Horizontal Radiation Pattern
<b>HSPA</b>	High Speed Packet Access
<b>ICNIRP</b>	International Commission on Non-Ionizing Radiation Protection
<b>ICT</b>	Information Communications and Technology
<b>IEEE</b>	Institute of Electrical and Electronics Engineers
<b>IMEI</b>	International Mobile Station Equipment Identity
<b>IMSI</b>	International Mobile Subscriber Identity
<b>IRPA</b>	International Radiation Protection Association

<b>LAN</b>	Local Area Network
<b>LGA</b>	Local Government Areas
<b>LOS</b>	Line of Sight
<b>ME</b>	Mobile Equipment
<b>NCC</b>	Nigerian Communications Commission
<b>NFMC</b>	National Frequency Management Council of the Federal Republic of Nigeria
<b>NIR</b>	Non-Ionizing Radiation
<b>RADAR</b>	Radio Detection and Ranging
<b>RF</b>	Radiofrequency
<b>RX</b>	Receiver
<b>S</b>	Power Density
<b>SAR</b>	Specific absorption rate
<b>SIM</b>	Subscriber Identity Module
<b>TDMA</b>	Time Division Multiple Access
<b>TRX</b>	Transceiver
<b>TV</b>	Television
<b>UNEP</b>	United Nations Environment Programme
<b>VBW</b>	Vertical Beam Width
<b>VRP</b>	Vertical Radiation Pattern
<b>WCDMA</b>	Wideband Code Division Multiple Access
<b>WHO</b>	World Health Organization
<b>Wi-Fi</b>	Wireless-Fidelity

## ABSTRACT

The proliferation of mobile telecommunication devices and radio transmitting antennas has precipitated global concern over possible health hazards associated with exposure to the generated electromagnetic radiations. Global System of Mobile (GSM) communications in Nigeria is enabled by over 30,000 Base Transceiving Stations (BTS) servicing over 140 million mobile subscribers. Data on the spectral analyses of Radiofrequency (RF) signals and the energy absorbed by the human brain from mobile phones in Nigeria are scarce. This has made it impossible for GSM risk assessments in the Nigerian environment. The objectives of this work were to delineate the energy contribution of each RF component, estimate energy absorbed in the brain from BTS and mobile phones to ascertain possible health risk to the public.

Lagos, Ibadan and Abuja were purposively selected for the study. A calibrated spectrum analyser coupled with an isotropic antenna was used to identify prominent RF signals within 900-2500 MHz band and to determine their exposure levels from 40 BTS in each city. The mean distances of maximum human exposure from these BTS were determined. The analyser, which measures specific bands, and a broadband Electromog meter for measuring total RF band were used to acquire RF spectra at the points of maximum exposure from 120, 100 and 80 BTS in Lagos, Ibadan and Abuja, respectively. The spectra were analysed to determine the power density of the various signals observed. The energy fractions transmitted to the brain tissue from 60 common mobile phones in active mode were computed in terms of Specific Absorption Rate (SAR), using a multi-layered model of the human head. The obtained level of exposure was compared to the standard prescribed by the International Commission on Non Ionizing Radiation Protection (ICNIRP). Data were analysed using descriptive statistics.

The distances of maximum exposure were  $183 \pm 58$ ,  $195 \pm 19$  and  $190 \pm 63$  m, in Lagos, Ibadan and Abuja, respectively. Nine major RF signals were identified at each point in the three cities. Five of these signals were satellite signals, within band 960-1700 MHz and producing a highest power density overall of  $9.6 \mu\text{W}/\text{m}^2$  in Lagos. The remaining four (within 935-960 MHz and 1805-2290 MHz) were from BTS, producing a highest power density overall of  $5411 \mu\text{W}/\text{m}^2$  in Abuja. The total power densities in the cities



ranged from 10-27500, 1-8430 and 108-90900  $\mu\text{W}/\text{m}^2$ , with only 23, 26 and 46% being from BTS in Lagos, Ibadan and Abuja, respectively. The SAR in brain tissue from BTS ranged from  $8.0 \times 10^{-9}$  –  $7.3 \times 10^{-5}$  W/kg. The SAR due to all emissions in the near field of the mobile phones ranged from 1–150 mW/kg. This showed that the energy absorption in the brain from mobile phones was higher than from the base stations. The highest SAR obtained was lower than the 2.0 W/kg exposure limit set by the ICNIRP.

Exposures to radiofrequency radiation are from nine major communication signals in most environments, with global system of mobile communications producing the highest. The currently obtained exposure level is within limits, indicating low health risk to the public.

**Keywords:** BTS signal power density, Radiofrequency exposure level, Spectral analyses, Brain specific absorption rate, Radiation related health risk

**Word count:** 496

## TABLE OF CONTENTS

<b>Title</b>	<b>Page</b>
Title Page	
Dedication	ii
Certification	iii
Acknowledgements	iv
List of Abbreviations	v
Abstract	vii
Table of contents	ix
List of Figures	xii
List of Tables	xv
<b>CHAPTER ONE: INTRODUCTION</b>	
1.1	Electromagnetic Radiation (EMR) 1
1.2	Radiofrequency (RF) Radiation 3
1.2.1	Production of RF Radiation 3
1.2.2	The Global system of mobile communication (GSM) 5
1.2.3	GSM Base Transceiver's Station (BTS) 7
1.2.4	The Code Division Multiple Access (CDMA) 9
1.2.5	Mobile Phones (Mobile Stations) 11
1.2.6	Mobile Telecommunication in Nigeria 11
1.3	EM Energy transmission and Absorption 14
1.3.1	Health Effect of Ionising Radiation 16
1.3.2	Health Effect of Non-ionising Radiation 16
1.3.2	RF Radiation Exposure Quantities and Units 17
1.4	Problem Statement and Justification of Study 19
1.5	Aims of Study 20
1.6	Objectives of Study 20
<b>CHAPTER TWO: LITERATURE REVIEW</b>	
2.1	Antennas 21
2.1.2	The Gain and Directivity of an Antenna 22

2.1.3	Antenna Radiation Pattern	27
2.1.4	Near and Far Field of an Antenna	31
2.2	Principle of RF Signal Detection and Measurement	33
2.3	Broad band Meters	36
2.4	Spectrum Analysers	37
2.5	Features of RF Exposure Assessment	42
2.5.1	Study Areas	42
2.5.2	Study sampling time or period	43
2.5.3	Exposure and Distance Relationship	43
2.6	Variation of Power Density with Distance	44
2.7	Assessments of RF Exposure in Nigeria	48
2.8	Biological Effect of RF Radiation Exposure	49
2.9	Limiting Human Exposure to RF Radiation	51
2.10	The ICNIRP RF Exposure Guideline	51
2.11	Brain Energy Absorption Model	55
2.11.1	Uniform Plane Waves in Free Space	55
2.11.2	Plane Wave Propagation in Lossy Materials	57
2.11.3	Power Flow in Lossy Materials	58
2.11.4	Plane Waves at the Boundary between Two Media	59
2.11.5	EM Waves Transmission in Human Head Tissues	63
2.11.6	EM Wave Transmission across each Boundary	63
 <b>CHAPTER THREE: MATERIALS AND METHODS</b>		
3.1	Study Areas	70
3.1.1	Lagos	70
3.1.2	Ibadan	72
3.1.3	Abuja	72
3.2	Instrumentation	75
3.2.1	The Spectrum Analyser	75
3.2.2	The Broadband Meter	77
3.3	Estimation of distance of maximum power density	77
3.3.1	Distance of maximum power density in the three cities	79
3.4	Assessment of all signals within 900 and 2500 MHz RF band	79

3.5	RF Exposure Measurements around Mobile Phones	82
3.6	Estimation of SAR within some Head Tissues	84
<b>CHAPTER FOUR: RESULTS AND DISCUSSION</b>		
4.1	Introduction	88
4.2	Components of RF Spectrum from each BTS Mast	88
4.2.1	Comparison of GSM Radiation Intensity with other RF intensities	101
4.3	Emitted Signals from the Mobile Phones	104
4.4	Electric Field Intensity around a Mobile Phone in Use	104
4.5	RF exposure within the Head tissues	108
4.6	Risk of RF radiation Exposure in the three cities	118
<b>CHAPTER FIVE: CONCLUSION</b>		
5.1	Summary	122
5.2	Contributions, Limitations and Suggestion for Further Studies	124
	<b>REFERENCES</b>	125

## LIST OF FIGURES

	<b>Page</b>
Figure 1.1: Schematic diagram of a radiofrequency transmitter	5
Figure 2.1: Examples of Directional antennas	23
Figure 2.2: Examples of Omni-directional antennas	24
Figure 2.3: GSM directional panel antenna showing dipole antennas arranged in it	25
Figure 2.4: The plot of the normalized power around a typical mobile telecommunication antenna against the vertical angular directions	28
Figure 2.5: The vertical and horizontal radiation pattern of a typical mobile telecommunication antenna with its power in dB	29
Figure 2.6: Radiation lobes and beam widths of the normalised power pattern of a directional antenna	30
Figure 2.7: Field regions of an antenna	32
Figure 2.8: The radiation field regions of a typical Mobile Phone	34
Figure 2.9: An illustration of a RF detection system	35
Figure 2.10: Block diagram showing the configuration of a Superheterodyne or sweptfrequency spectrum analyzer	39
Figure 2.11: Block diagram showing the configuration of a FFT frequency spectrum analyzer	40
Figure 2.12: Radiation beam from a tilted antenna on a typical BTS mast	45
Figure 2.13: An illustration of the variation of power density with distance around a typical BTS mast	46
Figure 2.14: The process of reflection and transmission undergone by an incident wave between two media $m_1$ and $m_2$	60
Figure 2.15: The layers of the human head	63
Figure 2.16: A six-tissue multi-layered planar model of the human head	64
Figure 2.17: The process of wave transmission and reflection across the head tissues	67
Figure 3.1: A map of the city of Lagos showing measurement positions	71
Figure 3.2: A map of the city of Ibadan showing measurement positions	73

Figure 3.3:	An Aerial map of the city of Abuja showing measurement positions	74
Figure 3.4:	An Aaronia SPECTRAN HF - 60105V4 spectrum analyser coupled with an Omnilog-90200 isotropic antenna manufactured by Aaronia AG	76
Figure 3.5:	A TES 92 Electrosmog broadband survey meter manufactured by Less EMF, NY USA	78
Figure 3.6:	Variation of power density of a GSM 1800 signals with distance around typical BTS masts in Lagos, Ibadan and Abuja	80
Figure 3.7:	Distribution of the distances of maximum power density in Lagos, Ibadan and Abuja	81
Figure 3.10:	Distribution of the distances of maximum power density in Ibadan	86
Figure 3.11:	Distribution of the distances of maximum power density in Abuja	87
Figure 4.1:	Typical spectrum of RF signals between 900 – 2500 MHz with indications of prominent frequency bands in Lagos, Ibadan and Abuja	89
Figure 4.2:	Screen shot of the spectrum analyser’s display showing the spectrum of GSM 900 (935 – 960 MHz) frequency band signal strengths	92
Figure 4.3:	Typical screen shot of the spectrum analyser’s display showing the spectrum of GSM 1800 (1805 – 1880) frequency band signal strengths	93
Figure 4.4:	Typical screen shot of the spectrum analyser’s display showing the spectrum of CDMA-1900 (1963 – 1990 MHz) frequency band signal strengths	94
Figure 4.5:	Typical screen shot of the spectrum analyser’s display showing the spectrum of 3G-2100 (2110 – 2290 MHz) frequency band signal strengths	95
Figure 4.6:	A typical spectrum of a GSM 1800 uplink signal band from a mobile phone in the active call mode	105
Figure 4.7:	A typical spectrum of a 3G-2100 uplink signal band from a mobile phone in the active call mode	106

Figure 4.8: Distribution of maximum Electric field intensity within the head tissues obtained from broadband measurements	112
Figure 4.9: Distribution of electric field intensity within the head tissues obtained from spectral measurements	113
Figure 4.10: Distribution of SAR within the head tissues obtained from broadband measurements`	116
Figure 4.11: Distribution of electric field intensity within the head tissues obtained from spectral measurements	117

## LIST OF TABLES

	<b>Page</b>
Table 1.1: Electromagnetic spectrum	2
Table 1.2: Some applications of RF radiation	6
Table 1.3: GSM frequency bands and their Absolute Radio Frequency Channel Number (ARFCN)	8
Table 1.4: Classification of GSM BTS transmission power	10
Table 1.5: Classification of GSM mobile phone transmitting power	12
Table 1.6: The maximum output power of CDMA Mobile Phones	13
Table 1.7: Mobile communication frequency bands allocated by the NCC in Nigeria	15
Table 2.1: Previous measurements of RF power density around some GSM masts in Nigeria	50
Table 2.2: ICNIRP, 1998 reference levels for public and occupational RF exposure at frequencies ( $f$ ) between 400 MHz and 300 GHz	53
Table 2.3: ICNIRP, 1998 basic restrictions for time varying electric and magnetic fields exposure at frequencies between 10 MHz to 10 GHz	54
Table 2.4: The dielectric parameters of the layers of the head tissues at 900 MHz, 1800 MHz and 2100 MHz	66
Table 3.1: Models and communication standards of the selected mobile phones	83
Table 3.2: Values of the transmittance, reflectance, attenuation coefficients, intrinsic impedance and phase angle in the head tissues at 900, 1800 and 2100 MHz	85
Table 3.3: Fraction of the average incident power density in each tissue	86
Table 4.1: Identities of the nine prominent signals in the three cities	90
Table 4.2: Ranges of power density of signal peaks within the spectra of the four BTS signal bands in the cities	96
Table 4.3: Ranges of power density of signal peaks within the spectra of the five satellite signal bands in the cities	97
Table 4.4: Ranges of the sum of power densities of all signal peaks within	



	thespectra of the four BTS signal bands in the three cities	98
Table 4.5:	Ranges of the sum of power densities of all signal peaks within thespectra of the five satellite signal bandsin the three cities	99
Table 4.6:	ICNIRP, 1998 reference levels for public exposure to RF radiation in the range 900 – 2500 MHz	100
Table 4.7:	Ranges of maximum power densities due to satellite and BTS signals in the three cities	102
Table 4.8:	The percentage contribution of GSM to the Total RF power densities in the three cities	103
Table 4.9:	Electric field strength in near field region of the mobile phones using broad band meter and a spectrum analyser	107
Table 4.10:	Summary of the resultant electric field intensityin the head tissues due to 2G mobile phones	109
Table 4.11:	Summary of the resultant electric field intensityin the head tissues due to 3G mobile phones	110
Table 4.12:	Summary of the SARin the head tissues due to 2G mobile phones	114
Table 4.13:	Summary of the SARin the head tissues due to 3G mobile phones	115
Table 4.14:	The ranges of the resultant <b>E</b> and SAR in the brain tissue due to BTS signals at the point of maximum intensities from BTS masts in each city	119

# CHAPTER ONE

## INTRODUCTION

### 1.1 Electromagnetic Radiation (EMR)

Radiation can simply be defined as the propagation of energy from a source into space, which is delivered to any material medium it passes through. Electromagnetic radiation (EMR) consists of both oscillating electric field  $\mathbf{E}$  and magnetic field  $\mathbf{H}$  which are perpendicular to each other and to the direction of propagation of the radiation. It is produced by accelerated charges and it propagates with the speed of light in space. The quantitative relationships between  $\mathbf{E}$ ,  $\mathbf{H}$  and the electromagnetic properties of a medium are given in the Maxwell's equations.

The arrangement of all EMRs according to their frequency, wavelength and energy is called the electromagnetic (EM) spectrum, as shown in Table 1.1. Electromagnetic spectrum extends from low frequency radiations used for long distance radiocommunication to gamma radiation at high-frequency (short-wavelength). Generally speaking, EMR covers wavelengths from  $10^{10}$  to  $10^{-12}$  m. The EM spectrum is generally studied for spectroscopic applications to characterize matter (Mehta, 2011). From the perspective of their effects on human health, EM spectrum can be divided into ionizing and non-ionizing radiations. Ionizing radiations are generally radiation types that have ability to ionize atoms and molecules thereby producing some reactive species that can cause damage at cellular level. Gamma rays and X-rays are two examples of ionizing EM radiations, while examples of particulate ionizing radiation include alpha and beta particles. Non-ionizing radiations such as light and radio waves do not have enough energy to ionize matter.

Table 1.1: Electromagnetic spectrum

<b>Spectrum of Electromagnetic Radiation</b>			
<b>Region</b>	<b>Wavelength (cm)</b>	<b>Frequency (Hz)</b>	<b>Energy (eV)</b>
Gamma Rays	$< 10^{-9}$	$> 3 \times 10^{19}$	$> 10^5$
X-Rays	$10^{-7} - 10^{-9}$	$3 \times 10^{17} - 3 \times 10^{19}$	$10^3 - 10^5$
Ultraviolet	$4 \times 10^{-5} - 10^{-7}$	$7.5 \times 10^{14} - 3 \times 10^{17}$	$3 - 10^3$
Visible Light	$7 \times 10^{-5} - 4 \times 10^{-5}$	$4.3 \times 10^{14} - 7.5 \times 10^{14}$	$2 - 3$
Infrared	$0.01 - 7 \times 10^{-5}$	$3 \times 10^{12} - 4.3 \times 10^{14}$	$0.01 - 2$
Microwave	$10 - 0.01$	$3 \times 10^9 - 3 \times 10^{12}$	$10^{-5} - 0.01$
Radio waves	$> 10$	$< 3 \times 10^9$	$< 10^{-5}$

## 1.2 Radiofrequency (RF) Radiation

Electromagnetic radiations within the frequency band 3 kHz – 300 GHz are generally referred to as Radiofrequency (RF) radiation. Radiofrequency radiations are the main types of EM radiation used for transmitting signals or information from one point to another through space. Radio transmission was initially made from experimental spark gap apparatus by Heinrich Rudolf Hertz 1887, transmitting signals wirelessly over several meters (Siwiak and Bahreini, 2007). Pioneer inventors like Nikola Tesla and Alexander Popov, improved on the earlier wave propagation experiments to produce a simple radio transmitting system comprising of resonant transmitters and receiver circuits by 1890.

Modern day applications of RF signals cut across different types of digital radio transmission technology and techniques in radio, television, mobile phone and satellite communication systems. The uses of RF radiation in modern communication technology also include RADAR communication systems in airports or airways traffic control, military missile guiding systems, microwave heaters and ovens. Some specific applications of RF radiation in communication technology and their corresponding frequency bands are presented in Table 1.2. All devices that emit RF radiation convert electrical power to EM power which is transmitted into space. The transmitted energy is absorbed to different extents by materials in the medium. The amount of energy carried by an electromagnetic field is determined by the electric field intensity  $E$  (V/m) and magnetic field strength  $H$  (A/m) of the EM wave.

### 1.2.1 Production of RF Radiation

Radio waves are generated from a radio transmitter and a common type of this transmitter is an audio transmitter used in AM and FM radio stations illustrated in Figure 1.1. The production of radiofrequency radiations starts from the acceleration of electrical charges through electrical oscillations in an electronic oscillator at a pre-set frequency. An Oscillator in its simplest form is an inductor, a capacitor, and at least one active device like a transistor to amplify an input signal. The generated signal voltage or current from the oscillator is weak and thereby transferred to a buffer amplifier where the signal voltage is increased to a level that can be modulated.

Table 1.2: Some applications of RF radiation

RF Application	Frequency Range
Radio Broadcasting (AM)	30 – 300 kHz
Radio Broadcasting (FM)	87.5 – 108 MHz
TV broadcasting	54 – 216 MHz
GSM Communication	400 – 1900 MHz
CDMA Communication	1900 – 2200 MHz
Wi-Fi (Wireless LAN)	2.4 – 5.9 GHz
Satellite links	3 – 30 GHz
Remote Sensing	30 – 300 GHz

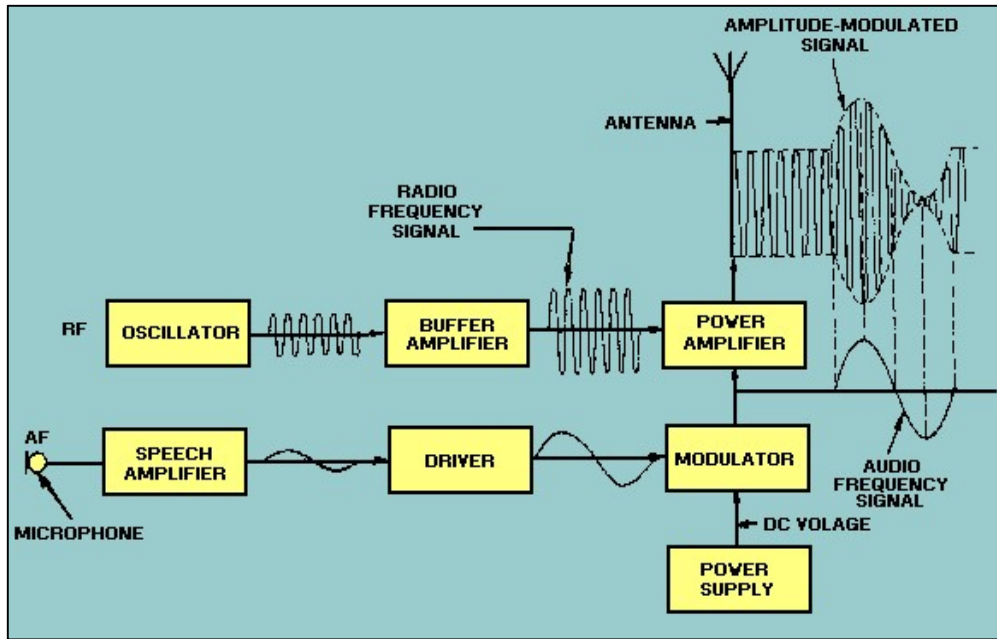


Figure1.1: Schematic diagram of a radiofrequency transmitter(Tpub, 2016)

Meanwhile, a baseband signal intended to be transmitted into space (such as an Audio Frequency (AF) signal received by a microphone) is amplified by the speech amplifier because its output current or voltage is weak. This intermediate amplification is necessary because the voice signal needs to have enough signal amplitude for it to be received by a speech driver. The speech driver acts like an amplifier, which increases the amplitude of the incoming baseband signal so that the modulator can receive it without any loss or distortion.

An RF modulator is a device that adds the baseband AF signal generated by the transducer (microphone) to an electronic signal carrier generated from the oscillator and outputs a radio frequency-modulated signal that is fed into a power amplifier. The power amplifier is a circuit that takes sufficient power from a power source and generates radiofrequency signals of a significant amount of RF output-power directly fed into an antenna, which transmits the signal into space.

### **1.2.2 The Global system for mobile communication**

One of the widespread applications of RF radiation in the 20th century is the development of the Global System for Mobile communication (GSM) originally called Groupe Spécial Mobile. It is a digital communication system created by European conference on postal and telecommunication administration in 1982 in order to develop a standard for mobile communication in over 212 countries in the world (Samra, 2008). The GSM works by using different carrier frequency bands, such as 450, 850, 900, 1800, and 1900 MHz bands, but only GSM 900 (P-GSM) and GSM 1800 (DCS1800) are used in Nigeria.

The different bands of GSM signals allocated around the world and their corresponding carrier frequencies are presented in Table 1.3. (Eberspächer et al., 2009). Out of all the available bands of GSM in the world, only GSM 900 (P-GSM) and GSM 1800 (DCS1800) are used in Nigeria. About 373 and 123 RF carrier channels of GSM 1800 and GSM 900 bands can be achieved, respectively. This shows that GSM 1800 offers more than double of GSM 900 speech channels for mobile phone users and therefore ideal for frequency reuse in a congested area.

Signal transfers during a call in a GSM network are made on a duplex frequency operation within designated frequency bands. In the duplex frequency operation mode, there is a link between the mobile phone and the Base Transceiver Station (BTS) (Uplink signal frequency) and also between the BTS and mobile phone (Downlink signal frequency), operating separately at a very small time difference so that callers can speak and hear at the same time. For effective operation, GSM bands are divided into several channels, having a pair of frequencies with a bandwidth of 200 kHz and a specific offset frequency that vary from one band to other. This division of the GSM spectrum into allocated frequencies is referred to as the Frequency Division Multiple Access (FDMA). The GSM makes use of digital speech and signalling channels, and it is considered to be a second generation (2G) mobile phone system.

### **1.2.3 GSM Base Transceiving Station (BTS)**

A GSM service provider divides a service area into cells. A cell is a coverage area which surrounds a BTS, in which a fixed number of mobile phone subscribers can connect to the network of a service provider. The BTS is a communication equipment that supports 1 to 16 two-way radio called a Transceiver (TRX), depending on the number of mobile phone subscribers in an area (Manjish, 2015). Each TRX can provide up to 8 basic communication channels on the same TDMA frame via the air interface (ETSI, 1996b). Each BTS consists of a power amplifier to enhance signal transmission via the BTS antennas.



Table 1.3: GSM frequency bands and their Absolute Radio Frequency Channel Number (ARFCN)

<b>GSM Frequency Band</b>	<b>GSM Frequency range</b>	<b>ARFCN (Channel Number)</b>
GSM 450 Band	450 – 458MHz (Uplink) and 460 – 468 MHz (Downlink)	259 – 293
GSM 480 band	478 – 486 MHz (Uplink) and 488 – 496 MHz (Downlink)	306 – 340
GSM 850	824 – 849MHz (Uplink) 869 – 894 MHz (Downlink)	128 – 251
GSM 900(P-GSM)	890 – 915MHz (Uplink) and 935 – 960 MHz (Downlink)	1 – 124
GSM 900(E-GSM)	880 – 915 MHz (Uplink) and 925 – 960 MHz (Downlink)	975 – 1023, 0 – 124
GSM 900(R-GSM )	876 – 880 MHz (Uplink) and 921 – 925 MHz (Downlink)	940 – 974, 0 –124
GSM 1800 (DCS1800)	1710 – 1785 MHz (Uplink) and 1805 – 1880 MHz (Downlink)	512 – 885
GSM 1900 (PCS1900)	1850 – 1910MHz (Uplink) and 1930 – 1990 MHz (Downlink)	512 – 810

Although GSM 900 has less communication channels than GSM 1800, it is generally rated better than GSM 1800. This is because the GSM 900 is mainly used for longdistance communications due to its longer wavelength than that of GSM 1800. The rating of a BTS within a cell is controlled and kept below a regulated level in order to prevent interferences with signals in neighbouring cells and also to prevent hazardous exposure to humans in an area. A typical classification of GSM 900 and GSM 1800 BTS transmission power is presented in Table 1.4.

#### **1.2.4 The Code Division Multiple Access (CDMA)**

While GSM uses both time and frequency divisions to allocate calls to users, The Code Division Multiple Access (CDMA) makes use of a spread spectrum transmission technology to allocate call slots to different users(Ipatov, 2000). The spread spectrum technique works by spreading all the mobile phone users uniformly over the available signal bandwidth at the same power,while each conversation is encoded with a pseudo-random digital sequence and a special coding scheme. The CDMA mobile system provides faster, larger capacity for voiceand data communications(5 times bigger than GSM systems),and a better communication hands off between two BTS(Harte et al., 2002; Kopp, 2005; Satooshi et al., 2002).

The CDMA mobile system operates within the down link frequencies of 1930 – 2170 MHz, and constitutes about 3 percent of mobile communications in Nigeria. The power rating of CDMA mobile systems range from 24 dBm (0.25 W) – 38 dBm (6.3 W) (ETSI, 2008). The maximum rated power of CDMA is about 1 percent of that power of GSM. Although the power ratings of CDMA are generally lower than GSM, CDMA mobile phones consume more battery power than GSM. This is due to the ability of CDMA mobile phones to work with many BTS at the same time, and because of the complex network of electronic components within the phones that works most of the time. The 3G (2100 MHz) mobile standard is based on CDMA technology and it is often used in backward compatibility with GSM systems.

Table 1.4: Classification of GSM BTS transmission power (ETSI, 1996a)

GSM 900		GSM 1800	
Transmission power class	Maximum output power in watts	Transmission power class	Maximum output power in watts
1	320 – 640	1	20 – 40
2	160 – 320	2	10 – 20
3	80 – 160	3	5 – 10
4	40 – 80	4	2.5 – 5
5	20 – 40		
6	10 – 20		
7	5 – 10		
8	2.5 – 5		

### **1.2.5 Mobile Phones (Mobile Stations)**

The mobile phone is a portable versatile two way radio system that transmit to and receive signals from a BTS (within a designated frequency band), when in the area covered by the BTS. It consists of a Subscriber Identity Module (SIM) card and Mobile Equipment (ME). Each SIM card has an International Mobile Subscriber Identity (IMSI) number that is unique, while the mobile phone has a unique International Mobile Station Equipment Identity (IMEI) number.

Mobile phones are low-powered devices ( $< 8W$ ) that operate typically between 450 and 2700 MHz. The power ratings of GSM and CDMA mobile phones are presented in Tables 1.5 and 1.6, respectively. The mobile phone only transmits power when it is turned on and hence the exposure to a user falls off rapidly with increasing distance from the mobile phone to the users head. Mobile phones derive the energy required for their operation from their batteries. The BTS controls the power output of the mobile phone, keeping the power level sufficiently high to maintain a good signal to noise ratio, and not too high to reduce interference, overloading and also to preserve the battery life (Ian, 2017). The human head is often within the region around a mobile phone, where the maximum RF energy is four times the average energy at the aperture of the phone's antenna in the active mode. Most mobile phones operate on several mobile communication bands like the third generation (3G), GSM (2G)/EDGE and WCDMA/ HSPA standards. This multi-band system of mobile phones is made possible by the one or more antennas that switch between different operating modes of the phones.

### **1.2.6 Mobile Telecommunication in Nigeria**

A revolution in the Nigerian telecommunication industry took place in 2001, when GSM was introduced. The GSM network services in Nigeria have since then expanded enormously in capacity, with the inclusion of the CDMA-1900 and 3G mobile telecommunication bands. It was reported that Nigeria's teledensity is over 99 percent, with over 140 million active mobile telecommunication lines (NCC, 2019). This huge number of active lines has attracted over 30,000 base transceiver stations and millions of mobile phone handsets within the country. About 98 percent of the BTS in Nigeria are used for GSM.

Table 1.5: Classification of GSM mobile phone transmitting power (ETSI, 1996c)

Power class	GSM 900 Maximum output power	GSM 1800 Maximum output power	Tolerance (dB) for conditions	
			Normal	Extreme
1		1 W (30 dBm)	$\pm 2$	$\pm 2.5$
2	8 W (39 dBm)	0.25 W (24 dBm)	$\pm 2$	$\pm 2.5$
3	5 W (37 dBm)	4 W (36 dBm)	$\pm 2$	$\pm 2.5$
4	2 W (33 dBm)		$\pm 2$	$\pm 2.5$
5	0.8 W (29 dBm)		$\pm 2$	$\pm 2.5$

Table 1.6: The maximum output power of CDMA Mobile Phones (ETSI, 2008).

Power class	WCDMA Band 1	WCDMA Band 2	Tolerance (dB) for conditions	
	Downlink (2110 – 2170 MHz) Maximum Output Power	Downlink (1930 – 1990 MHz) Maximum Output Power	Band 1 tolerance	Band 2 tolerance
1	+33dBm (2W)	-	+1.7/-3.7	± 2.5
2	+ 27dBm (0.5W)	-	+1.7/-3.7	± 2.5
3	+24dBm (0.25W)	+24dBm (0.25W)	+1.7/-3.7	± 2.5
4	+21dBm (126mW)	+21dBm (126mW)	+2.7/-2.7	± 2.5

The Nigerian Communications Commission (NCC) is the Independent national regulatory authority for the telecommunications industry in Nigeria. The Commission is responsible for allocating mobile telecommunication frequency band to service providers and providing healthy competitive environment among service providers as well as protecting the interest of the consumers in Nigeria. There are currently four major GSM service providers in Nigeria namely Mobile Telecommunications Network (MTN), Globacom (GLO) mobile, 9-Mobile and Airtel mobile and about two major CDMA-1900 (1900 MHz) service providers namely Visafone and Multilinks mobile.

While the number of GSM mobile phone subscribers in Nigeria recorded an increment of about 24 % from 2014 to 2018, the number CDMA-1900 mobile phone users had a setback of about 98 % within this period (NCC, 2019). Although the 3G mobile band is based on CDMA technology, it is often incorporated into the existing GSM systems. Therefore, most GSM users with an enabled internet facilities in Nigeria switch between GSM (2G) and 3G systems. The NCC frequency spectrum allocation for GSM, CDMA-1900 and 3G-2100 (2100 MHz) bands are presented in Table 1.7.

### **1.3 EM Energy transmission and Absorption**

Electromagnetic radiations transport energy in space and can deposit this energy in a material medium they interact with. The amount of energy available in EM radiations depends on their frequency or wavelength. High frequency or short wavelength radiations have higher photon energy levels, than the lower frequency or long wavelength radiations.

The interaction of EM radiations with a material medium can cause them to be scattered, absorbed or transmitted across the medium (Chaudhary et al., 2016). The mechanism by which EM radiation energy is absorbed in a medium is basically through electronic transitions, molecular vibrations and rotation in the atom of the medium (L'Annunziata and Baradei, 2003). Ionising radiations like X-rays with high quantum energies (far above 12.4 eV) can completely eject an electron from an atom, thereby resulting in photoionization and Compton scattering.

Table 1.7: Mobile communication frequency bands allocated by the NCC in Nigeria

Mobile Frequency Band	Transmission (TX) frequency (MHz)	Receiving (RX) frequency (MHz)	Number of Subscribers
GSM 900 (900 MHz)	935.00 – 960.00	890.00 – 915.00	
GSM 1800 (1800 MHz)	1805.00 – 1880.00	1710.00 – 1785.00	162,000,000
3G-2100 (2100 MHz)	2110.00 – 2150.00	1920.00 – 1960.00	
CDMA-1900 (1900 MHz)	1963.75 – 1988.75	1883.75 – 1908.75	124,000



Below 12.4 eV, absorption of EM radiation like the ultraviolet in a medium is mainly by electron transitions which results in effects such as Fluorescence (MTU, 2019). The infrared IR radiation has photon energy between 0.01 and 2 eV and is capable of producing molecular vibrations which results to heating in a medium. Radiofrequency (RF) radiation (microwave and radio waves) have low photon energies less than 0.01 eV and cannot cause ionisation in any medium. The absorption of RF radiation in a medium produces molecular rotations and torsion due to the interaction between the polar molecules of the medium and the applied high frequency electric field. The electric field of RF radiations can also set up ionic current by induction and produce the Joule heating in a medium (Cember and Johnson, 2009).

### **1.3.1 Health Effect of Ionising Radiation**

Ionising radiations have enough photon energies to cause ionisation in the human body. This process leads to the production of new undesired molecules, a change in the conductive properties, and a release of energy in the body (Ralph, 2012). This action causes free radicals to be produced in the cellular water which is about 70 – 90 percentage of the human tissue. The production of free radicals in body results in the formation of reactive molecule which damages deoxyribonucleic acid, enzymes, nuclei and chromosomes of the human cell (RPII, 2013). Generally, ionizing radiations are known to cause skin redness, hair loss, radiation burns, known as acute effects and Cancers and heritable mutations known as stochastic (probabilistic) effects.

### **1.3.2 Health Effect of Non-ionising Radiation**

The human body absorbs part of the non-ionising radiations like radio waves incident on them and at very high frequency can absorb almost all of the radiation energy, at the skin surface as heat such as infrared radiation. The major effect of absorbing RF radiation ranging from 10MHz – 300GHz by a human body is the production of heat in the body, leading to heat exhaustion and heat stroke (ACGIH, 1996). The production of heat is as a result of induced ionic current and Joule heating due to the reorientation of the electric dipoles in the body (ICNIRP, 1998). Other effects of RF radiation, which are not associated with temperature increment in the body are considered to be non-thermal effects such as DNA damage, increase in blood brain-barrier permeability and ocular impairment (Wolf and Wolf, 2004).

### 1.3.2 RF Radiation Exposure Quantities and Units

The tissues of the human body are lossy dielectric materials. A dielectric is a non-conductor of electricity, but exhibits electric polarization in finite amount of time when an electric field is applied to it (Feldman et al., 2005). The measure of how easy a dielectric medium can be polarized is called its relative permittivity  $\epsilon_r$  or dielectric constant. The dielectric constant is the ratio of the permittivity of a substance to the permittivity of free space and this is the electrical equivalent of relative magnetic permeability  $\mu_r$ .

The permittivity of a biological medium is complex in nature, with real and imaginary components. The real part of the complex permittivity ( $\epsilon'$ ) represents the polarisation in line with an incident EM field, while the imaginary part ( $\epsilon''$ ) represents the component of the polarisation in quadrature with the field (Feldman et al., 2005). The  $\epsilon''$  of a medium is attributed to bound charges and relaxation phenomena in the medium, which give rise to energy loss that is similar to the losses due to conduction charges that is quantified by the conductivity ( $\sigma$ ) of the medium (Ramo et al., 1994; Zhao et al., 2016).

The loss of EM energy in a dielectric medium (often as heat) is a function of the dielectric loss which is parameterised as loss tangent ( $\tan \delta$ ). The loss tangent in a dielectric medium can be expressed as,

$$\tan \delta = \frac{\epsilon''}{\epsilon'} = \frac{\sigma}{\omega \epsilon'} \quad (1.1)$$

where,  $\omega$  is the angular frequency of the incident wave. Similarly, magnetic loss tangent can be expressed as,

$$\tan \delta_m = \frac{\mu''}{\mu'} \quad (1.2)$$

It is therefore apparent that RF energy losses in the human body basically depend on parameters like permittivity, permeability and conductivity of the body, which are intrinsic characteristics of biological materials.

To accurately account for the absorbed RF energy in a human body, the intrinsic characteristics of the body must be known. The measurement of radiation energy absorbed by human organs in an EM field over a period of exposure is called dosimetry (Ahlbom et al., 2012).

The proportion of energy absorbed by human body in a given period of time in a radiofrequency electromagnetic field is referred to as the Specific absorption rate (SAR) (W/kg). The SAR was developed and has been used since 1974 (Gandhi, 1974). It is normally related to  $\mathbf{E}$  and can be expressed as (ANSI, 1982),

$$SAR = \frac{\sigma |\mathbf{E}|^2}{2\rho} \text{ (W/kg)} \quad (1.3)$$

$\sigma$  = conductivity  
 $\rho$  = Mass density

When an EM wave is incident upon an aperture of an area  $A$  of a medium the total power  $P$  flowing through  $A$  can be expressed as,

$$P = \int_A \mathbf{S} \cdot \hat{\mathbf{n}} dA \text{ (W)} \quad (1.4)$$

where,  $\hat{\mathbf{n}}$  is a unit vector normal to area  $A$  and  $\mathbf{S}$  is the Poynting vector, defined as,

$$\mathbf{S} = \mathbf{E} \times \mathbf{H} \quad (1.5)$$

$S$  is the power density ( $\text{W/m}^2$ ) carried by the wave along the direction of wave propagation. The power density,  $\mathbf{E}$  and  $\mathbf{H}$  are interrelated by Equation (1.6) (ICNIRP, 1998),

$$\mathbf{S} = \frac{\mathbf{E}^2}{377} = 377 \mathbf{H}^2 \text{ (W/m}^2\text{)} \quad (1.6)$$

where, 377 is the characteristic impedance of free space in Ohms. In biological media, the characteristic impedance is expressed as the complex intrinsic impedance  $\eta_c$ .

Practically, measurements of the amount of power flow in a lossy medium can be expressed as an average power density  $\mathbf{S}_{av}$  (Hayt and Buck, 2012) where,

$$\mathbf{S}_{av} = \hat{\mathbf{z}} \frac{|E_{x0}|^2}{2|\eta_c|} e^{-2\alpha z} \cos\theta_\eta \text{ (W/m}^2\text{)} \quad (1.7)$$

The magnitude of complex intrinsic impedance  $\eta_c$  in polar form is,

$$\eta_c = |\eta_c| e^{j\theta_\eta} \quad (1.8)$$

Where  $\theta_\eta$  is the phase difference between  $\mathbf{E}$  and  $\mathbf{H}$  components of a wave propagating in positive  $z$  direction within the lossy medium and  $\alpha$  is the attenuation constant of the medium expressed as,

$$\alpha = \omega \left\{ \frac{\mu\epsilon'}{2} \left[ \sqrt{1 + \left( \frac{\epsilon''}{\epsilon'} \right)^2} - 1 \right] \right\}^{\frac{1}{2}} \quad (1.9)$$

#### 1.4 Problem Statement and Justification of Study

The proliferation of mobile telecommunication devices and radio transmitting antennas has precipitated global concern over possible health hazards associated with exposure to the generated electromagnetic radiations (Ahaneku and Nzeako, 2012; Durduran et al., 2013; Oladapo et al., 2011; Wu et al., 2013). In Nigeria, communication BTS and masts are found averagely at every 500 m interval of distance in its major cities. People live as close as 10 m to these BTS and can be exposed to excessive RF radiation (Aderoju et al., 2014; Farai et al., 2012).

In densely populated Nigerian cities like Lagos, Ibadan and Abuja, assessments of RF power density are needed to be constantly made to avoid unnecessary health hazard to the populace. However, there are only few known studies to have assessed the level of RF power density around GSM masts and mobile phone handsets in the major cities of Nigeria, using both RF broadband and spectrum analyser (Mamilus et al., 2012; Ojuh and Isabona, 2015). There is a need to measure the power density of GSM signals around the numerous BTS and assess the level of RF emissions from mobile phones in major cities in Nigeria.

Assessments of RF exposure from communication systems in Nigeria are mainly done to evaluate GSM signal power density in an environment (Akintonwa et al., 2009; Akpolile et al., 2014; Ibitoye and Aweda, 2011). Most of these studies makes use of a broadband meters. A broadband meter measures the total RF power density at a point due the contributions of a wide range of frequencies. There is a need to assess RF emission characteristics of signal frequencies within the RF range (WHO, 2010), because these signals are used for different RF applications and may present different exposure scenarios that can be used to characterise RF exposure to the general population.

However, information on exposure of signals within 900 and 2500 MHz in Nigeria to humans is scanty. Therefore, there is the need to identify and assess various RF signals within 900 and 2500 MHz in each environment using a spectrum analyser.

The evaluation of SAR in the human head from various BTS masts and the numerous brands of mobile phones in Nigeria is necessary to determine their safety to the public. However, studies on the assessment of SAR in the human brain tissue, in the use of GSM and various brands of mobile phone sets in the country are scarce. There is the need to quantify RF exposure to the brain using a frequency selective meter and estimate any associated health risk in the use of mobile phones in Nigeria.

### **1.5 Aim of Study**

The aim of this study is to determine the power density due to each signal in the frequency range 900 – 2500 MHz and assess the health risks due to GSM signals from BTS masts and mobile phones in Nigeria.

### **1.6 Objectives of Study**

The objectives of this study are to,

1. Make spectral survey of RF signals around 40 randomly selected BTS masts in Lagos, Ibadan and Abuja in order to determine the general profile and estimate the point of maximum power density, representing the point of worst case scenario of power density.
2. Identify the major signals within 900 - 2500 MHz around the distance of maximum power density from BTS masts in each city and determine their respective power densities.
3. Measure the Electric field intensity (**E**) on the skin of the head during the use of mobile phones.
4. Extrapolate the fraction reaching the brain tissue from the intensity on the skin from both the BTS masts and the hand held mobile phones.
5. Estimate the radiological health risks using established guidelines.

## CHAPTER 2

### LITERATURE REVIEW

#### 2.1 Antennas

As introduced in chapter one, RF radiations are produced from the acceleration of electrical charges within the circuitry of a radio transmitter. The generated RF signal within the transmitter, after being amplified to the desired level of output signal power, must be fed into an antenna device in order to radiate it into space. An antenna is a device that converts high frequency alternating electric power into radio waves which can be transmitted by the radiating antenna or received by a receiving antenna (Schantz, 2003; Seybold, 2005; Straw, 2007).

Antennas can be used as transmitting (TX) or receiving (RX) antennas. These characteristics of the antenna is based on the reciprocity theorem of electromagnetics (Stutzman and Thiele, 2012), which establishes that the principle governing the characteristics of an antenna are the same when the antenna is used as an emitter or a receiver. A transmitting antenna radiates the RF energy applied to it into space, while the receiving antenna collects and converts the radio waves from space into an applied alternating voltage to the receivers amplifying circuits. An antenna can be classified into directional or Omni-directional antenna. Directional antennas concentrate the RF radiation from there elements to a preferred direction and suppress it in others.

Examples of Directional antennas are the Yagi, parabolic, Conical, sectorial and Horn antennas, presented in Figures 2.1 and 2.3. Omni-directional antennas on the other hand, are antennas that emit RF radiation equally in all directions. Examples of Omni-directional antennas are the Monopole and Dipole antennas, presented in Figure 2.2. Most BTS antennas in mobile communication are mostly directional antennas, which are made of well-arranged sectorial antennas with a rear reflector to concentrate emitted radiation to a desired point. An example of a GSM sectorial antenna is presented in Figure 2.3.

Electromagnetic waves are radiated from an antenna when a sinusoidal signal voltage from a radio transmitter is applied to a two-conductor transmission line that is connected to the antenna (Balanis, 2005). The two-conductor transmission line creates an EM fields between the conductors and transfers it to the antenna. Electric charges and current are created within the antenna, which in return produce free space waves that are detached from the antenna into space (Serway and Jewett, 2010).

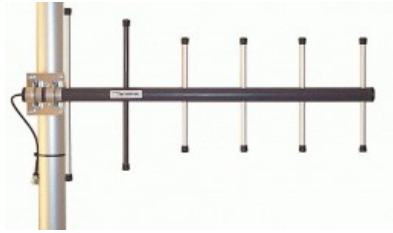
### 2.1.2 The Gain and Directivity of an Antenna

The gain ( $G$ ) of an antenna describe its ability to concentrate EM radiation in a particular direction and it is defined as the ratio of the antenna's radiation intensity ( $U$ ) (Watt per unit solid angle) at a point, to the radiation intensity ( $U_o$ ) that would be obtained at that point if the antenna were to be an isotropic antenna. The isotropic antenna is an antenna that radiates energy equally in all direction. The gain of an antenna is defined as:

$$G = \frac{U}{U_o} = 4\pi \frac{U}{P_{in}} \quad (2.1)$$

$P_{in}$  = Input power (W).

$U_o$  = Power accepted by the antenna



**Yagi antenna**



**Horn Antenna**



**Parabolic antenna**

Figure 2.1: Examples of Directional antennas.



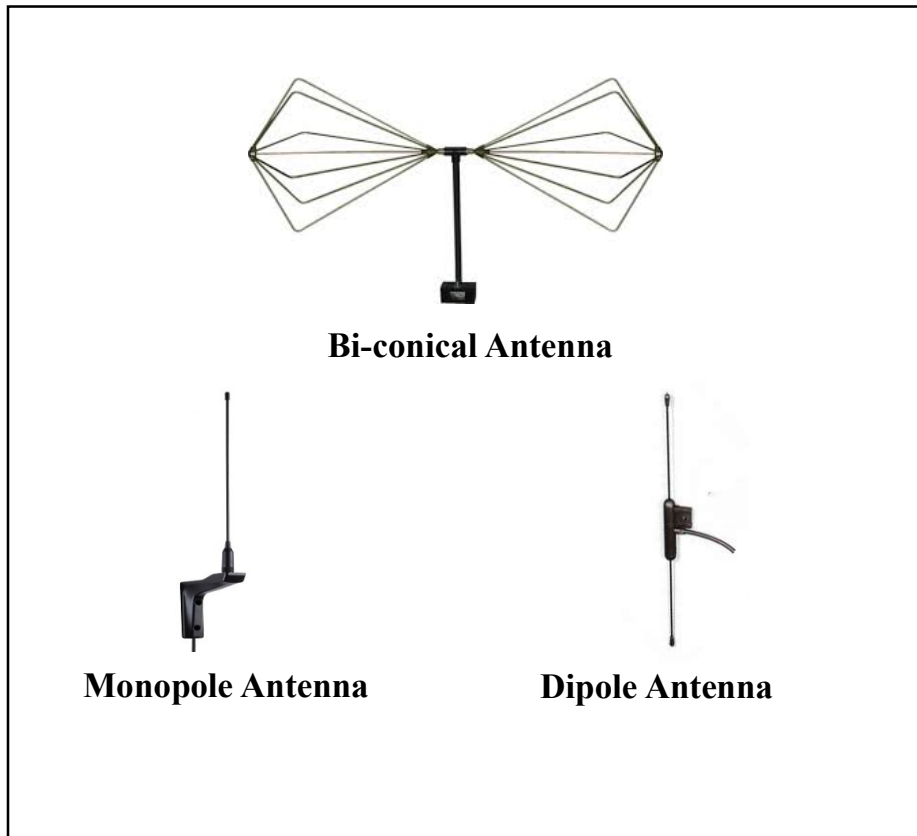


Figure 2.2: Examples of Omni-directional antennas

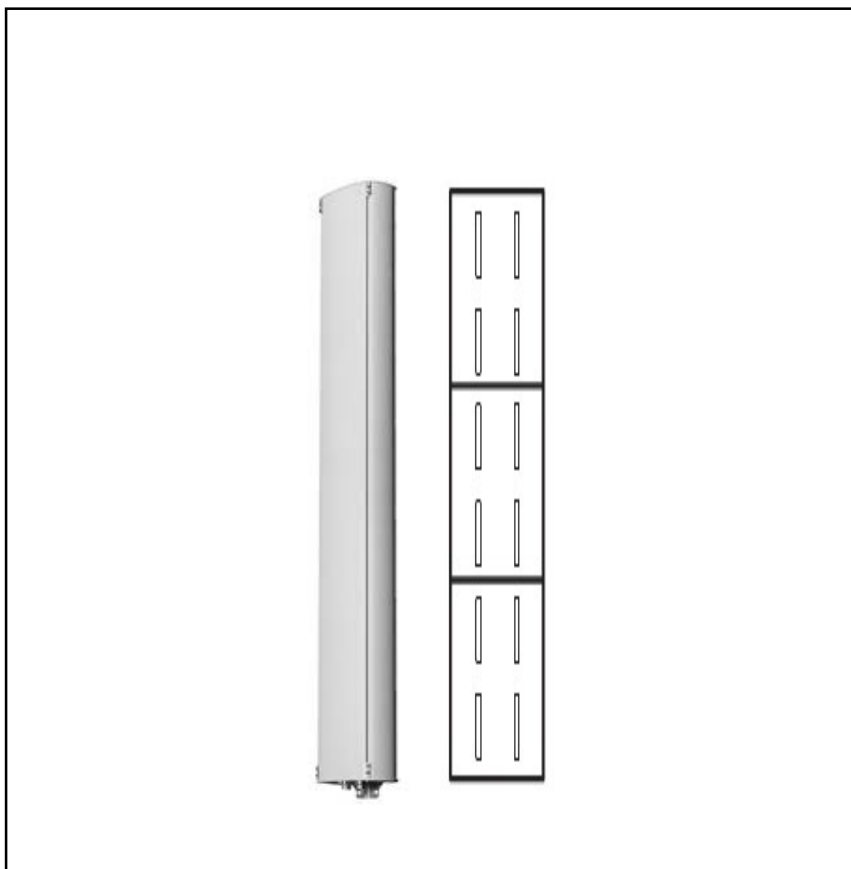


Figure 2.3: GSM directional sectorial antenna showing dipole antennas arranged in it

The gain can be related to the geometry of an antenna and the wavelength of the radiated waves from the antenna as,

$$G = \frac{4\pi\eta A}{\lambda^2} \quad (2.2)$$

Where,

A = Aperture (area of the antenna)

$\lambda$  = Wavelength of RF

$\eta$  = Antenna efficiency

The gain can also be used to calculate the power density ( $S$ ) ( $W/m^2$ ) of RF radiations received by the antenna of RF meters such as a spectrum analyzer using Equation (2.3) (Aaronia, 2011),

$$S = \frac{10^{\left(\frac{P-G}{10}\right)}}{1000} \times \frac{4\pi}{\lambda^2} \quad (2.3)$$

$P$  = power received by the antenna of the meter in dBm

$G$  = gain of the antenna in dBi

$\lambda$  = is wavelength of the received signal meters (m).

The directivity ( $D$ ) of an antenna is the ratio of the radiation intensity at a point in a given direction ( $U$ ) (Watt per unit solid angle), to the radiation intensity averaged over all directions expressed as (Balanis, 2005),

$$D = \frac{4\pi U}{P_{rad}} \quad (2.4)$$

$P_{rad}$  = the total radiated power in watts (W).

The directivity and the gain of an antenna are related by (Straw, 2007),

$$D = \frac{G}{\eta} \quad (2.5)$$

where  $\eta$  is referred to as the antenna efficiency (Seybold, 2005).

### 2.1.3 Antenna Radiation Pattern

The directivity of an antenna is based on the fact that it is required that EM radiations from an antenna are emitted to favour certain directions and to discriminate against noise or interference in other directions (Straw, 2007). The strength of the radiation is not the same around the antenna, but depends on the direction or angles around the antenna (Serway and Jewett, 2010). The radiation pattern of an antenna is generally expressed as the plot of measured electric field strength, magnetic field intensity or radiation power against the angle of direction of measurement around the antenna.

Graphical expression of radiation patterns are made in terms normalized  $\mathbf{E}$  field,  $\mathbf{H}$  field, radiation intensity, power and logarithmic scale or more commonly in the decibels (dB) scale. The normalized antenna's radiation property is obtained when the value of the property at a point is divided by its maximum value. The normalized power at a point around an antenna can be expressed as,

$$P_{normalised} = \frac{P}{P_{max}}(2.6)$$

A typical plot of the radiation pattern of a mobile telecommunication antenna is shown in Figure 2.4. The radiation pattern in a spherical dimension is shown in Figure 2.5. As indicated in Figure 2.5, radiation patterns can be obtained in the vertical or elevation directions called the vertical radiation pattern VRP or in the horizontal or azimuth directions called the horizontal radiation pattern HRP. The radiation pattern of an antenna is divided into different parts that are referred to as lobes.

The lobes are divided into the major or main, minor, side, and back lobes. A major lobe contains the direction of maximum radiation from the antenna. A minor lobe is the radiation lobe that is less than the major lobe and it consists of the side and the back lobes. Figure 2.6 presents the various lobes, the beam width and the angular distance they occupy. The Half Power Beamwidth (HPBW) is the angular distance between two identical half power points on the opposite sides of the main beam. The half power points are located in the directions where the value of the radiation intensity or radiated power of the antenna is half its maximum value, called the 3dB points. The First Null Beamwidth (FNBW) is the angular distance between the first nulls of the pattern.

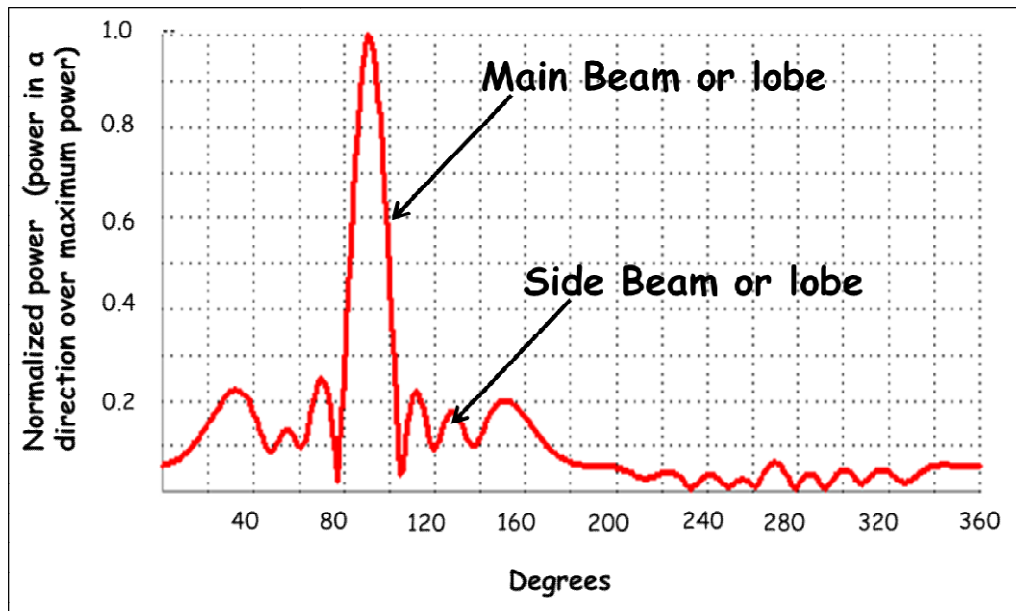


Figure 2.4: The plot of the normalized power around a typical mobile telecommunication antenna against the vertical angular directions (ITU, 2013).

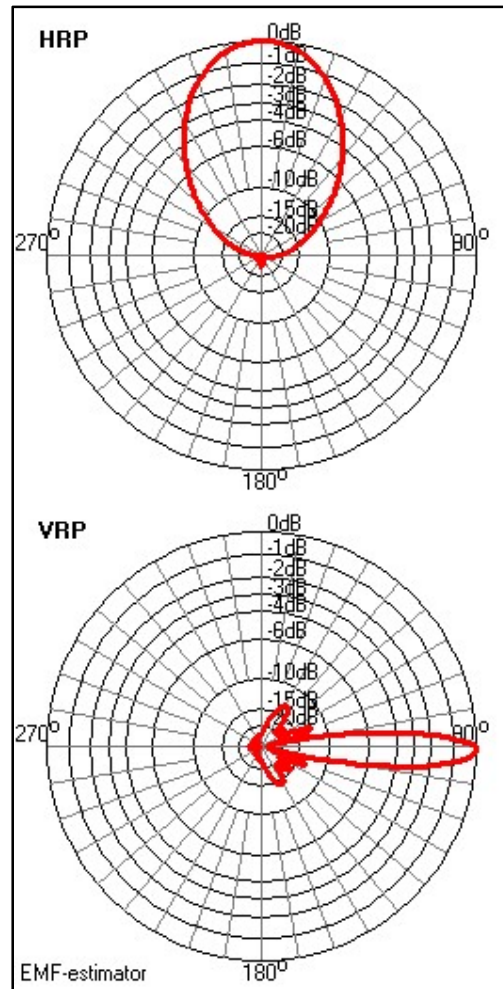


Figure 2.5: The vertical and horizontal radiation pattern of a typical mobile telecommunication antenna with its power in dB(ITU, 2013).

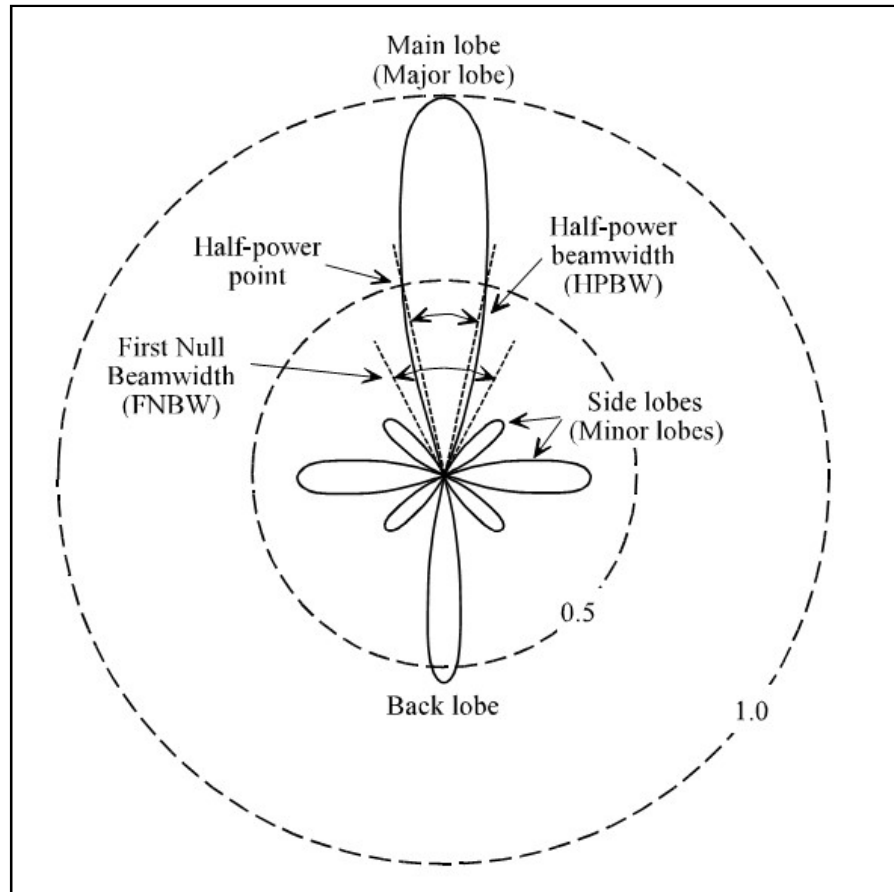


Figure 2.6: Radiation lobes and beam widths of the normalised power pattern of a directional antenna (Balanis, 2005).

#### 2.1.4 Near and Far Field of an Antenna

The near field of an antenna is the region where reactive energy flows back and forth during successive emission of RF waves from an antenna. Reactive energy is stored in very close to the antenna, contributing to the total energy at regions near the antenna (Cember and Johnson, 2009). The near field can be divided into the reactive non-radiative (reactive) and radiative field regions. The non-radiative field region exists in the distance  $R_d$  expressed as,

$$R_d = 0.62 \times \sqrt{\frac{D^3}{\lambda}} \quad (2.7)$$

Distances greater than  $R_d$  is the radiative near field region, as shown in Figure 2.7. There is an uneven distribution of  $\mathbf{E}$  and  $\mathbf{H}$  in the near field region an antenna, thereby making the ratio of  $\mathbf{E}$  to  $\mathbf{H}$  to differ substantially from the  $377\Omega$  impedance of free space. This is the reason why the power density is not suitable in determining RF exposure in the near field of an antenna (ICNIRP, 1998). The maximum Energy ( $W_m$ ) in the near field of an antenna as in mobile communication systems like the BTS and a mobile phone is four times the average Energy ( $W_o$ ) at the aperture of the antenna (Cember and Johnson, 2009) i.e.,

$$W_m = 4W_o \quad (2.8)$$

The far field region of an antenna starts at a distance  $f_d$  from the antenna. The distance  $f_d$  from the antenna can be expressed as,

$$f_d = \frac{2D^2}{\lambda} \quad (2.9)$$

where,  $D$  is largest dimension of the antenna and  $\lambda$  is the wavelength of the emitted signal. Meaningful measurements of power density can be made in the far field region of an antenna.



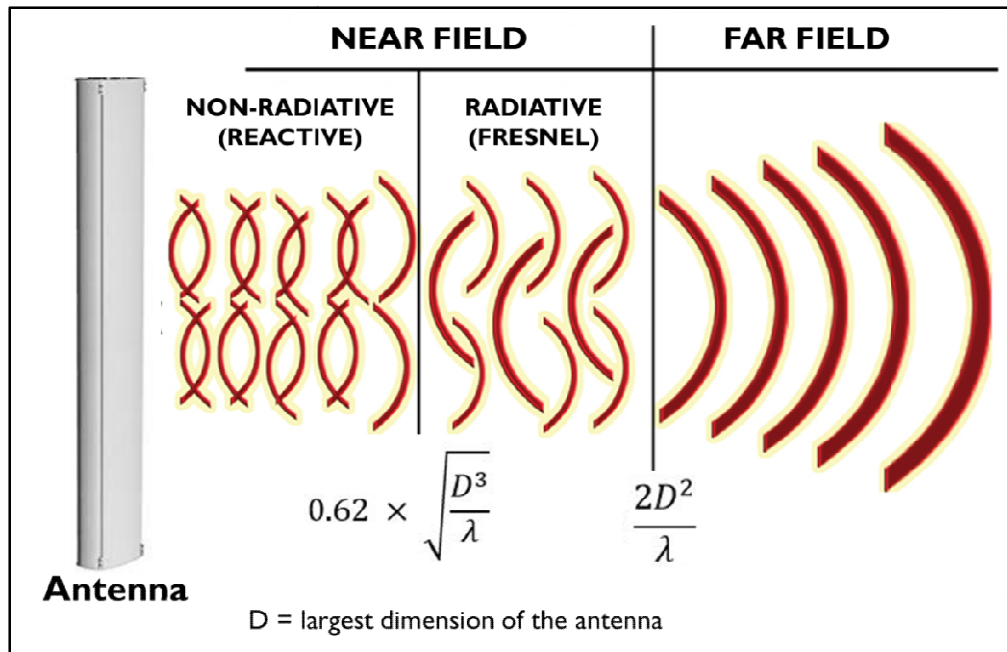


Figure 2.7: Field regions of an antenna.

For example, the largest dimension ( $D$ ) for a typical mobile phone ranges from 1 – 5 cm (Al-Mously and Yahya, 2010). For a mobile phone antenna with  $D = 5$  cm, the  $f_d$  at 900 MHz is 1.5 cm, 3 cm at 1800 MHz and 3.5 cm at 2100 MHz. This shows that, a caller's head is always in the near field of the mobile phone during an active call. The brain of a caller may be exposed to high level of power density at this region, leading to the heating of the brain tissues. The thickness of most mobile phones is typically between 0.5 and 1.5 cm and this range of distances are within the near field of the antenna as illustrated in Figure 2.8.

## 2.2 Principle of RF Signal Detection and Measurement

Radiofrequency signals in space carry energies that can be converted into a measurable electric current or voltage by a RF receiver. The detection of RF signals in a receiver starts from a receiving antenna, which receives the signal as an induced voltage that causes current to flow into a RF tuner or filter. The RF tuner selects the desired signal frequency from a band of frequencies. The selected signal is usually of low voltage or current, which is amplified by feeding it into a signal amplifier. The amplifier increases the amplitude of the signal for adequate detection by the detector. The detected signal is transferred into a power or DC amplifier before the value of the signal power density or electric field intensity of the signal is indicated on the meter. An illustration of a RF detection system is presented in Figure 2.9.

The mode of signal detection in an RF receiver depends on the frequency at which the signal is being transmitted. At low frequencies (below 100 kHz), power and hence power density is measured indirectly. The detected signals are measured by the received voltage  $V$  or current  $I$ , according to Ohm's law:

$$I = \frac{V}{R} \quad (2.10)$$

where,  $R$  is the impedance of the detection medium. The power is then calculated from the values of the voltage or current. At very high frequencies, direct power measurement is more accurate than when it is calculated from voltage and current, because of the large variation in the detector's impedance as the frequency of signal increases. Therefore at frequencies above 1GHz, direct measurement of power is more reliable than taking current and voltage measurements (Agilent, 2001).

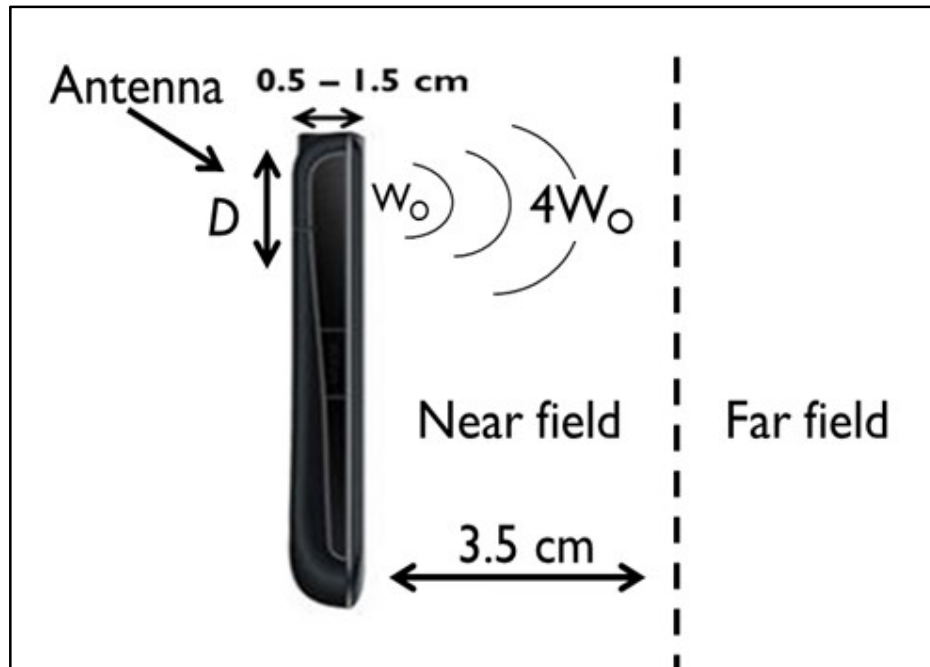


Figure 2.8: The radiation field regions of a typical Mobile Phone

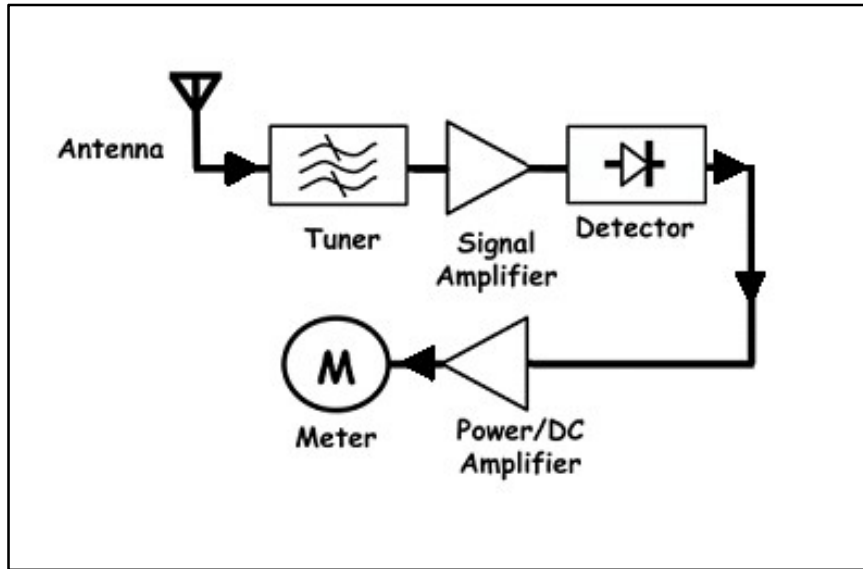


Figure 2.9: An illustration of a RF detection system

As earlier stated, signals of various frequencies may induce a signal voltage across the antenna system of a receiver but the tuner circuit selects the frequency of the desired radio signal from other frequencies received by the antenna. The tuner circuit is made up of inductors and capacitors connected together to create a resonating current similar to the frequency of the desired signal. The amplitude of the signal that is selected by the tuner is amplified for proper detection by the RF amplifier.

There are three major devices for detecting the average power at RF and microwave frequencies (Agilent, 2001). These detectors are a thermistor, a thermocouple and a diode detector. Many RF receivers contain the crystal diode, because of its ability to detect extremely low and high frequency signal powers. A crystal diode is a non-linear device that rectifies the high frequency signal energy received from a receiver's antenna, into an output voltage which is proportional to the antenna's power input

At a higher signal power levels, thermistor and the thermocouple are often used as RF detection device. Thermistors are power sensors that operate by changing resistance due to a change in temperature. The change in temperature results from converting high frequency RF or microwave energy into heat within its element (Delisle, 2014). Thermocouples are based on the fact that dissimilar metals generate a voltage due to temperature differences at a hot and a cold junction of the two metals. When RF radiation or microwave signal is introduced to the elements of a thermocouple, there is a temperature change in these elements which gives rise to a voltage drop across them.

### **2.3 Broad band Meters**

Broadband meters are RF detector that measure the  $E$  or power density of all the signals within a wide RF band. They are similar to power meters that are often used in the radar and navigation systems that depended primarily on the peak power radiated (Skolnik, 1962). The Broad band meters make use of thermistors, a thermocouple or diode as a RF detector device (Agilent, 2001; Haim and Shimshon, 2002). Power measurements are often made by comparing the output power coming out of an amplifier, relative to that going into it. These measurements are usually in the decibel (dB) units expressed as:

$$P(dB) = 10 \log_{10} \left( \frac{P}{P_{ref}} \right) \quad (2.11)$$

where,  $P$  is the detected power and  $P_{ref}$  is the reference power or input power. To avoid the number of zeros that are sometimes involved in low power signal measurements, microwave power measurements are often expressed in terms of dBm,

$$P(dBm) = 10 \log_{10} \left( \frac{P}{1m} \right) \quad (2.12)$$

The measured power by the broadband meter is expressed in terms of power density, electric and magnetic field units at its digital or analog display. All commercially available broadband meter have the same basic functionality, i.e. they can integrate the power of individual signal frequencies that make up a wide band of frequency. Although relatively inexpensive, broadband meters are limited by their inability to identify each frequency within the detected RF band.

Few of the broadband meters that have been used in some RF studies are the ALRF05 by Toms Gadgets (Enyinna and Avwir, 2010) and EMR-300 by Wandel & Golterman (Shurdi et al., 2010). Most of these meters can cover the frequency range of 100 kHz – 3 GHz and they have a tri-axial antenna that can detect Eof signals and display its value up to 600V/m.

## 2.4 Spectrum Analysers

A spectrum analyser is required in the study of radiocommunication signals in the frequency domain. It is therefore one of the most-versatile and widely used RF measuring instrument. A spectrum analyser basically measures the magnitude of the strength of signal against its frequency. There are two classes of spectrum analysers which are the Superheterodyne and Fast Fourier Transform (FFT) based spectrum analysers.

In a superheterodyne or swept spectrum analyser, the power of a received signal is limited by the RF attenuator to prevent the signal from damaging the delicate electronic components within the spectrum analyser. The obtained signal may be accompanied by other undesired signal frequencies, it is therefore transferred into a low pass filter that allow only the desired signal to go through it as long as the

frequency of the desired signal is lower than cut-off frequency of the filter. The signal from the low pass filter is mixed or swept through a fixed signal frequency generated from the local oscillator, at the mixer. The mixer converts the base band or carrier frequency into a different signal usually of lower frequency called the Intermediate Frequency (IF). The signal conversion is done in order to improve the performance of the spectrum analyser by reducing unacceptable signal loss before the signal detection is done.

The obtained IF signal is amplified and sent to the envelope detector. The envelope detector is a circuit that converts the amplitude of the modulated signal (in this case the IF signal) to the envelope of the original (base band) signal. For the detected signal to be displayed in the frequency and time domain, the ramp generator is employed. The ramp generator is a circuit that drives the sweep generator of the local oscillator by creating a linear rising and falling output signal voltage with time. The detected signal is displaced on the screen of the spectrum analyser as bar indicating the frequency and power level of the signal. The configuration of a superheterodyne spectrum analyzer is shown in Figure 2.10.

The FFT spectrum Analyser on the other hand, samples one or several base band signals through sampler and converts the signal from analogue to digital format using the analogue to digital converter. Analysis of the obtained digital signal is done using a Fourier transformation before the resultant frequency and power level of the signal is displayed on the screen. The FFT spectrum analyser is more expensive and often more specialized than the superheterodyne spectrum analyzer. Figure 2.11 presents a simplified configuration of a FFT frequency spectrum analyzer.

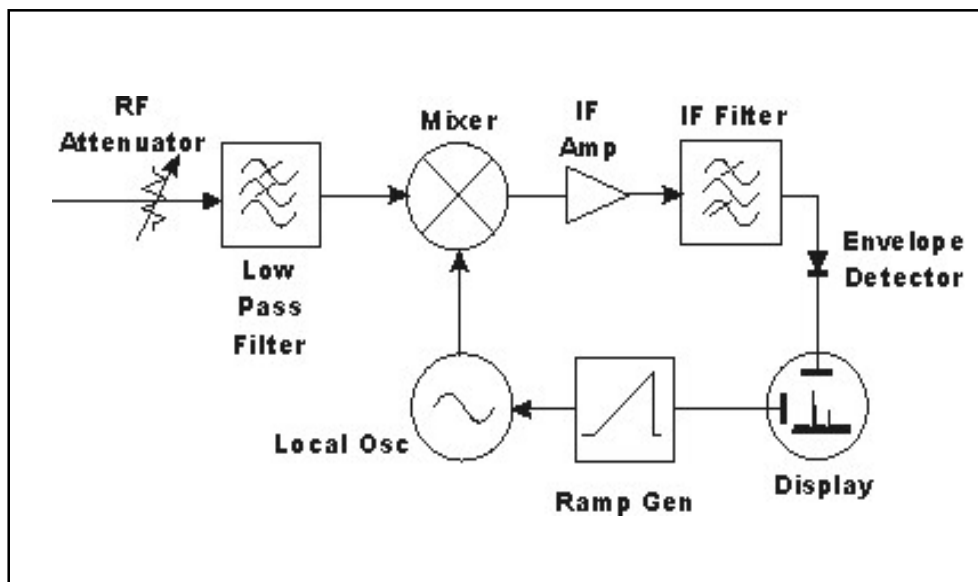


Figure 2.10: Block diagram showing the configuration of a Superheterodyne or swept frequency spectrum analyzer



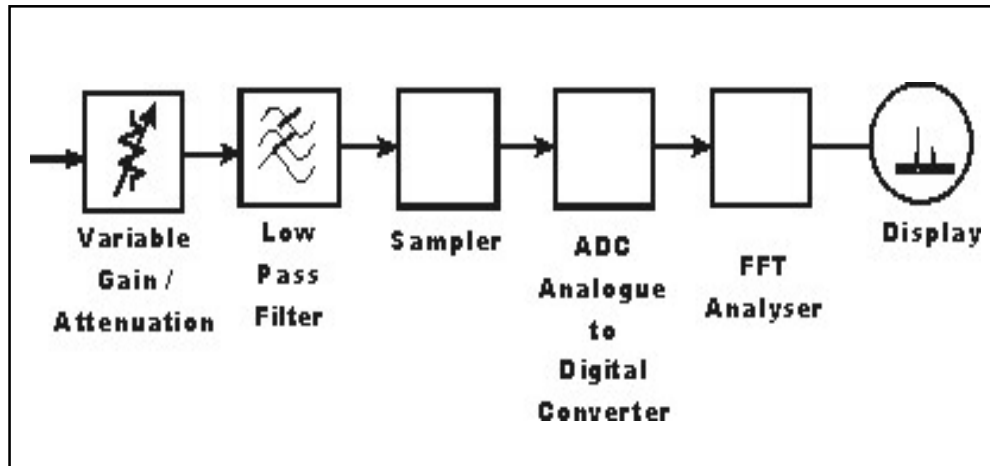


Figure 2.11: Block diagram showing the configuration of a FFT frequency spectrum analyzer

The superheterodyne spectrum analyzer is widely used because it can operate in a wide range of frequencies of many GHz, but can only detect signals in continuous wave mode of transmission. This is because superheterodyne spectrum analysers are slow in capturing the phase information of a given signal sweep.

The FFT spectrum analyzer alternatively, can capture a sample very quickly and then analyse it. Therefore, an FFT analyzer can capture short lived or one-shot phenomena in signal measurements. However, the FFT spectrum analyzer has a limited (narrower) frequency bandwidth, which is caused by the sampling rate of the analogue to digital converter in it.

There are different models of spectrum analysers used in various studies around the world. The Tektronix 2712 (9 kHz to 1.8GHz) (ARPANSA, 2000), the Narda SRM 3006 (9kHz to 6GHz)(Frei et al., 2010), the Agilent E4408B (9 KHz up to 26.5GHz) (Pérez-vega et al., 2008) and the Advantest R3131 by Rohde & Schwarz (Haumann et al., 2002) are few popular models of spectrum analysers around the world.

Some of these spectrum analysers are portable or handheld and can measure the magnitude of RF fields as well as comparing the measured quantity to various limits (maximum permissible exposures) on RF exposure. All spectrum analysers are accompanied by a probe or antenna that is capable of performing narrowband spectrum measurements. Antennas accompanying a spectrum analyser can either be a directional or an isotropic one. Both types of antennas during measurements are positioned at about 1.4 to 2.0m above the ground level (Ismail et al., 2010).

## **2.5 Features of RF Exposure Assessment**

Radiofrequency exposure assessments are aimed at estimating the maximum level of power density due to mobile communication signals in an environment. There are techniques and steps that are taken during RF measurements to obtain a data that can be used to draw meaningful conclusions during the analysis of the data. These steps are determined by some factors that are associated with location (study area), instrumentation, planning and logistics.

### **2.5.1 Study Areas**

The area or place where a RF exposure assessment is carried out can either be in an urban or rural area. An urban area is relatively congested with human population and many facilities like the BTS masts. With many BTS masts in urban areas, several measurements of power density are required to account for the level of RF exposure to the public. The use of a spectrum analyser is necessary to characterise the various sources of RF radiation in these areas. This type of assessment may require a method to cut the time spent on the field and also reduce the overhead cost of carrying out of a study.

In some studies of RF exposure around world, the study areas were first stratified and some relevant locations were selected to reduce time and cost. In Australia, this method was used to measure RF power density around GSM masts (ARPANSA, 2000). The study area was quite large and fourteensuitable spots were selected for measurements within two neighbourhoods at different statesof the country. A study in Spain by Perez-Vega et al (2008) was done in Santander metropolis with a broadband meter. Measurements in this study were made along the streets of the town in a car running at low speed, while to recording the RF exposure from BTS masts in the town (Pérez-vega et al., 2008).

The number of BTS masts and the mobile communication teledensity in some areas are the main reason why RF exposure assessments are carried out in them. In Nigeria, two LGAs in Rivers State were considered for RF exposure assessments because of the numerous masts and mobile phones in them than the other 21 LGAs (Biebuma and

Esekhaigbe, 2011). Specific locations where BTS masts are sited are also targeted in some studies (Okonigene and Yesufu, 2009).

### **2.5.2 Study sampling time or period**

The time taken to acquire RF exposure data in an area may be different for various studies. The idea of varying the time of exposure during measurements is as a result of the variation in the temperature response (thermal effect) of the human body to RF radiation. Radiofrequency radiation exposure to a human tissue will constantly increase the temperature of the tissue with time and 67% of the constant increase in temperature may occur at about 6 minutes which is referred to as the thermal time constant. Safety guidelines by most international organizations and scientific bodies are based on this concept of exposure time (ICNIRP, 1998).

Measurements are often based on 6 – 30 minutes time averages recommended by some international standards (Shurdi et al., 2010), while some studies make use of continuous data logging, where measurements were made for as long as 24 hours period (ARPANSA, 2000; Frei et al., 2009).

### **2.5.3 Exposure and Distance Relationship**

The importance of measurement distance from the source of RF radiation (usually an antenna) can be of great significance. Most antennas are installed on masts and are pointing in a given direction for precise signal coverage in an area. Radiofrequency workers may be exposed to the near field region of these antennas, but since this region is not always accessible it is rarely studied. To prevent occupational hazard during antenna maintenance, the IEEE (IEEE, 2002) proposes that a distance of 20 cm should be maintained in front of the active antennas. For far field radiation assessments, some studies have considered RF measurement from the foot of a BTS to a distance which sometimes range from 100 m – 1 km at different intervals of distance (Akpilile et al., 2014; Haumann et al., 2002; Mousa, 2011)

## 2.6 Variation of Power Density with Distance

Most GSM BTS antennas are directional antennas made up of a reflecting panel that contains arranged dipole antennas. They are mounted on a BTS mast at typically at 15 – 50 m above the ground, depending on the terrain and nearby structures. In practice, three of these antennas are mounted on a mast, each covering 120 degree sector around the mast to ensure azimuthal coverage. The antenna is slightly tilted (typically at  $5^\circ$  –  $10^\circ$ ) to allow the main beam hits the ground at 30 – 300 m from the foot of the mast within which we have the maximum RF intensity on the ground (Sambo et al., 2015). The distance of maximum power density on the ground, represents the region of worst-case scenario of exposure around a mast.

Because the antenna is always positioned on the mast at a considerable height from the ground, RF measurements taken at ground level or at a certain height (typical between 1.2 and 2.0 m) from ground level around the mast are within the far field region of the antenna. Radiofrequency measurements are made in clear view (line of sight (LOS)) of the antenna in the direction of measurement. The antenna is clearly visible without any physical obstruction to the RF measuring instrument.

Power densities at various distances from the BTS vary as the measurements are taken. This is mainly due to the radiation intensity from the antenna, which varies inversely with the square of the distance from the antenna. The height ( $H$ ), tilt angle ( $\psi$ ) and the vertical beam width ( $VBW$ ) of the antenna are also a contributing factor to this process. An illustration of a typical GSM mast in an environment is presented in Figure 2.12. The illustration of the changes in power density at different distances from the foot of a typical BTS up to 300 m, indicating the distance of maximum power density is presented in Figure 2.13.

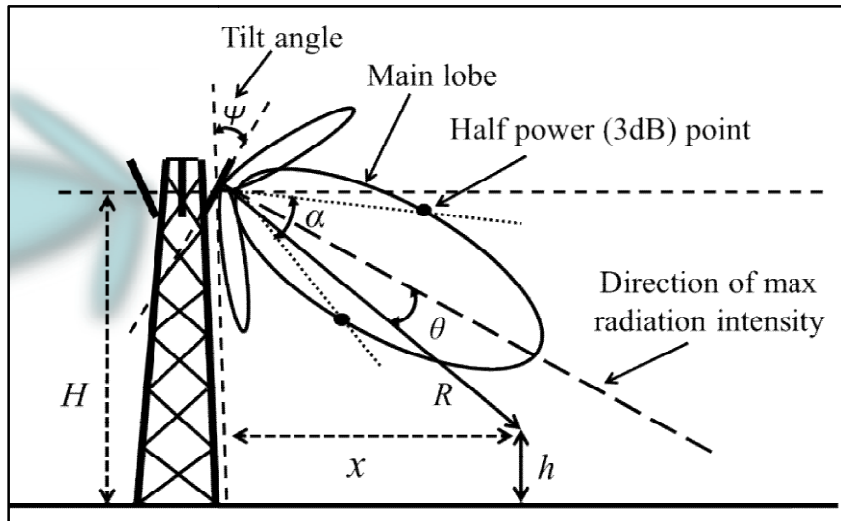


Figure 2.12: Radiation beam from a tilted antenna on a typical BTS mast(Balanis, 2005; Sambo et al., 2015)

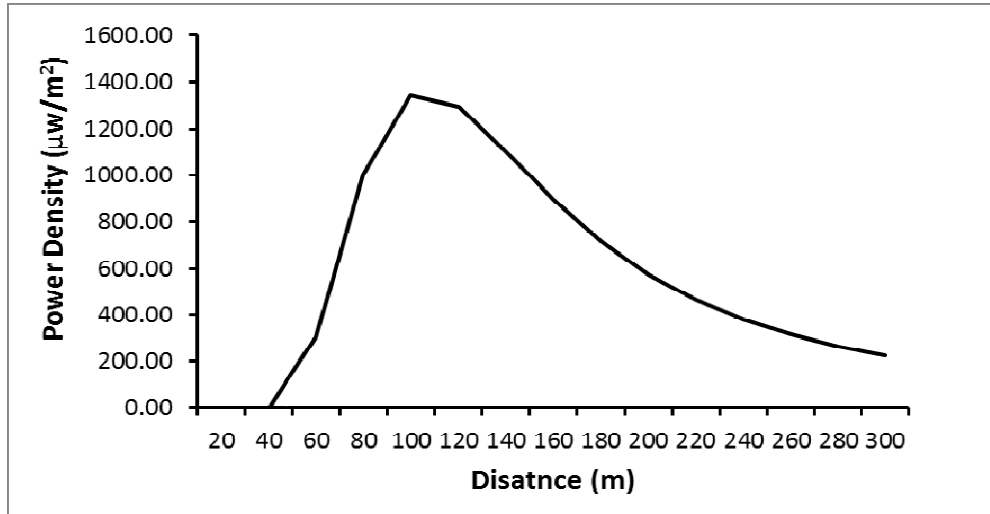


Figure 2.13: An illustration of the variation of power density with distance around a typical BTS mast (Linhares et al., 2013)

In figure 2.12,

$\alpha$  = vertical beam width (VBW)

$\theta$  = solid angle between a receiver's direction and the direction of maximum radiation intensity from the antenna.

$R$  = distance between the antenna and the receiver.

$x$  = distance between the foot of the measurement point.

$h$  = height of the RF meter from the ground level.

The power density at a point from a typical antenna with a gain and a power output ( $P_o$ ) can be generally obtained by (Milligan, 2005):

$$\mathbf{S} = \frac{P_o G}{4\pi R^2} \quad (2.13)$$

Due to the nature of the radiation pattern of an antenna, power density ( $\mathbf{S}$ ) below a BTS antenna is angular dependent (ITU, 2013). Therefore in the vertical plane ( $\theta$ ):

$$\mathbf{S}(\theta) = \frac{P_o G(\theta)}{4\pi R^2} \quad (2.14)$$

Radiation pattern ( $U$ ) of directional antennas can be modeled by (Kraus, 1988; Lo and Lee, 1993; Tai and Pereira, 1976) as,

$$U(\theta) = \cos^n(\theta) \quad (2.15)$$

Therefore, the power density at a point in a direction at a solid angle  $\theta$  to the centre of the antenna can be expressed as (Linhares et al., 2013),

$$\mathbf{S} = \frac{P_o G_{max}}{4\pi R^2} \cos^n \theta \quad (2.16)$$

$G_{max}$  = antenna maximum gain

$P_o G_{max}$  = the Equivalent Isotropically Radiated Power (EIRP)

$$n = \left( \frac{\log 0.5}{\log(\cos \frac{\alpha}{2})} \right) \quad (2.17)$$

The value of  $\cos^n \theta$  in Equation (2.15) is the normalized power or intensity of the radiation pattern of directional antennas at a point determined by  $\theta$ .



By considering the antenna and the measurement heights in Figure 2.12, Equation (2.15) can be modified as:

$$S = \frac{EIRP}{4\pi((H-h)^2+x^2)} \cos^n \theta \quad (2.18)$$

The equivalent power density of the RF waves can be calculated at various points around the BTS mast with Equation (2.18). With access to BTS antenna parameters in an area, the variation of power density against distance around a BTS mast can be modeled with Equation (2.18) as shown in Figure 2.13. The data on GSM BTS antenna parameters in Nigeria are not always readily available. Only hypothetical values of the antenna parameters can be generated from the various antenna manufacturers' data and existing literature.

## **2.7 Assessments of RF Exposure in Nigeria**

The assessment of RF radiation from wireless communication devices and its impact on human health have been in progress in many countries around the world for quite some time. Many studies have focused on environmental RF exposure assessments, epidemiological studies, animal/cellular studies and computational modelling (Cooper et al., 2004; Durney et al., 1986; Gandhi, 1974; Gandhi et al., 2012; Imaida et al., 1998; Islam et al., 2006; Mann and Roschke, 1996; Maskarinec et al., 1994; Samaras and Kuster, 2000; Yee, 1966). The study of RF radiation exposure in Nigeria became a popular area of research interest, few years after the introduction of GSM in 2001. Although the popularity of GSM has increased overtime, studies on RF radiation from GSM devices are not sufficient to establish RF exposure criteria in Nigeria, as has been done in some other countries.

RF exposure assessments in Nigeria are usually carried out to estimate GSM signal power density around BTS masts in each neighbourhood (Akintonwa et al., 2009; Farai et al., 2012). There are few known studies to have employed a spectrum analyzer in assessing the level of RF exposure around BTS in Nigeria (Okonigene and Yesufu, 2009). These studies neither considered other component RF signals within 900 – 2500 MHz frequency range, nor evaluate the contributions of GSM Band to the total RF spectrum in an environment. The dearth of studies on RF exposure around BTS has

resulted to the scarcity of data on spectral power density of various RF signals in our environment. Some of the few RF exposure assessments around BTS masts in Nigeria are presented in Table 2.1.

## **2.8 Biological Effect of RF Radiation Exposure**

All biological materials absorb part of the RF radiation that is incident on them. When RF radiation is absorbed by the human body, it is known to produce some effects which are categorised into thermal and non-thermal effects. Thermal effects are referred to as the responses of human body to a measurable rise in the temperature of a body that is exposed to RF radiation.

The production of heat in human body is as a result of time varying RF field which causes the drift of electrons, the polarisation of charges and the repositioning of electric dipoles in the body (ICNIRP, 1998). Heating effects of RF radiation in biological materials usually occur at frequencies between 10MHz – 300GHz. A temperature increase of about 2 °C can result to health hazards like heat exhaustion and stroke in humans (ACGIH, 1996).

When the human body responds to an incident RF radiation in a manner that its temperature is not increased, then the response is considered to be non-thermal in nature (Eger and Neppe, 2009; Hardell et al., 2005; Hyland, 2000). It is possible that RF radiations can interfere with processes related to DNA replication and repairs by subtly altering their molecular conformation, but does not have enough energy to break them apart (Hyland, 2003). Other non-thermal effects of RF radiation may be leukaemia, nervous tissue tumour, increased blood brain-barrier permeability, ocular impairment, stress associated change in immune system, reproductive change, changes in cell morphology and many more (ICNIRP, 1998; NRPB, 1992).

Table 2.1: Previous measurements of RF power density around some GSM masts in Nigeria

Author	Location	Distance to BTS	Maximum level of exposure	Instrument
(Akpolile et al., 2014)	Delta State	60 m – 360 m	5.66 $\mu\text{W}/\text{m}^2$	Broad band
(Isabona and Ojuh, 2015)	Benin city	0 m – 100m	1.20 $\text{mW}/\text{m}^2$	Broad band
(Oluwajobi et al., 2014)	Minna	100 m – 400 m	2.70 $\text{mW}/\text{m}^2$	Broad band
(Enyinna and Avwir, 2010)	Rivers State	2 m – 100 m	31.00 $\text{mW}/\text{m}^2$	Broad band
(Farai et al., 2012)	Ibadan	10 m – 200 m	53.40 $\text{mW}/\text{m}^2$	Broad band
(Ushie et al., 2013)	Lokoja	0 m – 125 m	1.73 $\text{mW}/\text{m}^2$	Broad band
(Akintonwa et al., 2009)	Lagos	0 m – 200 m	14.00 $\text{W}/\text{m}^2$	Broad band
(Ajetunmobi, 2014)	Ijebu Ode	0 m – 150 m	20.86 $\text{mW}/\text{m}^2$	Broad band
(Olorunfemi et al., 2016)	Ile-Ife	Not specified	1361 $\mu\text{W}/\text{m}^2$	Broad band/GIS
(Briggs-Kamara et al., 2018)	Port Harcourt	0 m – 100 m	4.90 $\mu\text{W}/\text{m}^2$	Broad band
(Ahaneku et al., 2015)	Nsukka	50 m – 300 m	0.19 $\text{mW}/\text{m}^2$	Spectrum analyzer
(Okonigene and Yesufu, 2009)	56 Towns	0 m – 1500 m	59.00 $\mu\text{W}/\text{m}^2$	Spectrum analyzer
(Umar et al., 2017)	Kaduna	20 m – 100 m	58.08 $\text{nW}/\text{m}^2$	Spectrum analyzer
(Aminu et al., 2014)	Kaduna	25 m – 200 m	31.00 $\mu\text{W}/\text{m}^2$	Spectrum analyzer

## **2.9 Limiting Human Exposure to RF Radiation**

There is a general concern for possible the health hazards which may be linked to RF radiation exposure due to the numerous BTS masts and mobile phone units around the world (Alenoghena et al., 2014; Hutter et al., 2006; Linhares et al., 2014; Wolf and Wolf, 2004). Several experimental and epidemiological studies on the effect of RF exposure on man and animal have been carried out over the years. Many of the scientific literatures and research papers from these studies were put together using internationally accepted criteria to setup RF exposure guidelines.

Various scientific bodies and organisation around the world organizations have established guidelines for the control occupational and public RF radiation exposures. These organisations publish and update safety recommendations which are meant to limit exposure levels that can result in thermal and sometimes non-thermal effects.

### **2.10 The ICNIRP RF Exposure Guideline**

The ICNIRP was established by the International Radiation Protection Association (IRPA) in 1992 as an independent organization, to examine the health risks in the use of the various types of non-ionizing radiation, develop an exposure guide and deal with all aspects of non-ionizing radiation protection.

The ICNIRP with the help of the IRPA and the environmental health division of the World Health Organization (WHO), made a document on health criteria related to NIR. This document consists of summaries of NIR characterisations, methods of NIR measurements in biological materials, various effects of NIR and the evaluation of health risks of NIR exposure (ICNIRP, 1998).

The main objective of the ICNIRP 1998 publication is to provide guidelines that will provide protect RF workers and the public against adverse effects of NIR. The ICNIRP guideline is based on scientific data alone. The data are gotten from epidemiological studies of cancer risk (NRPB, 1992), meta-analysis of reproductive outcomes (Shaw and Croen, 1993), residential cancer studies (Wertheimer and Leeper, 1979), Occupational studies (Savitz and Loomis, 1995), Cellular and animal studies and direct and indirect effects of electromagnetic fields (Bernhardt, 1988).

The numbers of published epidemiological research on the effect of RF radiation around the world are limited and inconclusive. It was established that both epidemiological studies and studies on human volunteers are fully in support of the health effects that are related to temperature increase in excess of 1°C, at the frequency range of 100 kHz–300 GHz in the human body tissue. The ICNIRP 1998 guideline protects mainly against thermal effects of various NIR in humans. The summary of the ICNIRP 1998 document is that, there are evidences from different studies that exposure of the whole body of humans to approximately 30 minutes of EMF and a SAR in the entire human body of less than 4 W/kg will increase the body temperature with about 1 °C. At SAR greater than 4 W/kg, this temperature increase will exceed of 1°C and can lead to an irreversible thermal damage to the human tissues.

These ICNIRP guidelines are classified into two categories, which are the basic restrictions and the reference levels. The basic restrictions were established directly from known health effects of NIR; while the reference levels were established to ascertain the compliance with basic restrictions during the practical assessment of NIR exposure. Generally, the ICNIRP reference levels are the main standard for limiting NIR exposure to humans. The reference and basic restriction levels for preventing occupational and public RF exposure hazard due to mobile communications are presented in Table 2.2 and 2.3, respectively.

Table 2.2: ICNIRP, 1998 reference levels for public and occupational RF exposure at frequencies ( $f$ ) between 400 MHz and 300 GHz

Frequency range	Electric field strength ( $\text{Vm}^{-1}$ )	Magnetic field strength ( $\text{Am}^{-1}$ )	Magnetic field ( $\mu\text{T}$ )	Equivalent plane wave power density ( $S_{\text{eq}}$ ) ( $\text{Wm}^{-2}$ )
Public exposure				
400 – 2000 MHz	$1.375f^{1/2}$	$0.0037f^{1/2}$	$0.0046f^{1/2}$	$f/200$
2 – 300 GHz	61	0.16	0.20	10
Occupational exposure				
400 – 2000 MHz	$3f^{1/2}$	$0.008f^{1/2}$	$0.01f^{1/2}$	$f/40$
2 – 300 GHz	137	0.36	0.45	50

Table 2.3: ICNIRP, 1998 basic restrictions for time varying electric and magnetic fields exposure at frequencies between 10 MHz to 10 GHz

Exposure characteristics	Frequency range	Current density for head and trunk (mA m <sup>-2</sup> ) (rms)	Whole body average SAR (Wkg <sup>-1</sup> )	Localized SAR (head and trunk) (Wkg <sup>-1</sup> )	Localized SAR (limbs) (Wkg <sup>-1</sup> )
Occupational exposure	10 MHz – 10 GHz	–	0.4	10	20
General exposure	10 MHz – 10 GHz	–	0.08	2	4

## 2.11 Brain Energy Absorption Model

An EM wave can propagate in both free space (vacuum) and in matter. When propagating in matter (solids, liquids or gas), it can lose part of the energy it carries as it propagates through them. A material, in which appreciable EM energy is absorbed, usually to produce heat, is referred to as a lossy material. The heat generated manifest by temperature rise in such materials. Most biological materials are lossy materials. In this section, the principles of EM propagation in free space and a lossy medium are discussed. A model to assess fraction of energy transmitted to and absorbed within the human brain tissue is obtained from existing principles and models of wave propagation in matter.

### 2.11.1 Uniform Plane Waves in Free Space

Electromagnetic waves are composed of  $\mathbf{E}$ (V/m) and  $\mathbf{H}$ (A/m), which are perpendicular to each other in space and to the direction of propagation. The response of different materials to EM waves can be studied by using the popular four Maxwell's equations, which in free space (air) are of the form,

$$\nabla \times \mathbf{H} = \epsilon_0 \frac{\partial \mathbf{E}}{\partial t} \quad (2.19)$$

$$\nabla \times \mathbf{E} = -\mu_0 \frac{\partial \mathbf{H}}{\partial t} \quad (2.20)$$

$$\nabla \cdot \mathbf{H} = 0 \quad (2.21)$$

$$\nabla \cdot \mathbf{E} = 0 \quad (2.22)$$

where  $\epsilon_0$  is permittivity of free space measured in farads per meter (F/m),  $\mu_0$  is the permeability of free space measured in Henry per meter (H/m).

These equations describe the spatial variation of  $\mathbf{E}$  and  $\mathbf{H}$  in a direction normal to their orientation. A wave can be described by the  $x$  component of  $\mathbf{E}$  and  $\mathbf{H}$ , when moving in the  $z$  orthogonal direction at time  $t$ . The time variation of the  $x$  component of  $\mathbf{E}$  and  $\mathbf{H}$  of this wave shows that it will move or propagate in space in  $z$  direction with the speed of light and this can be mathematically expressed as (Hayt and Buck, 2012),

$$\frac{\partial^2}{\partial z^2} = \frac{1}{\mu_0 \epsilon_0} \frac{\partial^2 E_x}{\partial t^2} \quad (2.23)$$

$$\frac{\partial^2}{\partial z^2} = \frac{1}{\mu_0 \epsilon_0} \frac{\partial^2 H_x}{\partial t^2} \quad (2.24)$$



Equations (2.23) and (2.24) can be transformed to Equation (2.25), by squaring both sides of the equations and reducing the similar terms. Equation (2.25) represents the propagation velocity of the wave in vacuum (air)

$$\frac{\partial z}{\partial t} = \frac{1}{\sqrt{\mu_0 \epsilon_0}} = 3 \times 10^8 \text{ m/s} \quad (2.25)$$

A general solution to Equations (2.23) and (2.24) depicts a forward and backward waves propagating in space (Ulaby et al., 1994). The solution can be translated into a real instantaneous sinusoidal function of a specified frequency in the form of a forward and backward propagating cosine waves (Hayt and Buck, 2012),

$$E(z, t) = |E_{x0}| \cos(\omega t - kz + \phi) + |E_{x0}| \cos(\omega t + kz + \phi) \quad (2.26)$$

where  $\phi$  is the reference phase,  $k$  is the propagation constant or wave number and  $\omega$  is the angular frequency.

$$k = \frac{\omega}{c} = \frac{2\pi}{\lambda} \text{ (rad/m)} \quad (2.27)$$

$$\omega = 2\pi f \text{ (rad/s)} \quad (2.28)$$

The frequency  $f$  is measured in cycle per seconds Hertz (Hz) and  $c$  is the speed of light measured in meters per seconds (m/s) and  $|E_{x0}|$  is the magnitude of the amplitude of  $\mathbf{E}$ .

A time-dependent sinusoidal wave of cosine form can be expressed in the phasor form. Expressing the wave function in its phasor form or phasor domain helps to suppress the time domain aspect of the function, thereby allowing a simpler way of solving the function. The phasor of a sinusoidal time-dependent wave function contains only the amplitude and phase information of the function. Equation (2.26) can be expressed in its phasor form as:

$$E(z, t) = \Re[|E_{x0}| e^{j(\pm kz + \phi)} e^{\pm j\omega t}] \quad (2.29)$$

where the symbol  $\Re$  represent the real part of the wave function and also,

$$j = \sqrt{-1} \quad (2.30)$$

$$|E_{x0}| e^{j\phi} = E_{x0} \quad (2.31)$$

Substituting Equation (2.31) in Equation (2.29), it can be modified as,

$$\mathbf{E}(z, t) = \Re[E_{x0} e^{j(\pm kz)} e^{\pm j\omega t}] \quad (2.32)$$

$$\mathbf{E}(z, t) = \Re[E_{sx} e^{\pm j\omega t}] \quad (2.33)$$

From Equation (2.33), the phasor form of the electric field component of the forward and backward wave is,

$$\mathbf{E}_s(z) = \hat{\mathbf{x}}E_{sx} = \hat{\mathbf{x}}E_{xo}e^{j(\pm kz)} \quad (2.34)$$

Where  $\mathbf{E}_s$  is the phasor electric field strength, while  $E_{sx}$  is the wave complex amplitude in  $x$  direction with a phase angle  $\phi$ .

### 2.11.2 Plane Wave Propagation in Lossy Materials

A dielectric material is a poor conductor of electricity, but a good agent of electrostatic processes. Dielectric materials respond to the passage of EM waves by producing polar charges within them. They can be classified into a low-loss, lossless, lossy or high-loss dielectric material. A lossless dielectric is a perfect dielectric material such as vacuum or air with no power loss when EM waves propagate through it. A lossy material absorbs power from the EM waves that propagates through it. A biological tissue such as the human tissue is a lossy material and hence, will absorb RF radiation passing through it.

A lossy material absorbs energy from the propagating wave, making the propagation constant of the wave to be complex in nature (Ulaby et al., 1994). For a linear, isotropic and homogeneous lossy medium the complex propagation constant  $\gamma$  can be expressed as,

$$\gamma = \alpha + j\beta \quad (2.35)$$

where,  $\alpha$  and  $\beta$  are given by

$$\alpha = \omega \left\{ \frac{\mu\epsilon'}{2} \left[ \sqrt{1 + \left(\frac{\epsilon''}{\epsilon'}\right)^2} - 1 \right] \right\}^{\frac{1}{2}} \quad (2.36)$$

$$\beta = \omega \left\{ \frac{\mu\epsilon'}{2} \left[ \sqrt{1 + \left(\frac{\epsilon''}{\epsilon'}\right)^2} + 1 \right] \right\}^{\frac{1}{2}} \quad (2.37)$$

where,  $\epsilon$ ,  $\mu$ ,  $\sigma$ ,  $\alpha$  and  $\beta$  are electric permittivity, magnetic permeability, conductivity, attenuation constant (Np/m) and phase constant (rad/m) of the medium, respectively.

The quantities  $\epsilon'$  and  $\epsilon''$  are real and imaginary part of complex permittivity  $\epsilon_c$  expressed as,

$$\epsilon_c = \epsilon' - j\epsilon'' \quad (2.38)$$

Where,

$$\varepsilon' = \varepsilon \quad (2.39)$$

$$\varepsilon'' = \frac{\sigma}{\omega} \quad (2.40)$$

The intrinsic impedance  $\eta_c$  of the lossy material is also complex and can be expressed as,

$$\eta_c = \sqrt{\frac{\mu}{\varepsilon_c}} = \sqrt{\frac{\mu}{\varepsilon'}} \left(1 - j \frac{\varepsilon''}{\varepsilon'}\right)^{-\frac{1}{2}} \quad (2.41)$$

### 2.11.3 Power Flow in Lossy Materials

An EM wave upon an aperture area  $A$  of a lossy material with an outward surface of unit vector  $\mathbf{n}$ , has a total power  $P$  flowing through  $A$  equal to,

$$P = \int_A \mathbf{S} \cdot \hat{\mathbf{n}} dA \quad (W) \quad (2.42)$$

Where  $\mathbf{S}$  represents the Poynting vector or power density ( $W/m^2$ ) expressed as,

$$\mathbf{S} = \mathbf{E} \times \mathbf{H} \quad (2.43)$$

The energy absorbed in a lossy medium can be expressed in terms of the average power density (Hayt and Buck, 2012). The average power density is generally expressed as,

$$\mathbf{S}_{av} = \frac{1}{2} \Re[\mathbf{E}_s \times \mathbf{H}_s^*] \quad (W/m^2) \quad (2.44)$$

The average power density of an EM wave moving in  $z$  direction, having an  $E$  component only along the  $x$  direction in free space can be expressed as,

$$\mathbf{S}_{av} = \hat{\mathbf{z}} \frac{|E_{xo}|^2}{2\eta} \quad (W/m^2) \quad (2.45)$$

For a lossy medium, the quantities  $\gamma$  and  $\eta_c$  are complex and this modifies Equation (2.45) as,

$$\mathbf{S}_{av} = \hat{\mathbf{z}} \frac{|E_{xo}|^2}{2|\eta_c|} e^{-2\alpha z} \cos\theta_\eta \quad (W/m^2) \quad (2.46)$$

The magnitude of complex intrinsic impedance  $\eta_c$  in polar form is,

$$\eta_c = |\eta_c| e^{j\theta_\eta} \quad (2.47)$$

where  $\theta_\eta$  is phase difference between  $\mathbf{E}$  and  $\mathbf{H}$  within the lossy material.

### 2.11.4 Plane Waves at the Boundary between Two Media

When an EM wave which incidents normally on the surface of a medium  $m_1$  passes through the medium encounters another medium  $m_2$ , the wave will be partly reflected and partly transmitted at the boundary between the two media. This is illustrated in Figure 2.14. The constitutive parameters of these media are the permittivity  $\epsilon$ , permeability  $\mu$ , conductivity  $\sigma$  and the intrinsic impedance  $\eta$ .

The incident wave is made up of both an electric field strength  $\mathbf{E}^i$  and magnetic field strength  $\mathbf{H}^i$ , moving along a unit vector  $\mathbf{k}^i$  in the positive  $z$  direction. When the incident wave reaches the boundary between  $m_1$  and  $m_2$ , part of the wave is reflected back into  $m_1$ . The remaining wave crosses the boundary into  $m_2$  and continues to move in the positive  $z$  direction. The reflected wave consists of  $\mathbf{E}^r$  and  $\mathbf{H}^r$ , moving along a unit vector  $\mathbf{k}^i$  in the negative  $z$  direction. The  $\mathbf{H}^r$  will undergo a 180 degree phase change after reflection. The transmitted wave consists of  $\mathbf{E}^t$  and  $\mathbf{H}^t$ , moving in the same direction as the incident wave.

The phasor form of the incident wave in  $m_1$  can be expressed as,

$$\mathbf{E}_s^i(z) = \hat{\mathbf{x}} E_{x0}^i e^{-jk_1 z} \quad (2.48)$$

$$\mathbf{H}_s^i(z) = \hat{\mathbf{z}} \times \frac{\mathbf{E}_s^i(z)}{\eta_1} = \hat{\mathbf{y}} \frac{1}{\eta_1} E_{x0}^i e^{-jk_1 z} \quad (2.49)$$

That of the reflected wave is,

$$\mathbf{E}_s^r(z) = \hat{\mathbf{x}} E_{x0}^i e^{+jk_1 z} \quad (2.50)$$

$$\mathbf{H}_s^r(z) = -\hat{\mathbf{z}} \times \frac{\mathbf{E}_s^r(z)}{\eta_1} = -\hat{\mathbf{y}} \frac{1}{\eta_1} E_{x0}^i e^{+jk_1 z} \quad (2.51)$$

The field component of the transmitted wave in  $m_2$  is,

$$\mathbf{E}_s^t(z) = \hat{\mathbf{x}} E_{x0}^i e^{-jk_2 z} \quad (2.52)$$

$$\mathbf{H}_s^t(z) = \hat{\mathbf{z}} \times \frac{\mathbf{E}_s^t(z)}{\eta_2} = \hat{\mathbf{y}} \frac{1}{\eta_2} E_{x0}^i e^{-jk_2 z} \quad (2.53)$$

$E_{x0}^i$ ,  $E_{x0}^r$  and  $E_{x0}^t$  are, the amplitude of the incident, reflected and transmitted electric field strengths at the boundary respectively, where  $z = 0$ . The relationship between these component fields can be obtained by enforcing the boundary conditions between  $m_1$  and  $m_2$ . The underlying boundary condition is that the tangential component of the total  $\mathbf{E}$  ( $\mathbf{E}_s^T$ ) and total magnetic field strength  $\mathbf{H}$  ( $\mathbf{H}_s^T$ ) is continuous across the boundary.

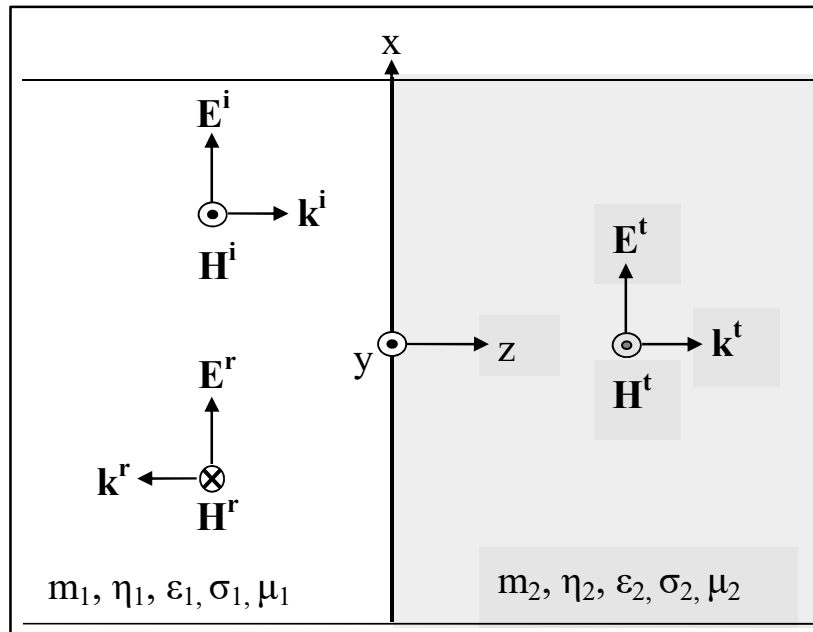


Figure 2.14: The process of reflection and transmission undergone by an incident wave between two media  $m_1$  and  $m_2$ (Ulaby et al., 1994)

The total  $\mathbf{E}$  and  $\mathbf{H}$  components in  $m_1$  is,

$$\mathbf{E}_s^{\mathbf{T}1}(z) = \mathbf{E}_s^i(z) + \mathbf{E}_s^r(z) = \hat{\mathbf{x}}(E_{x0}^i e^{-jk_1 z} + E_{x0}^r e^{+jk_1 z}) \quad (2.54)$$

$$\mathbf{H}_s^{\mathbf{T}1}(z) = \mathbf{H}_s^i(z) + \mathbf{H}_s^r(z) = \hat{\mathbf{y}} \frac{1}{\eta_1} (E_{x0}^i e^{-jk_1 z} - E_{x0}^r e^{+jk_1 z}) \quad (2.55)$$

The total  $\mathbf{E}$  and  $\mathbf{H}$  components in  $m_2$  is,

$$\mathbf{E}_s^{\mathbf{T}2}(z) = \mathbf{E}_s^t(z) = \hat{\mathbf{x}} E_{x0}^t e^{-jk_2 z} \quad (2.56)$$

$$\mathbf{H}_s^{\mathbf{T}2}(z) = \mathbf{H}_s^t(z) = \hat{\mathbf{y}} \frac{1}{\eta_2} E_{x0}^t e^{-jk_2 z} \quad (2.57)$$

At the boundary ( $z = 0$ ), if the tangential components are continuous, therefore,

$$\mathbf{E}_s^{\mathbf{T}1}(0) = \mathbf{E}_s^{\mathbf{T}2}(0) \quad (2.58)$$

$$\mathbf{H}_s^{\mathbf{T}1}(0) = \mathbf{H}_s^{\mathbf{T}2}(0) \quad (2.59)$$

From Equations (2.54) and (2.59),

$$E_{x0}^i + E_{x0}^r = E_{x0}^t \quad (2.60)$$

$$\frac{E_{x0}^i}{\eta_1} - \frac{E_{x0}^r}{\eta_1} = \frac{E_{x0}^t}{\eta_2} \quad (2.61)$$

Solving Equations (2.60) and (2.61) for  $E_{x0}^r$  and  $E_{x0}^t$  with respect to  $E_{x0}^i$ , then,

$$E_{x0}^r = \left( \frac{\eta_2 - \eta_1}{\eta_2 + \eta_1} \right) E_{x0}^i \quad (2.62)$$

$$E_{x0}^t = \left( \frac{2\eta_2}{\eta_2 + \eta_1} \right) E_{x0}^i \quad (2.63)$$

The ratio of incident and reflected  $\mathbf{E}$  at the boundary between  $m_1$  and  $m_2$  is referred to as the reflection coefficient ( $\Gamma$ ), while that of the transmitted and incident  $\mathbf{E}$  is the transmission coefficient ( $\tau$ ).  $\Gamma$  and  $\tau$  can be obtained from Equations (2.62) and (2.63) as,

$$\Gamma = \frac{E_{x0}^r}{E_{x0}^i} = \frac{\eta_2 - \eta_1}{\eta_2 + \eta_1} \quad (2.64)$$

$$\tau = \frac{E_{x0}^t}{E_{x0}^i} = \frac{2\eta_2}{\eta_2 + \eta_1} \quad (2.65)$$

Therefore,

$$E_{x0}^r = \Gamma E_{x0}^i \quad (2.66)$$

$$E_{x0}^t = \tau E_{x0}^i \quad (2.67)$$

Where,

$$\tau = 1 + \Gamma \quad (2.68)$$

In a lossy medium the propagation constant  $k_1$  and  $k_2$  is  $\gamma_1$  and  $\gamma_2$  respectively, while  $\eta_1$  and  $\eta_2$  are the complex intrinsic impedance  $\eta_{c1}$  and  $\eta_{c2}$ .

The average incident, reflected and transmitted power at the boundary between two lossy media, will obey the law of conservation of power i.e.,

$$\mathbf{S}_{av}^i = \mathbf{S}_{av}^r + \mathbf{S}_{av}^t \quad (2.69)$$

$\mathbf{S}_{av}^i$  is the incident average power density and  $\mathbf{S}_{av}^r$  is the reflected average power density in the first medium.  $\mathbf{S}_{av}^t$  is the transmitted average power density in the second medium where,

$$\mathbf{S}_{av}^i = \frac{|E_{x0}^i|^2}{2\eta_{c1}} e^{-2\alpha z} \cos\theta_\eta \quad (2.70)$$

$$\mathbf{S}_{av}^r = |\Gamma|^2 \mathbf{S}_{av}^i \quad (2.71)$$

$$\mathbf{S}_{av}^t = |\tau|^2 \mathbf{S}_{av}^i \quad (2.72)$$

Therefore,

$$|\tau|^2 = 1 - |\Gamma|^2 \quad (2.73)$$

$|\tau|^2$  is the ratio of  $\mathbf{S}_{av}^t$  to  $\mathbf{S}_{av}^i$  referred to as Transmittance ( $T$ ), while  $|\Gamma|^2$  is the ratio of  $\mathbf{S}_{av}^r$  to  $\mathbf{S}_{av}^i$ , Referred to as reflectance ( $R$ ).

### 2.11.5 EM Waves Transmission in Human Head Tissues

The human head consists of mainly six thin layers of tissues. These tissues illustrated in Figure 2.15, include the Skin, Fat, Bone, Dura, cerebro-spinal fluid (CSF) and the brain. Each tissue absorbs EM waves according to its electric and magnetic properties. Across each boundary, there are multiple reflections which progressively reduce the amplitude of the waves. To study the interaction of EM wave with each layer of tissue, the planar multi-layered model of the human head was developed (Abdalla and Teoh, 2005).

The multi-layered model of human head approximates the head tissues to a flat multi-layered arrangement of different thicknesses  $z_1$  to  $z_5$  and absorption coefficients  $\alpha_1$  to  $\alpha_5$ . As illustrated in Figure 2.16, there exist the boundaries  $b_1 - b_5$  between the tissues and the thicknesses  $z_1$  to  $z_5$  in the model. The conductivity  $\sigma$ , mass density  $\rho$  and the relative permittivity  $\epsilon_r$  of each of these tissues are given in Table 2.4 (Gretel et al., 2006; ITIS, 2016; Sabbah et al., 2011). The approximate value of relative permeability  $\mu_r$  of the human tissue is 1.

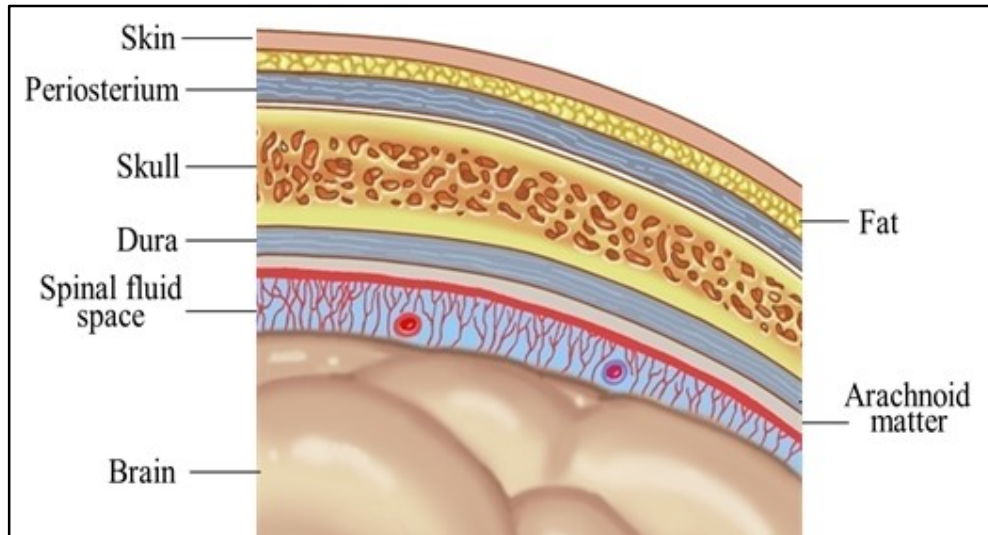


Figure 2.15: The layers of the human head (Earsite, 2015).



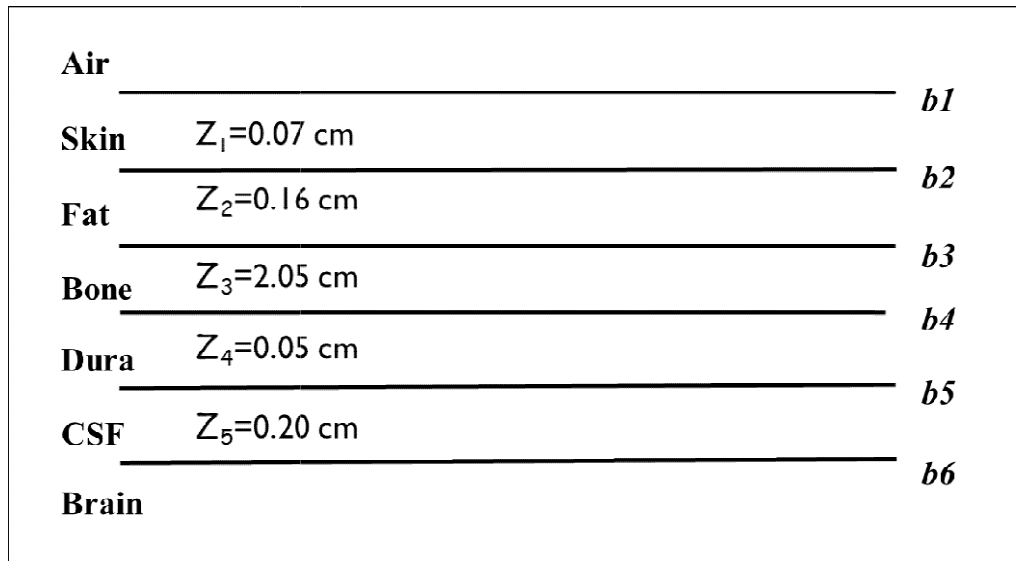


Figure 2.16: A six-tissue multi-layered planar model of the human head

Table 2.4: The dielectric parameters of the layers of the head tissues at 900 MHz, 1800 MHz and 2100 MHz (Gretel et al., 2006; ITIS, 2016; Sabbah et al., 2011).

Tissue	900 MHz		1800 MHz		2100 MHz		$\rho$ (kg/m <sup>3</sup> )
	$\epsilon_r$	$\sigma$ (S/m)	$\epsilon_r$	$\sigma$ (S/m)	$\epsilon_r$	$\sigma$ (S/m)	
Skin	41.400	0.867	38.900	1.180	38.400	1.310	1109
Fat	5.460	0.051	5.350	0.078	5.320	0.090	911
Bone	12.450	0.140	11.800	0.275	11.600	0.328	1908
Dura	44.400	0.961	42.900	1.320	42.500	1.470	1174
CSF	68.700	2.410	67.200	2.920	66.800	3.150	1007
Brain	52.700	0.940	50.100	1.390	49.500	1.570	1045

### 2.11.6 EM Wave Transmission across each Boundary

A normally incident EM wave with an average power density  $\mathbf{S}_o$ , will interact with the first boundary ( $b_1$ ) of the head tissues and part of the incident power will be transmitted across this boundary, while the rest is reflected in a back into the air (Abdulrazzaq and Aziz, 2013). The average power density across  $b_1$  can be expressed as,

$$\mathbf{S}_1 = \mathbf{S}_o |\tau_1|^2 \quad (2.74)$$

$|\tau_1|^2$ , is the transmittance ( $T$ ) at the first boundary ( $b_1$ ) and refers to the fraction of incident power density across  $b_1$  between the air and the skin. Both the transmittance ( $T$ ) and the reflectance ( $R$ ) can be obtained from Equations (2.64), (2.65) and (2.68). For the various boundaries between the tissues above the brain, their transmittance and reflectance are expressed as  $T_1 - T_5$  and  $R_1 - R_5$ .

Part of the power across  $b_1$  is absorbed by the skin tissue and the remaining part on getting to  $b_2$  is partially reflected and back propagates towards  $b_1$ . The back propagating wave will again be absorbed by the skin and the rest will undergo a partial reflection on getting to  $b_1$ . The total power across  $b_2$  is the sum of the direct and the partially reflected powers from  $b_1$ , after part of them have been absorbed by the skin. Some of the power across  $b_2$  will be absorbed within the fat. The rest of the power on getting to  $b_3$  will be reflected back to  $b_2$ . The reflected power undergoes a partial reflection at  $b_2$  and forward propagates towards  $b_3$ , where some of it crosses into the bone. The total power across  $b_3$  is the sum of the direct and the partially reflected powers from  $b_2$ , after part of them have been absorbed by the fat.

This process will continue until the wave signal gets to  $b_6$ , as illustrated in Figure 2.17. The total power density across  $b_2$  can be expressed as,

$$\mathbf{S}_{av}^o T_1 T_2 e^{2\alpha_1 z_1} + \mathbf{S}_{av}^o T_1 T_2 R_1 R_2 e^{4\alpha_1 z_1} \quad (2.75)$$

$$\mathbf{S}_{av}^o [T_1 T_2 e^{2\alpha_1 z_1} (1 + R_1 R_2 e^{2\alpha_1 z_1})] \quad (2.76)$$

Where,

$$T_1 T_2 e^{2\alpha_1 z_1} (1 + R_1 R_2 e^{2\alpha_1 z_1}) = F_2 \quad (2.77)$$

$F_2$  = fraction of the incident average power density ( $\mathbf{S}_{av}^o$ ) across  $b_2$

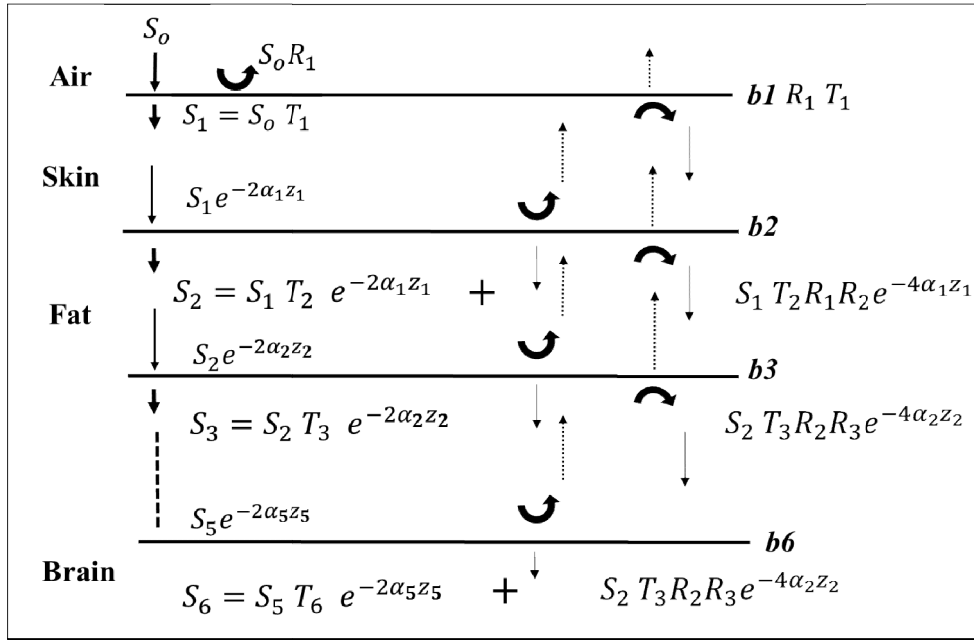


Figure 2.17: The process of wave transmission and reflection across the head tissues

The total power density across  $b_3$  is expressed as,

$$\mathbf{S}_{av}^o [F_2 T_3 e^{2\alpha_2 z_2} (1 + R_2 R_3 e^{2\alpha_2 z_2})] \quad (2.78)$$

Where,

$$F_2 T_3 e^{2\alpha_2 z_2} (1 + R_2 R_3 e^{2\alpha_2 z_2}) = F_3 \quad (2.79)$$

Across  $b_4$  (total power density at the Dura),

$$\mathbf{S}_{av}^o [F_3 T_4 e^{2\alpha_3 z_3} (1 + R_3 R_4 e^{2\alpha_3 z_3})] \quad (2.80)$$

Where,

$$F_3 T_4 e^{2\alpha_3 z_3} (1 + R_3 R_4 e^{2\alpha_3 z_3}) = F_4 \quad (2.81)$$

Across  $b_5$  (total power density at the CSF),

$$\mathbf{S}_{av}^o [F_4 T_5 e^{2\alpha_4 z_4} (1 + R_4 R_5 e^{2\alpha_4 z_4})] \quad (2.82)$$

Where,

$$F_4 T_5 e^{2\alpha_4 z_4} (1 + R_4 R_5 e^{2\alpha_4 z_4}) = F_5 \quad (2.83)$$

Across  $b_6$  (power density at the Brain),

$$\mathbf{S}_{av}^o [F_5 T_6 e^{2\alpha_5 z_5} (1 + R_5 R_6 e^{2\alpha_5 z_5})] \quad (2.84)$$

Where,

$$F_5 T_6 e^{2\alpha_5 z_5} (1 + R_5 R_6 e^{2\alpha_5 z_5}) = F_6 \quad (2.85)$$

$F_1$  to  $F_6$  are the fraction of the average incident power density ( $\mathbf{S}_{av}^o$ ), at the different instances when the transmitted power crosses  $b_1$  to  $b_6$ .

A steady state is reached across  $b_6$ , where the net power transmission across each boundary and the fraction of incident power density in each tissue are constant. At the steady-state transmission of the propagating waves, many co-propagating waves produce the effect of a single wave at definite amplitude and phase (Hayt and Buck, 2012). The net average power density across the various boundaries at the steady state is determined by the net power density across the last boundary ( $b_6$ ). This is because the total power across  $b_6$  is the remaining part of total power that is transmitted across  $b_1$ . The total power across  $b_1$  is the sum of the direct power across  $b_1$  and total reflected power at  $b_1$  the due to multiple reflections from all the other boundaries ( $b_2$  to  $b_6$ ).

If the fraction of the incident power density across  $b_6$  is  $F_6(F_{Brain})$ , the overall fraction of the incident power density in each tissues is presented in Equations (2.86) to (2.91).

$$F_{Skin} = \frac{F_6}{T_2 T_3 T_4 T_5 T_6 e^{-2(\alpha_1 z_1 + \alpha_2 z_2 + \alpha_3 z_3 + \alpha_4 z_4 + \alpha_5 z_5)}} \quad (2.86)$$

$$F_{Fat} = \frac{F_6}{T_3 T_4 T_5 T_6 e^{-2(\alpha_2 z_2 + \alpha_3 z_3 + \alpha_4 z_4 + \alpha_5 z_5)}} \quad (2.87)$$

$$F_{Bone} = \frac{F_6}{T_4 T_5 T_6 e^{-2(\alpha_3 z_3 + \alpha_4 z_4 + \alpha_5 z_5)}} \quad (2.88)$$

$$F_{Dura} = \frac{F_6}{T_5 T_6 e^{-2(\alpha_4 z_4 + \alpha_5 z_5)}} \quad (2.89)$$

$$F_{CSF} = \frac{F_6}{T_6 e^{-2(\alpha_5 z_5)}} \quad (2.90)$$

$$F_{Brain} = F_6 \quad (2.91)$$

where,  $F_{Skin}$  to  $F_{CSF}$  are the net fractions of  $\mathbf{S}_{av}^o$  in the tissue, when there is a net power transmission across b6. The use of Equations (2.86) to (2.91) in the calculation of the fraction power density of a RF radiation reaching brain will be discussed in chapter three.

## **CHAPTER THREE**

### **MATERIALS AND METHODS**

#### **3.1 Study Areas**

The cities of Lagos, Ibadan and Abuja were purposely selected for this study because they are renowned cities in Nigeria with considerable size of mobile communication facilities (NBS, 2018; NPC, 2006).

##### **3.1.1 Lagos**

Lagos is a mega city that is made up of many districts and local government areas (LGA), which constitute over 80 percent of the land mass of Lagos state. The city is located at latitude 6.4550°N and longitude 3.3841°E of Nigeria. There are about 20 local government areas (LGA) in Lagos state and the city hosts about 9.1 million people with about 2.2 million households (NPC, 2006). Most developed part of Lagos is often referred to as the Metropolitan Lagos. These areas include both the islands of the former municipality of Lagos and the mainland suburbs. The metropolitan Lagos encompasses about 16 of the 20 LGA of Lagos State. The metropolitan part of Lagos contains about 85% of the whole population of Lagos (Olowu, 1992; Rasaki, 1988). There are a considerable number of tall buildings in Lagos comparable to some cities in the world. Lagos has one of the largest and most extensive network of roads in West Africa (Mason-Jones and Cohen, 2012).

The city of Lagos is one of the hubs of Information Communications and Technology (ICT) in the West Africa (Zeng, 2008). There are 19 million active GSM voice lines in Lagos state (NBS, 2018). This study was carried out within 10 LGA in the state, hosting about 48 percent of active line in the state. A map of Lagos showing 120 points where RF measurements were made is presented in Figure 3.1.

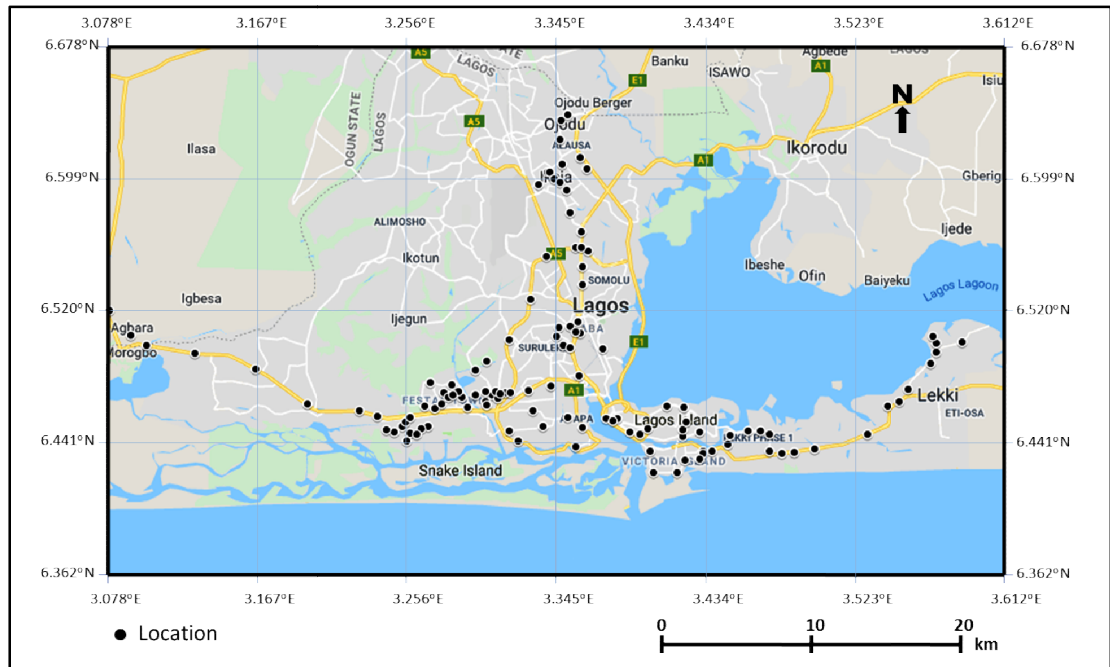


Figure 3.1: A map of the city of Lagos showing measurement positions (Base map from Google map, 2019)



### **3.1.2 Ibadan**

Ibadan is the capital city of Oyo state in Nigeria, is located at latitude 7.3964°N and longitude 3.9167°E of the country. The city of Ibadan is in the south-western region of Nigeria, 128 km inland northeast of Lagos and 530 km southwest of Abuja. The city is a major link transit between the coastal region and the areas to the north. The core areas of Ibadan are within 6 LGA of Oyo state (Tomori, 2007). The city holds about 3 million people and a 0.4 million households. The city of Ibadan is the third largest metropolitan region by population, in Nigeria (NPC, 2006).

Ibadan since the era of the Western Region government in Nigeria has possessed a number of sophisticated, liberal, scientific and cultural community on the continent of Africa. The city has one of the best road networks in Nigeria and hosts quite a number of financial institutions in the country. There are about 8 million GSM active lines in Oyo state (NBS, 2018) and Ibadan hosts 60 percent of the active lines in the state (edirectsms, 2016). A map of the Ibadan showing 100 points where RF measurements were made is presented in Figure 3.2.

### **3.1.3 Abuja**

The Federal Capital Territory (FCT) and some of its surrounding areas are referred to as Abuja. The city of Abuja is located at latitude 9.0667°N and longitude 7.4833°E of Nigeria. There are 6 LGA in the FCT holding about 1.4 million people with about 0.3 million households (NPC, 2006). It was reported by United Nations that Abuja grew at the rate of 139.7% between 2000 and 2010, making it one of the fastest growing cities in the world (Boumphrey 2010). The city by 2015 still grew annually by 35%, which makes it the fastest growing city in Africa (Abuja fact, 2005). The road network in Abuja is wider and better than most other cities in Nigeria.

The main district of Abuja houses the top bracket sections of society and business ventures. The city has the reputation of being very exclusive and expensive. This study was carried out within 3 local government areas of Abuja, which covers the municipal area of the city. There are about 5 million active GSM lines in the FCT and Abuja hosts about 56 percent of its active lines (edirectsms, 2016). A map of the Abuja showing 80 points where RF measurements were made is presented in Figure 3.3.

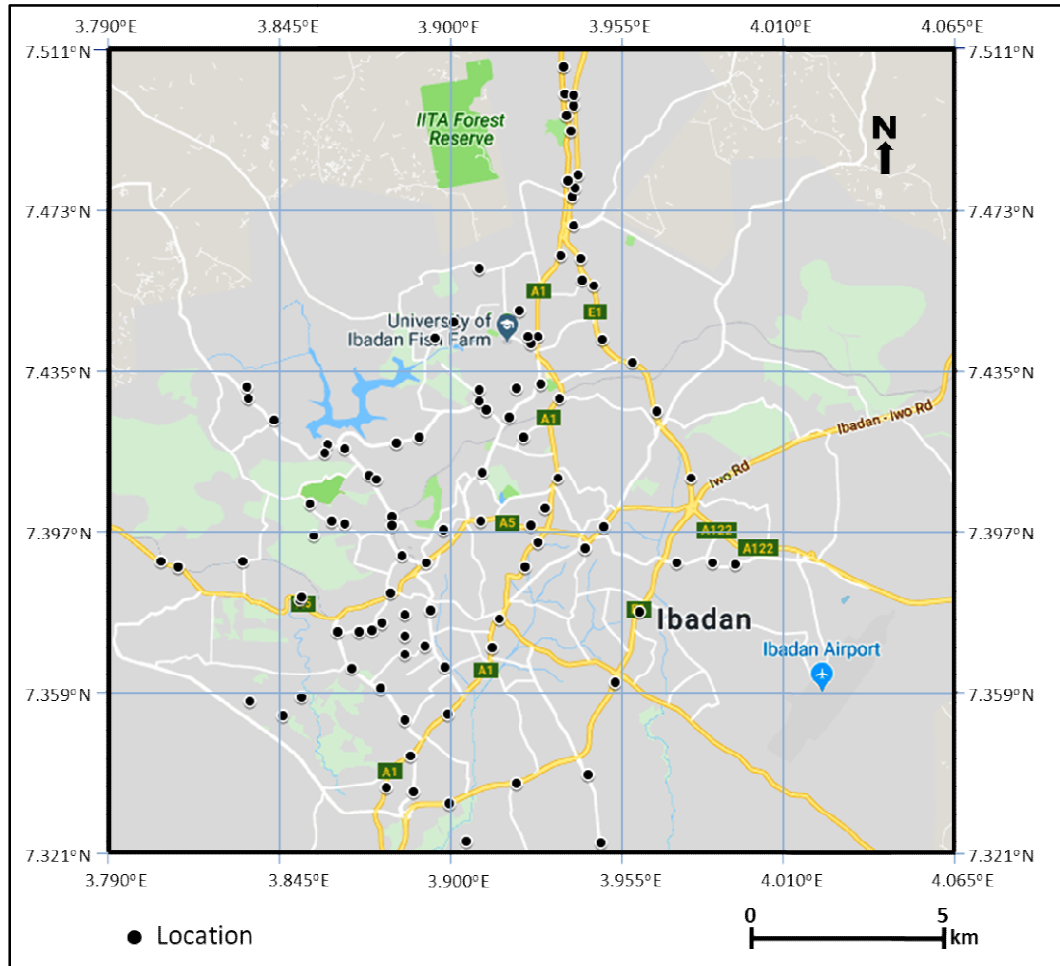


Figure 3.2: A map of the city of Ibadan showing measurement positions (Base map from Google map, 2019)

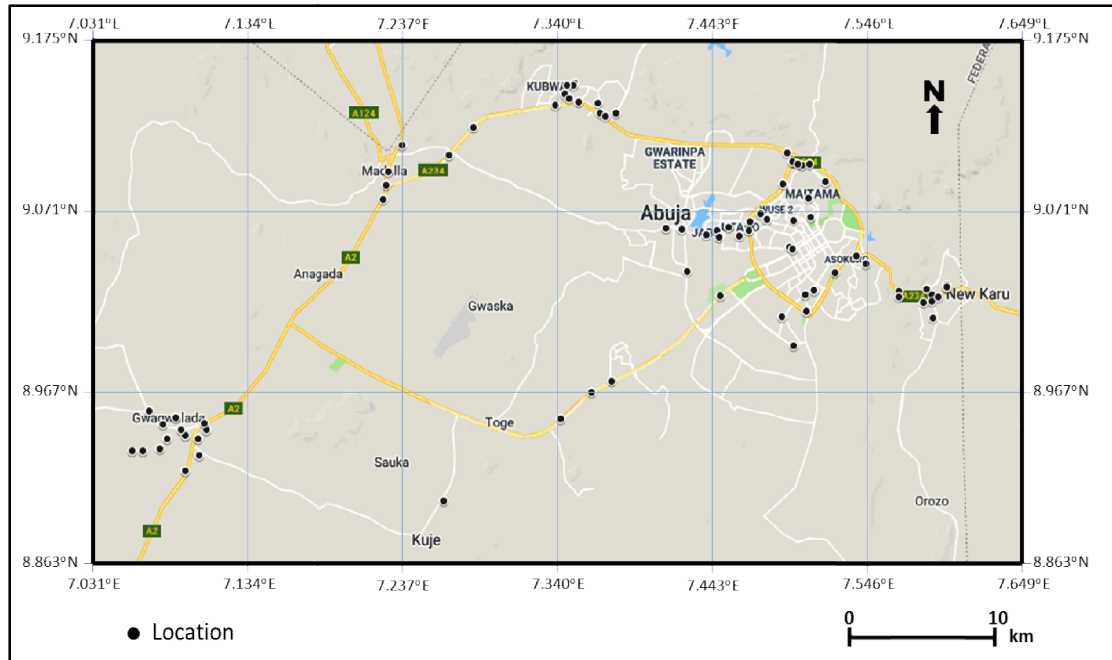


Figure 3.3: An Aerial map of the city of Abuja showing measurement positions (Base map from Google map, 2019)

## 3.2 Instrumentation

Measurements of RF radiation energy around some selected BTS masts and mobile phones were made with a calibrated spectrum analyzer and a broadband meter in the cities of Lagos, Ibadan and Abuja. A Global Positioning System (GPS) was also employed during the study to locate the positions of each measurement point. The specifications and characteristics of these RF meters are discussed in this section.

### 3.2.1 The Spectrum Analyser

The spectrum analyser employed in this study is a hand held type, called SPECTRAN HF - 60105V4 by Aaronia AG which has been factory calibrated for RF spectral analyses within the frequency range from 1 MHz to 9.4 GHz. The sensitivity of the spectrum analyser to RF signals is between  $-170$  dB and  $+20$  dB power levels and a frequency resolution of 200 kHz – 50 MHz. The instrument is coupled with a factory calibrated Omnilog-90200 tri-axial antenna to receive RF radiation from the environment in all directions. A picture of SPECTRAN HF - 60105V4 hand held spectrum analyser coupled with the antenna is presented in Figure 3.4. This antenna detects RF signal within the range from 700 – 2.5 GHz. Also accompanying the spectrum analyser is a computer interface where a computer with a pre-installed Aaronia RF analyses software programme is connected for on-field and post-field data analyses.

Measurements of  $\mathbf{E}$  (V/m),  $\mathbf{H}$  (A/m), signal strength (dBm) and  $\mathbf{S}$  ( $\text{W}/\text{m}^2$ ) can be taken separately or simultaneously by the spectrum analyser. By default, the spectrum analyser measures received signal strength in dBm unit and automatically convert it to  $\mathbf{E}$  and  $\mathbf{H}$ . During RF measurements around the BTS masts, the spectrum analyser was mounted on a tripod stand, which is about 1.5 m tall from the ground level. The spectrum analyser was set to record the peak values of power density during each measurement. When RF measurements were made around the mobile phones, the spectrum analyser was also set to record the peak values of  $\mathbf{E}$  during and the meter was placed within the near field region of the mobile phones.



Figure 3.4: An Aaronia SPECTRAN HF - 60105V4 spectrum analyser coupled with an Omnilog-90200 isotropic antenna manufactured by Aaronia AG

### **3.2.2 The Broadband Meter**

The broadband meter employed in this study is a factory calibrated TES-92 Electromog survey meter, manufactured by Less EMF, NY USA. This meter was designed to sum up or integrate the energies of all RF signals within the frequency range of 50 – 3500MHz. The TES-92 Electromog meter has an inbuilt isotropic antenna, but can also determine **E** or **H** in a spot along any chosen coordinate. A picture of TES-92 Electromog survey meter is presented in Figure 3.5. In this study, the broadband meter was positioned at about 1.2 m above the ground level at a spot where measurements of power density were made. The meter was also used to measure the total **E** in the near field of the selected mobile phones in this study.

### **3.3 Estimation of distance of maximum power density**

As discussed in chapter 2, the variation of power density with distance from a mast depends on factors such as the height of the antenna and its angle of tilt. These will vary from mast to mast and hence the distribution of power density with distance. From the foot of each, the point of maximum radiation intensity was determined from mast. For a survey aimed at health hazard assessment as in the case of this work, the point of maximum power density represents the point of worst-case scenario around a mast and hence, the point of interest around the masts.

To determine the distance of maximum power density from BTS masts in the cities of Lagos, Ibadan and Abuja, a preliminary study was conducted. In this study, the variation of power density of GSM signals versus distance was determined from the spectral measurements around 40 randomly selected BTS masts in the cities of Lagos, Ibadan and Abuja. The distance of maximum power density within the foot of each mast and a distance of 300 m from the masts was obtained from the profile of power density with distance. The average distance of maximum power density for each city was determined.



Figure 3.5: A TES 92 Electromog broadband survey meter manufactured by Less EMF, NY USA

### **3.3.1 Distance of maximum power density in the three cities**

The typical variation of power density of a GSM signals (mainly GSM 900 and GSM 1800 signal) with distance from the foot of BTS masts up to 300 m in Ibadan, Lagos and Abuja is presented in Figure 3.6. The obtained average distance of maximum power density of GSM signals around BTS masts is  $183 \pm 58$  m,  $195 \pm 19$  m, and  $190 \pm 63$  m in Lagos, Ibadan and Abuja, respectively. The distribution of the distances of maximum power density in the three cities is presented in Figures 3.7. The weighted mean distance of maximum power density for the three cities was  $189 \pm 50$  m.

### **3.4 Assessment of all signals within 900 and 2500 MHz RF band**

Measurements of power density of all signals including GSM, CDMA-1900, 3G-2100 and other signals within 900 to 2500 MHz band made the calibrated spectrum analyser and broad band meter around the estimated distances of maximum power density from 100, 120, and 80 BTS masts in Ibadan, Lagos and Abuja, respectively. Efforts were made to align each point of measurement with the Line of Sight (LOS) of the antenna from the foot of each mast.

The prominent signals obtained within the acquired spectrum around each mast, were identified from data book on national frequency allocation (8.3 KHz to 300 GHz) by the national frequency management council of the federal republic of Nigeria (NFMC, 2014). The power density of each signal was obtained at each point in order to estimate its contribution to the environment. An individual is exposed to RF radiations typically between 50 MHz to 3.5 GHz in each environment. This constitutes the radiation dose each person is exposed to due signals from various RF sources including BTS and satellite signals. The sum of power density of all signals from 50 MHz to 3.5 GHz around the selected BTS masts in each city was obtained with the broadband meter. RF signals within this broad band encompass all signals used in most applications in Nigeria. These include radio, TV and RADAR applications, most (or some) of which were not in NCC data book. This RF range can thus be regarded as the range of ambient RF radiation in each neighbourhood.



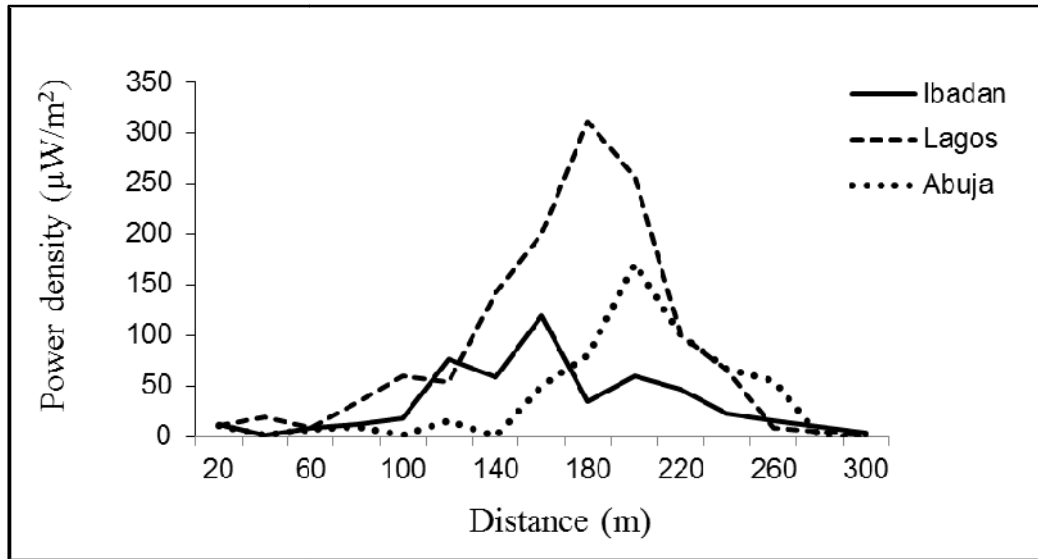


Figure 3.6: Variation of power density of a GSM 1800 signals with distance around typical BTS masts in Lagos, Ibadan and Abuja

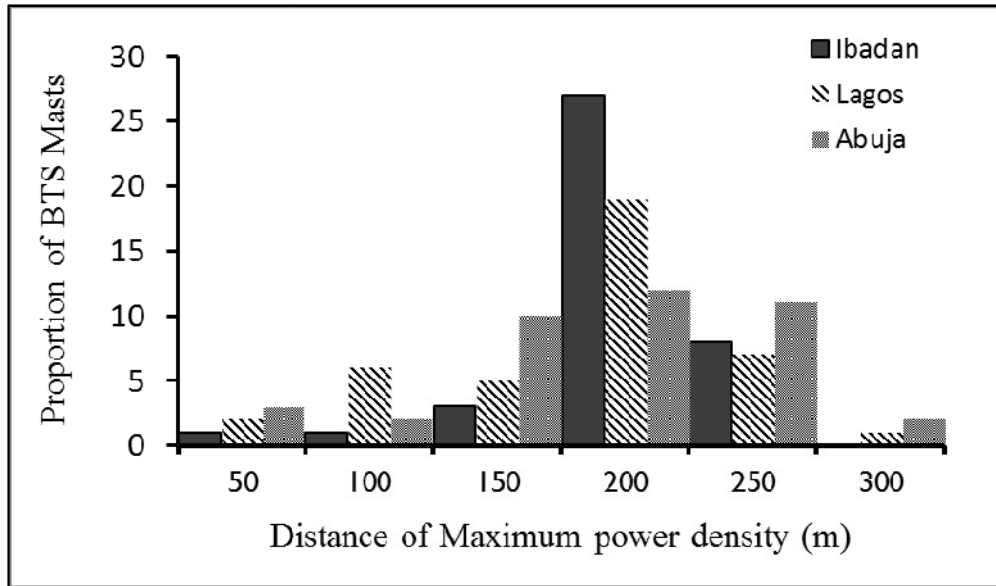


Figure 3.7: Distribution of the distances of maximum power density in Lagos, Ibadan and Abuja

As stated in chapter two, GSM 900 and GSM 1800 signals occupying 935 – 1880 MHz frequency band, CDMA-1900 and 3G-2100 occupying 1883 – 2150 MHz band are from BTS masts in each environment. The total power densities of these signals, as well as other signals that were not from BTS masts within the obtained spectrum at each spot were estimated. The percentage contributions of these signals to the ambient RF radiation at each spot were calculated. Precautions were taken not allow human interference with the receiving antennas of the two RF instruments. An average of 3 minutes was allowed for the instrument to stabilise before readings were taken.

### **3.5 RF Exposure Measurements around Mobile Phones**

As stated in chapter two, the maximum level of power radiated by a mobile phone is within the near field region of its antenna and for a typical mobile phone near field region is less than 3 cm from the phone. To estimate the level of RF radiation emitted from mobile phones, electric field measurements were made with both the spectrum analyser and the broadband meter at a distance less than 1 cm from 60 common mobile phones in Nigeria. Out of the selected mobile phones, 30 of them work mainly on GSM standard during an active call, while the other 30 phones work on the 3G-2100 mobile standard. The selected mobile phones are presented in Table 3.1.

During measurement, each phone was put in the active mode by calling and answering a call on it. The mobile phones were firmly attached to a tripod stand at 1.5 m above the ground level, while background measurements of  $E$  were taken with the broadband meter when no calls were either made or received from them. The 1.5 m height of the RF meter is close the region of the head of a reference man whose height is 1.7 m. Measurements of  $E$  were then made in near field region (about 10 mm) of the selected mobile phones when they were actively making and receiving a call. The difference between the results of background broadband measurements and other measurements when the phones were active was taken to represent the value of the  $E$  from the phones in the active call mode.

Table 3.1: Models and communication standards of the selected mobile phones

Models of mobile phones working on GSM standard		Models of mobile phones working on 3G Standard	
1	Sony Ericsson K800i	31	Malata i-11
2	i-Tel IT 2090	32	Samsung SM-G530H
3	Samsung GT-E2252	33	Prestigio PSP350
4	Nokia 113	34	HTC Desire 626S
5	Samsung GT-E1205T	35	BlackBerry SQW 100-1
6	Nokia 222	36	King Zone S2
7	Nokia Asha 202	37	Blackberry E145
8	BLU Energy X-plus	38	HTC Wildfire SAS10e
9	BlackBerry 9810	39	Sony Ericsson Xperia TX
10	Nokia 103	40	Blackberry BEC1
11	Infinix X551	41	Samsung SM-A310F
12	Nokia RM-1035	42	Nokia Lumia RM-978
13	ZTE Z222	43	Alcatel One touch
14	Tecno P5	44	Samsung core prime
15	Nokia 108	45	Tecno M3
16	Nokia 1209	46	Samsung GT-S6810P
17	Nokia 105	47	Samsung GT-S5282
18	Nokia 1100	48	Apple iphone-5
19	Tecno T6115	49	Lenovo A520
20	Tecno T605	50	Samsung GT -S7562
21	Tecno 608	51	Tecno W2
22	Nokia 1280	52	i-Tel 1508
23	Nokia 5130c-2	53	Lenovo A1010
24	Nokia Lumia 520	54	Tecno Y2
25	Nokia 2626	55	Infinix smart
26	Nokia 2720a-2	56	Lenovo A369i
27	Solo S355	57	Gionee P2
28	Vodafone Smatt II	58	Huawei G power
29	Samsung GT-S5301	59	Infinix note 3
30	Tecno T340	60	Huawei Ascend Y520

The spectrum analyser detects and measures the peak  $E$  that is associated with the transmission signal from the mobile phones during an active call, while the broadband meter measures the total  $E$  that is associated with all signals from 50 MHz to 3.5 GHz emitted from the phones. Measurements were made in an environment that is free of disturbances that can suddenly spike up the intensity of  $E$  during measurements. Some of these disturbances include active calls from other nearby mobile phones, human and vehicular movements and high level of Wi-Fi signals. The peak values of  $E$  were recorded when the readings from both meters were stable.

### **3.6 Estimation of SAR within some Head Tissues**

The estimate of SAR in the brain tissue due to RF radiation in the selected 60 mobile phones was made from the obtained  $E$  around the mobile phones and the obtained fraction of average power density getting to the brain. The determination of the fraction of the average incident power density in each tissue of the human head was discussed in chapter three. By making use of use of Equations (2.36) to (2.73) and the dielectric parameters of the layers of the head tissues at 900 MHz, 1800 MHz and 2100 MHz presented in Table 2.4, the values of the transmittance  $T$ , reflectance  $R$ , attenuation coefficients  $\alpha$ , intrinsic impedance  $\eta$  and phase angle  $\theta$  in the head tissues was be obtained and presented in Table 3.2.

The fraction of average incident power density in each tissue of the head was obtained by applying the values of tissues parameters at different signal frequencies in Table 3.2 to Equations (2.75) to (2.91) in chapter two. The obtained fractions of average incident power density in tissues of the head at different signal frequencies are presented in Table 3.3.

The values of  $E$  measured around the selected mobile phones using both the spectrum analyser and the broadband meter corresponds to the  $E$  present at the skin of the head. The obtained value of  $E$  at the skin was used to calculate the average power density in other tissues of the head using Equation (2.45) and hence the corresponding  $E$  in them using Equation (3.1) and the fractions of average incident power density in them in Table 3.3. The obtained  $E$  within each tissue was used to calculate the SAR in them by using Equation (3.2).

Table 3.2: Values of the transmittance, reflectance, attenuation coefficients, intrinsic impedance and phase angle in the head tissues at 900, 1800 and 2100 MHz

900 MHz						
Boundary						
	b1	b2	b3	b4	b5	b6
T	0.465	0.782	0.959	0.905	0.985	0.989
R	0.535	0.218	0.041	0.095	0.015	0.011
Tissue						
	Skin	Fat	Bone	Dura	CSF	Brain
$\alpha$	24.899	4.099	7.438	26.615	52.044	24.056
$\eta$	59.347	161.493	107.023	57.411	48.334	52.545
$\theta$	8.923	1.429	2.602	9.555	19.673	8.522
1800 MHz						
Boundary						
	b1	b2	b3	b4	b5	b6
T	0.476	0.79	0.962	0.903	0.987	0.994
R	0.524	0.21	0.038	0.097	0.013	0.006
Tissue						
	Skin	Fat	Bone	Dura	CSF	Brain
$\alpha$	35.292	6.344	15	37.582	65.723	36.697
$\eta$	60.84	163.12	109.93	57.98	47	53.63
$\theta$	6.218	1.102	2.627	6.623	11.746	6.439
2100 MHz						
Boundary						
	b1	b2	b3	b4	b5	b6
T	0.478	0.791	0.963	0.902	0.987	0.994
R	0.522	0.209	0.037	0.098	0.013	0.006
Tissue						
	Skin	Fat	Bone	Dura	CSF	Brain
$\alpha$	39.464	7.341	18.035	42.082	71.312	41.715
$\eta$	61.21	163.58	110.88	58.22	47	53.94
$\theta$	5.952	1.093	2.71	6.347	10.876	6.271

Table 3.3: Fraction of the average incident power density in each tissue

	900 MHz	1800 MHz	2100 MHz
$F_{\text{Skin}}$	0.525	0.532	0.533
$F_{\text{Fat}}$	0.396	0.400	0.399
$F_{\text{Bone}}$	0.375	0.377	0.375
$F_{\text{Dura}}$	0.250	0.184	0.162
$F_{\text{CSF}}$	0.240	0.175	0.153
$F_{\text{Brain}}$	0.193	0.134	0.114

$$|E_r| = \left[ \frac{S_{av}^o(F)(2\eta_c)}{e^{-2\alpha z} \cos\theta_{\eta_c}} \right]^{\frac{1}{2}} \quad (\text{V/m}) \quad (3.1)$$

$$SAR = \frac{\sigma |E_r|^2}{2\rho} (\text{W/kg}) \quad (3.2)$$

Where,

$F$  = the fraction of  $S_{av}^o$  in the tissue of interest

$\sigma$  = conductivity of the tissue

$\rho$  = mass density of the tissue



## CHAPTER FOUR

### RESULTS AND DISCUSSION

#### 4.1 Introduction

The focus of this study as stated in chapter one is to identify prominent RF signals within 900 and 2500 MHz band using spectral analysis, determine the contribution of each signal to the ambient RF radiation intensity in each environment and relate this to the health implication of GSM to humans. The methods of measurement with both RF spectrum analyser and broadband meter around some selected BTS masts in the cities of Lagos, Ibadan and Abuja and around 60 common mobile phones in Nigeria have been discussed in chapter three. This chapter is focused on the presentation and analysis of the results of the spectrum analyser and broadband meter as well as measurement within the near-field of the phone.

#### 4.2 Components of RF Spectrum from each BTS Mast

The typical spectrum of RF signals within 900 and 2500 MHz obtained at the distance of maximum power density from each of the randomly selected 120, 100 and 80 BTS masts in Ibadan, Lagos and Abuja, respectively are presented in Figure 4.1, indicating signals of the nine most prominent frequency bands. Except for small variations in the intensities of the peaks, it is observed that features of the peaks for all locations are quite similar. Using the NFMC (NFMC, 2014) information, the identities of nine frequency bands giving rise to these peaks and their utilization (or source) are summarised in Table 4.1. The intensities of GSM 900 and GSM 1800 bands are labelled as 1 and 7, respectively in the typical spectrum. The numbers 8 and 9 are due to CDMA-1900 and 3G-2100 networks, of which CDMA-1900 signals are only available in some masts, as typically observed in Figure 4.1. The numbers 2 to 6 are mainly signals from radiosondes, radio navigation, broadcast and mobile satellites, as identified in Table 4.1.

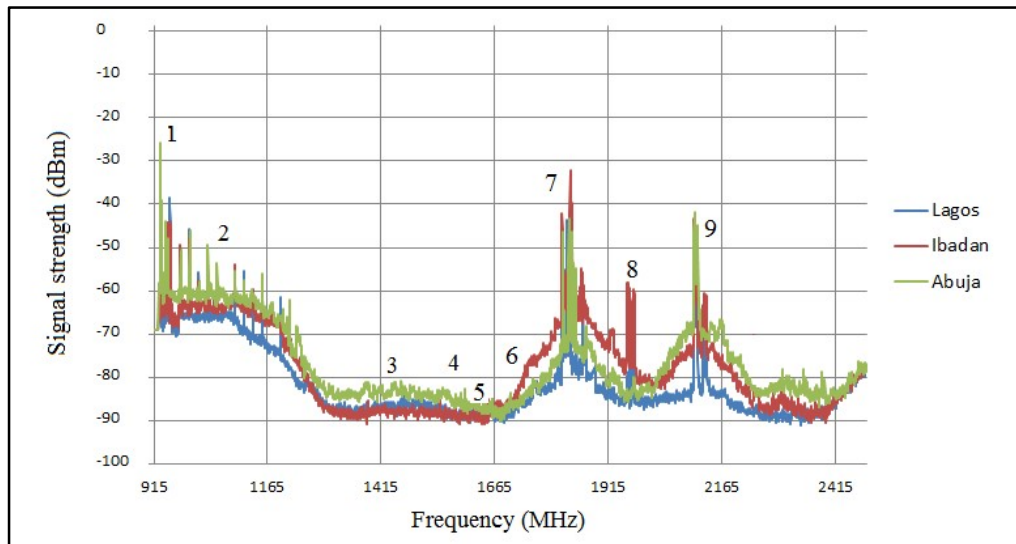


Figure 4.1: Typical spectrum of RF signals between 900 – 2500 MHz with indications of prominent frequency bands in Lagos, Ibadan and Abuja

Table 4.1: Identities of the nine prominent signals in the three cities (NFMC, 2014)

	Frequency Band (MHz)	Nigerian Utilization of Signal Band
1	935 - 960	GSM 900 signal forward link
2	960 -1215	Aeronautical radio-navigation
3	1452 - 1492	Broadcast-Satellite (1467 – 1492 MHz digital audio broadcasting)
4	1518 - 1610	Mobile Satellite (down link for BGAN implementation) (down link 1544 – 1545 MHz dedicated worldwide to distress and safety)
5	1661 -1668	Radio Astronomy
6	1668 – 1700	Weather Forecasting (Radiosondes)
7	1805 - 1880	GSM 1800 signal forward link
8	1963 -1990	CDMA-1900 signal forward link
9	2110 - 2290	3G networks; WIMAX (2204 – 2285); LTE (2226 – 2333)

As shown in Figures 4.1, the intensities of the identified satellite signals are generally low (below -70 dBm) in the three cities.

In order to examine details of each of the nine peaks in the typical spectrum, the frequency span of the spectrum analyser was reduced to match the frequency range of the 9 bands giving rise to the peaks. The resolution of the spectrum analyser was also increased from 3 MHz to 300 kHz thereby revealing the clusters of peaks which make up peaks 1 to 9 in the typical spectrum. The resulting spectra around GSM 900, GSM 1800, CDMA (1963 – 1990 MHz) and 3G networks (2100 – 2290 MHz) are presented in Figures 4.2, 4.3, 4.4 and 4.5, respectively.

The ranges of power densities of all signal peaks within the spectrum obtained in each city are presented in Tables 4.2 and 4.3, respectively for the four BTS signal bands and the five satellite communication signal bands. As discussed in chapter three, the radiation dose which an individual is exposed to due to the presence of a BTS mast in each environment is the sum of the radiation energies of all signal peaks within the obtained spectrum for GSM 900, GSM 1800, CDMA-1900 and 3G- 2100 band, presented in Table 4.4. The radiation dose an individual is exposed due to satellites signals is the sum of the radiation energies of signal peaks in the spectrum of the five satellite communication band identified in this work and presented in Table 4.5.

The threshold for which an individual can be exposed to in many parts of the world including Nigeria was recommended by the ICNIRP. The ICNIRP guideline is based on quantities like the power density  $S$ ,  $E$  and SAR. When an obtained exposure level in an area is lower than the reference level, it means that the basic restriction is not exceeded. Table 4.6 presents the reference level or threshold for public exposure to RF radiation in the range 900 – 2500 MHz.

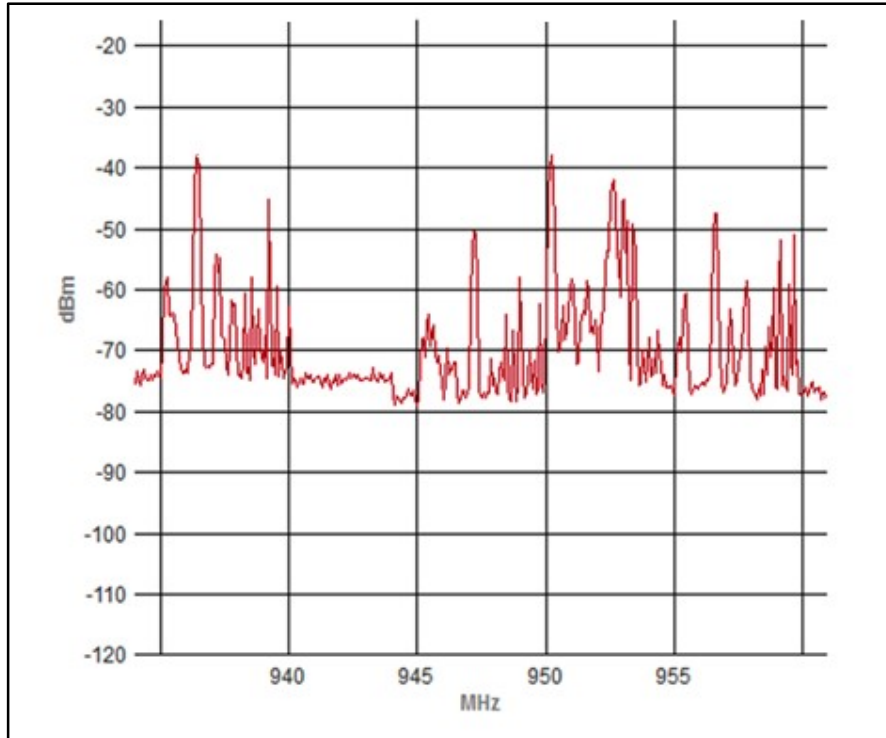


Figure 4.2: Screen shot of the spectrum analyser's display showing the spectrum of GSM 900 (935 – 960 MHz) frequency band signal strengths

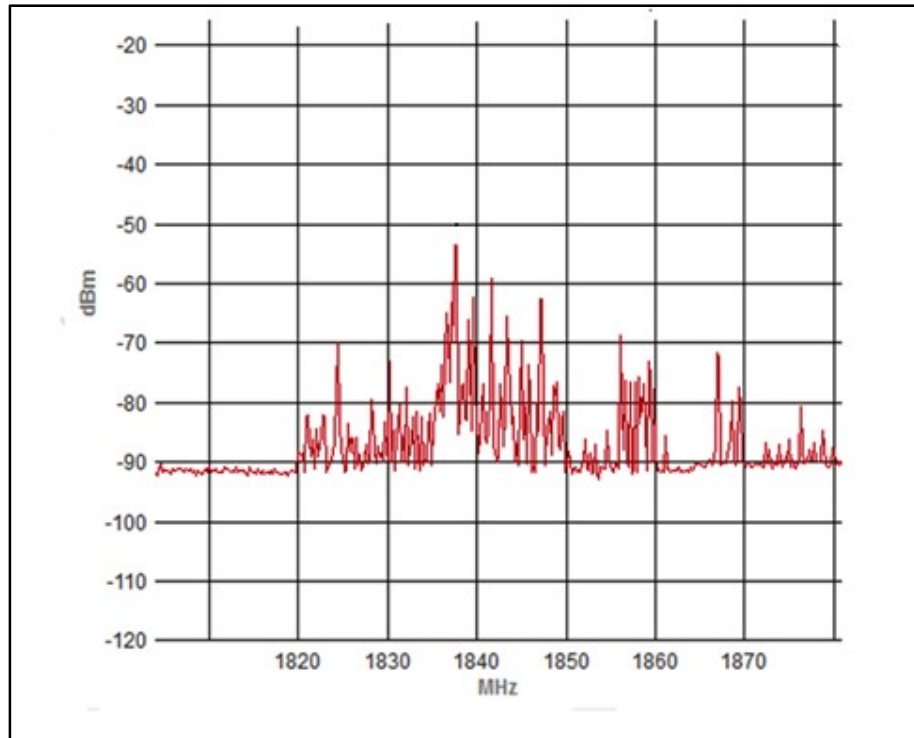


Figure 4.3: Typical screen shot of the spectrum analyser's display showing the spectrum of GSM 1800 (1805 – 1880) frequency band signal strengths

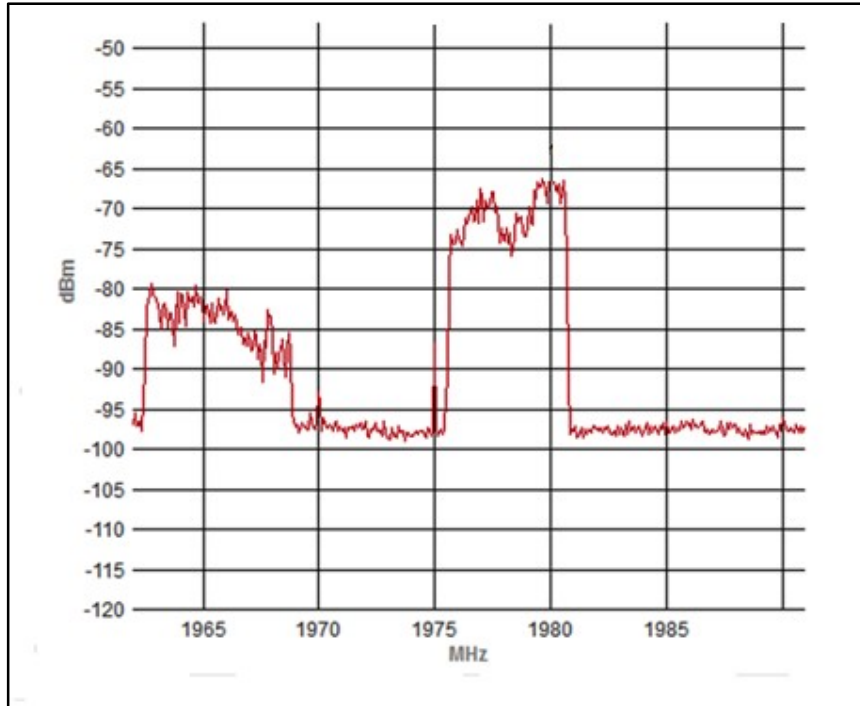


Figure 4.4: Typical screen shot of the spectrum analyser's display showing the spectrum of CDMA-1900 (1963 – 1990 MHz) frequency band signal strengths

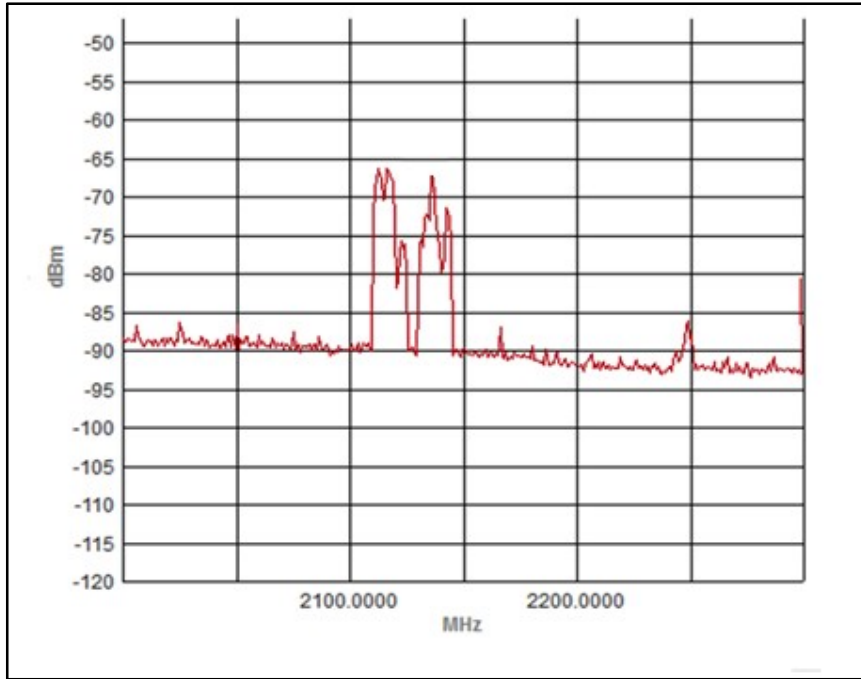


Figure 4.5: Typical screen shot of the spectrum analyser's display showing the spectrum of 3G-2100 (2110 – 2290 MHz) frequency band signal strengths



Table 4.2: Ranges of power density of signal peaks within the spectra of the four BTS signal bands in the cities

Power Density ( $\mu\text{W}/\text{m}^2$ )						
Frequency Band	Lagos		Ibadan		Abuja	
	Max	Min	Max	Min	Max	Min
GSM 900	447.56	0.01	162.49	0.01	5411.26	0.13
GSM 1800	425.95	0.11	158.65	0.01	1263.00	0.03
CDMA-1900	10.00	0.01	57.52	0.01	175.30	0.01
3G-2100	118.50	0.01	116.82	0.01	423.78	0.06

Table 4.3: Ranges of power density of signal peaks within the spectra of the five satellite signal bands in the cities

Satellite Frequency Band	Power Density ( $\mu\text{W}/\text{m}^2$ )					
	Lagos		Ibadan		Abuja	
	Max	Min	Max	Min	Max	Min
960 -1215	9.585	0.120	4.74	0.740	8.177	0.231
1452 - 1492	1.247	0.001	0.02	0.001	2.387	0.001
1518 - 1610	0.048	0.001	0.02	0.001	0.048	0.001
1661 -1668	0.019	0.001	0.004	0.001	0.016	0.001
1668 – 1700	0.006	0.001	0.003	0.001	0.010	0.001

Table 4.4: Ranges of the sum of power densities of all signal peaks within the spectra of the four BTS signal bands in the three cities

Sum of Power Densities ( $\mu\text{W}/\text{m}^2$ )						
Frequency Band	Lagos		Ibadan		Abuja	
	Max	Min	Max	Min	Max	Min
GSM 900	1845.754	0.204	737.590	0.098	2915.907	0.191
GSM 1800	665.488	0.278	695.981	0.058	7045.068	0.064
CDMA-1900	11.390	0.010	68.300	0.010	252.780	0.010
3G-2100	124.030	0.010	176.150	0.010	873.730	0.280

Table 4.5: Ranges of the sum of power densities of all signal peaks within the spectra of the five satellite signal bands in the three cities

Sum of Power Densities ( $\mu\text{W}/\text{m}^2$ )						
Satellite Frequency Band	Lagos		Ibadan		Abuja	
	Max	Min	Max	Min	Max	Min
960 -1215	23.898	0.425	11.978	1.978	20.570	0.705
1452 - 1492	3.113	0.022	0.070	0.023	5.988	0.023
1518 - 1610	0.165	0.048	0.096	0.049	0.166	0.049
1661 -1668	0.051	0.006	0.014	0.006	0.044	0.006
1668 – 1700	0.031	0.018	0.024	0.019	0.041	0.019

Table 4.6: ICNIRP, 1998 reference levels for public exposure to RF radiation in the range 900 – 2500 MHz

	Frequency Band			
	900 MHz	1800 MHz	1900 MHz	2100 MHz
Electric Field Intensity ( <b>E</b> ) (V/m)	41	58	60	61
Power Density ( <b>S</b> ) (W/m <sup>2</sup> )	4.5	9	9.5	10
Specific Absorption Rate (SAR) (W/kg)	2	2	2	2

#### **4.2.1 Comparison of GSM Radiation Intensity with other RF intensities**

As stated in chapter one, GSM radiation is just one set of non-ionizing radiation type in most environments. We have established the presence of some satellite communication radiation types in the band 900 – 2500 MHz being investigated in this work. The ratio of the maximum intensities of the satellite signals to maximum intensities of GSM signals is presented as SS/GSM in Table 4.6 for the three cities. We can observe that this is generally below 1% in the cities showing the insignificance of satellite signals to human radiation exposure when compared with GSM signals in the cities. The maximum value of power densities in the cities have been taken to represent the worst case health scenario.

As discussed in chapter one, most applications of RF radiation in our environment is within the range of 50 MHz to 3.5 GHz, whereas, our investigation with the spectrum analyser covers the band 900 – 2500 MHz within which BTS signals are located. The many other radiation frequencies below and above these range contribute to human exposure at a rate which increases with increase in RF applications. In other to see the current level of exposure outside the GSM, we wish to examine the result of measurement with the broadband meter, which integrates the entire RF bands.

The ranges of the maximum broadband power density around each BTS mast in the three cities are presented in Table 4.7 alongside the maximum GSM power density in each city. From the table, it is concluded that the mean overall contribution of GSM to overall power density due to all RF signals in a typical environment is about 28%.

Table 4.7: Ranges of maximum power densities due to satellite and BTS signals in the three cities

Power Densities ( $\mu\text{W}/\text{m}^2$ )					
	Satellite		BTS		(SS/BTS) %
	Max	Min	Max	Min	
Lagos	24.17	0.63	2546.91	2.41	0.90
Ibadan	12.08	2.07	1594.91	0.40	0.80
Abuja	25.37	0.80	7931.69	0.87	0.30

Table 4.8: The percentage contribution of GSM to the Total RF power densities in the three cities

Power Densities ( $\mu\text{W}/\text{m}^2$ )					
	GSM		Total RF (broadband)		Mean (GSM/Total) %
	min	max	min	max	
Lagos	2.27	2511.24	9.90	27500.00	20
Ibadan	0.16	1418.03	0.84	8430.00	22
Abuja	0.53	7911.05	108.90	90900.00	42



### **4.3 Emitted Signals from the Mobile Phones**

Typical spectrum of the RF radiation from the 60 selected phones when making a call is presented in Figures 4.6 and 4.7. The spectrum of typical uplink signal frequencies of a mobile phone operating on GSM (2G) at 1800 MHz is shown in Figure 4.6. The spectrum in Figure 4.7 is that of a typical 3G-2100 signal emitted from a mobile phone. It is no surprise that most of the GSM mobile phones transmitted at GSM 1800 uplink frequencies, because as stated in chapter one GSM 1800 offers more than double of GSM 900 speech channels for mobile phone users and therefore ideal for frequency reuse in a congested area like the cities under study.

The spectrum in Figure 4.6 shows that apart from the emitted RF radiation due to the communication signal frequency from the 2G phones, the phones during a phone call were also emitting RF radiation continuously at different frequencies between 1710 and 1785 MHz. The spectrum in Figure 4.7 confirm that the 3G phones in this study works on WCDMA mobile standard and that the emitted RF radiation from the phones was due to signals within a frequency band of about 5 MHz.

### **4.4 Electric Field Intensity around a Mobile Phone in Use**

The background measurements of **E** when phones are switched on but no phone calls are being made around the selected mobile phones were made with the broadband meter. This represents the sum of **E** due to the RF signals in the environments where measurements were being taken and the **E** due to current flow within circuitry of phones when no phone calls are made by them. The ranges of the obtained background **E** around the 60 selected 2G and 3G phones were from 0.03 – 0.76 V/m and 0.02 – 0.70 V/m, respectively. When the mobile phones were in active mode (in a state of making and receiving a call), **E** measurements in the near field region of the phones were made and the ranges of **E** obtained from broadband and spectral measurements around the selected mobile phones are presented in Table 4.9.

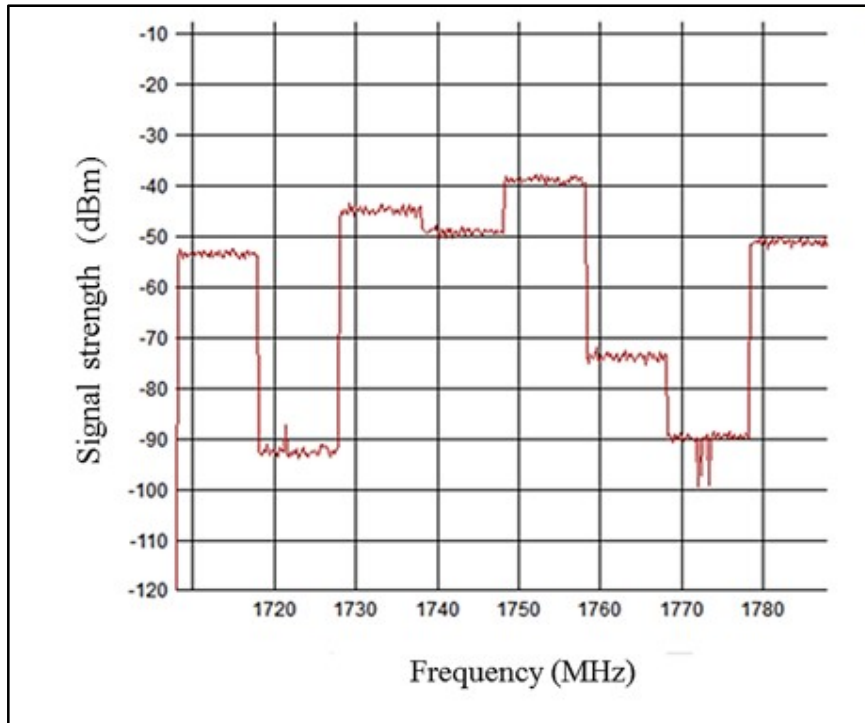


Figure 4.6: A typical spectrum of a GSM 1800 uplink signal band from a mobile phone in the active call mode

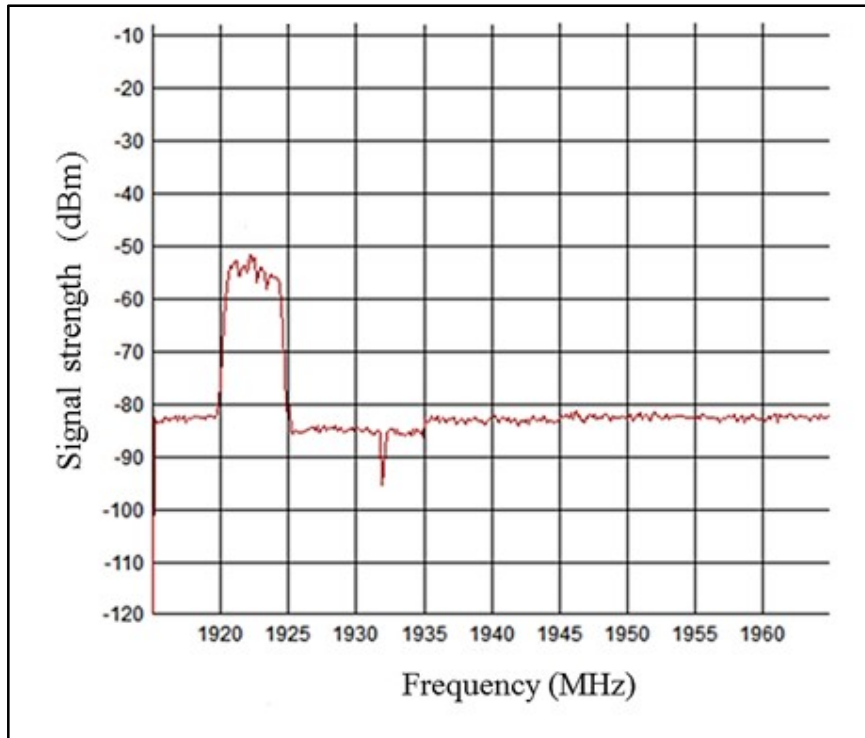


Figure 4.7: A typical spectrum of a 3G-2100 uplink signal band from a mobile phone in the active call mode

Table 4.9: Electric field strength in near field region of the mobile phones using broad band meter and a spectrum analyser

E (V/m) around the 3G Phones					
	Background	Broad Band		Spectral	
		incoming call	outgoing calls	incoming calls	outgoing calls
Maximum	0.70	30.21	33.01	0.19	0.20
Minimum	0.02	2.92	3.60	0.04	0.03
Average	0.19	13.72	14.45	0.10	0.11
Standard Deviation	0.23	6.97	6.73	0.04	0.05

E (V/m) around the 2G Phones					
	Background	Broad Band		Spectral	
		incoming calls	outgoing calls	incoming calls	outgoing calls
Maximum	0.76	74.49	76.52	0.22	0.33
Minimum	0.03	6.88	19.70	0.09	0.08
Average	0.31	43.41	48.08	0.16	0.17
Standard Deviation	0.24	18.23	16.21	0.04	0.05

The  $E$  associated mainly to a signal during a phone call from spectral measurements in the near field region of the 3G mobile phones is about 64% of that of 2G mobile phones on the average. This shows that an individual whose head is within the near field region of a 2G mobile phone is prone to a higher level of RF radiation exposure than from a 3G mobile phone. It was observed that radiation emissions during incoming calls are slightly lower than the outgoing calls for both 2G and 3G mobile phones.

From Table 4.9, it was also observed that there is a large difference between the measured values of  $E$  from the two instruments. The large difference is due to the fact that the broadband meter during measurements, integrate the values of the  $E$  emitted the phones due to various frequencies as shown in the spectrum in Figures 4.6 and 4.7, while the spectrum analyser measure the peak  $E$  due to the signal frequency that is being used to communicate between the phone and the BTS. The average value of  $E$  emitted due to a communication signal in the near field region of 2G and 3G mobile phones is about 0.35 and 0.76% of the total  $E$  in the region of the phones, respectively.

#### **4.5 RF exposure within the Head tissues**

As discussed in chapter four, RF radiation exposure in 6 tissues of the human head was estimated from the results of  $E$  obtained from broad band and spectral measurements in the near field region of 60 common mobile phones in Nigeria. The results of the externally obtained  $E$  around the mobile phones in section 4.4 and the estimated fractions of power density in each tissue, which was determined from the multi-layered planar model of the head discussed in chapter two, were used to estimate the resultant  $E$  within the different head tissues.

The obtained resultant  $E$  in the various head tissues from both broadband and spectral measurements around the phones in Table 4.10 and 4.11, shows that the estimated values of  $E$  in the fat tissue is higher than on the skin tissue and the other head tissues.

Table 4.10: Summary of the resultant electric field intensity in the head tissues due to 2G mobile phones

<b>E (V/m) due to Broadband Measurements around 2G mobile Phone</b>						
Incoming calls						
	Skin	Fat	Bone	Dura	CSF	Brain
Maximum	30.963	43.824	34.943	17.782	15.723	14.571
Minimum	2.858	4.045	3.226	1.641	1.451	1.345
Average	18.044	25.539	20.363	10.362	9.163	8.491
Standard deviation	7.577	10.725	8.552	4.352	3.848	3.566
Outgoing calls						
	Skin	Fat	Bone	Dura	CSF	Brain
Maximum	31.803	45.013	35.891	18.264	16.150	14.966
Minimum	8.189	11.591	9.242	4.703	4.159	3.854
Average	19.985	28.287	22.554	11.478	10.149	9.405
Standard deviation	6.739	9.539	7.606	3.870	3.422	3.171
<b>E (V/m) due to Spectral Measurements around 2G mobile Phone</b>						
Incoming calls						
	Skin	Fat	Bone	Dura	CSF	Brain
Maximum	0.093	0.131	0.105	0.053	0.047	0.044
Minimum	0.008	0.012	0.010	0.005	0.004	0.004
Average	0.065	0.092	0.073	0.037	0.033	0.030
Standard deviation	0.021	0.029	0.024	0.012	0.011	0.010
Outgoing calls						
	Skin	Fat	Bone	Dura	CSF	Brain
Maximum	0.136	0.192	0.153	0.078	0.069	0.064
Minimum	0.008	0.012	0.009	0.005	0.004	0.004
Average	0.072	0.101	0.081	0.041	0.036	0.034
Standard deviation	0.024	0.035	0.028	0.014	0.012	0.012

Table 4.11: Summary of the resultant electric field intensity in the head tissues due to 3G mobile phones

E (V/m) due to Broadband Measurements around the 3G mobile Phones						
Incoming calls						
	Skin	Fat	Bone	Dura	CSF	Brain
Maximum	12.609	17.786	14.208	6.773	5.956	5.481
Minimum	1.218	1.718	1.373	0.654	0.575	0.530
Average	5.725	8.076	6.452	3.075	2.704	2.182
Standard deviation	2.909	4.103	3.278	1.563	1.374	1.265
Outgoing calls						
	Skin	Fat	Bone	Dura	CSF	Brain
Maximum	13.776	19.432	15.523	7.400	6.507	5.989
Minimum	1.503	2.120	1.693	0.807	0.710	0.653
Average	6.029	8.504	6.793	3.238	2.847	2.621
Standard deviation	2.809	3.962	3.165	1.509	1.327	1.221
E (V/m) due to Spectral Measurements around the 3G mobile Phones						
Incoming calls						
	Skin	Fat	Bone	Dura	CSF	Brain
Maximum	0.081	0.114	0.091	0.043	0.038	0.038
Minimum	0.018	0.026	0.021	0.010	0.009	0.005
Average	0.041	0.058	0.047	0.022	0.020	0.017
Standard deviation	0.018	0.025	0.020	0.009	0.008	0.009
Outgoing calls						
	Skin	Fat	Bone	Dura	CSF	Brain
Maximum	0.085	0.120	0.096	0.046	0.040	0.037
Minimum	0.011	0.016	0.012	0.006	0.005	0.005
Average	0.044	0.063	0.050	0.024	0.021	0.019
Standard deviation	0.022	0.031	0.025	0.012	0.010	0.009

The high value of  $E$  in fat tissue is due mainly to its lower relative permittivity. This can be seen in the table of dielectric parameters for the head tissues at different frequency in chapter two, where the relative permittivity of the fat is seen to be lower than all the other tissues of the head. The relative permittivity or dielectric constant of a dielectric medium like the fat tissue is the measure of its ability to generate or retain electric flux in the process of being polarized by an external electric field. The internally generated electric field by the polarization of the dipole molecules in the medium opposes the external electric field producing it, thereby reducing the effective electric field in the medium. This opposition or resistance depends on the permittivity and hence the dielectric constant of the medium. Therefore a medium like fat with low relative permittivity will yield more electric flux because it offers little opposition to the electric field during the polarization of its molecules.

The estimated value of  $E$  on the skin tissue is about 70% of that in the fat tissue. It was observed that the estimated value of  $E$  in the brain tissue is about 45% of what is on the skin tissue. The distribution of maximum  $E$  in the tissues of the head is illustrated in Figures 4.8 and 4.9. The estimated values of the resultant  $E$  in the head tissues was used to estimate the SAR in each of the tissues and is summarized in Tables 4.12 and 4.13. Typical distributions of the maximum values of the obtained SAR in these tissues are presented in Figures 4.10 and 4.11. The value of the obtained SAR within the skin tissue, calculated from both broad band and spectral measurements of external  $E$  around the mobile phones is higher than other tissues.



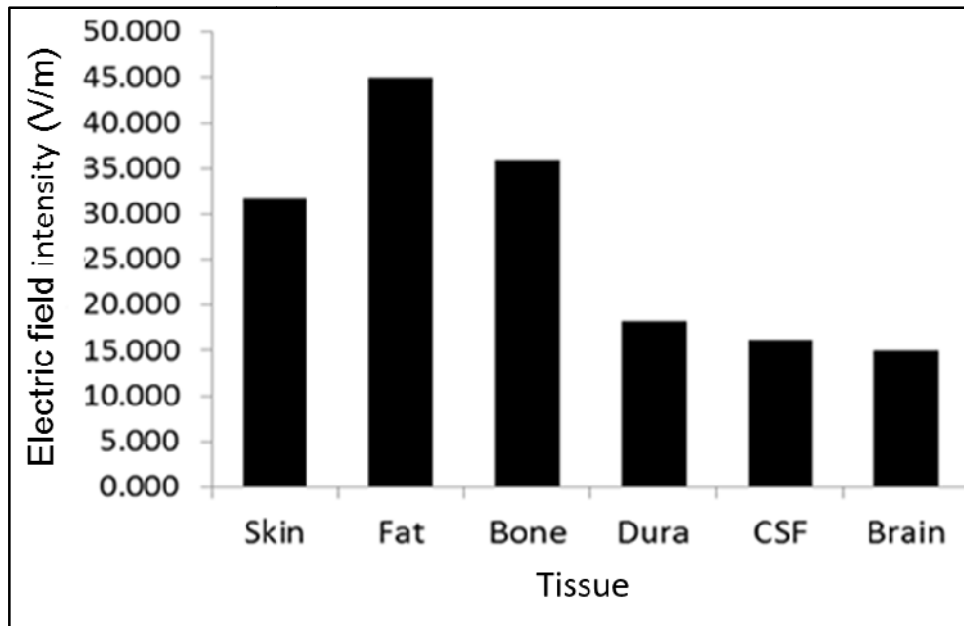


Figure 4.8: Distribution of maximum Electric field intensity within the head tissues obtained from broadband measurements

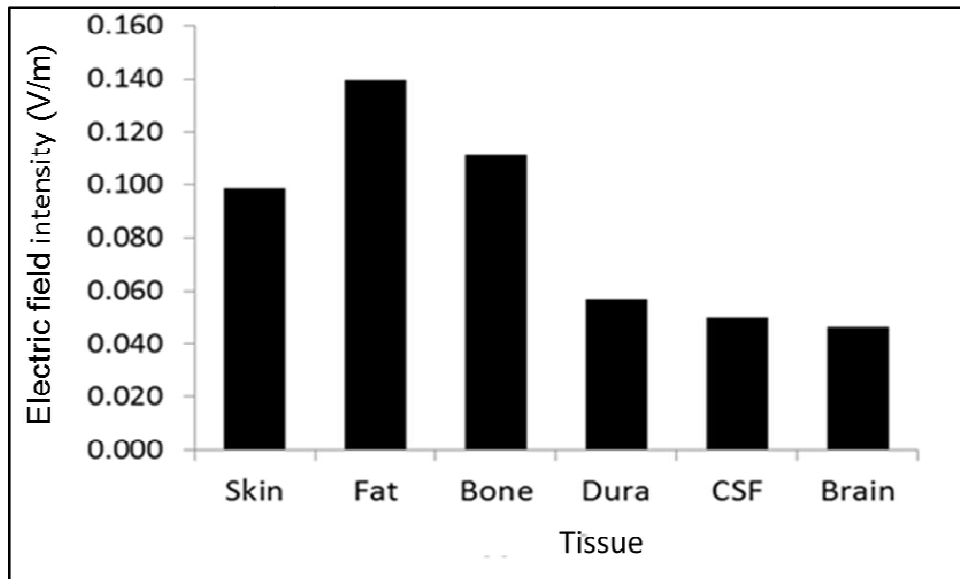


Figure 4.9: Distribution of electric field intensity within the head tissues obtained from spectral measurements

Table 4.12: Summary of the SAR in the head tissues due to 2G mobile phones

SAR (W/kg) due to Broadband Measurements around 2G mobile Phone						
Incoming calls						
	Skin	Fat	Bone	Dura	CSF	Brain
Maximum	0.510	0.082	0.088	0.178	0.358	0.141
Minimum	0.004	0.001	0.001	0.002	0.003	0.001
Average	0.203	0.033	0.035	0.071	0.142	0.056
Standard deviation	0.141	0.023	0.024	0.049	0.099	0.039
Outgoing calls						
	Skin	Fat	Bone	Dura	CSF	Brain
Maximum	0.538	0.087	0.093	0.188	0.378	0.149
Minimum	0.036	0.006	0.006	0.012	0.025	0.010
Average	0.236	0.038	0.041	0.082	0.166	0.065
Standard deviation	0.138	0.022	0.024	0.048	0.097	0.038
SAR ( $\mu$ W/kg) due to Spectral Measurements around 2G mobile Phone						
Incoming calls						
	Skin	Fat	Bone	Dura	CSF	Brain
Maximum	4.588	0.740	0.791	1.599	3.224	1.016
Minimum	0.038	0.006	0.007	0.013	0.027	0.008
Average	2.451	0.395	0.423	0.854	1.722	0.543
Standard deviation	1.303	0.210	0.225	0.454	0.916	0.289
Outgoing calls						
	Skin	Fat	Bone	Dura	CSF	Brain
Maximum	9.816	1.582	2.752	3.421	6.898	2.718
Minimum	0.036	0.006	0.010	0.012	0.025	0.010
Average	3.037	0.489	0.851	1.058	2.134	0.841
Standard deviation	1.895	0.305	0.531	0.660	1.332	0.525

Table 4.13: Summary of the SAR in the head tissues due to 3G mobile phones

SAR (mW/kg) due to Broadband Measurements around the 3G mobile Phones						
Incoming calls						
	Skin	Fat	Bone	Dura	CSF	Brain
Maximum	93.906	15.626	17.352	28.721	55.477	22.569
Minimum	0.876	0.146	0.162	0.268	0.518	0.211
Average	24.192	4.026	4.470	7.399	14.292	5.814
Standard deviation	23.187	3.858	4.285	7.092	13.698	5.573
Outgoing calls						
	Skin	Fat	Bone	Dura	CSF	Brain
Maximum	112.091	18.652	20.713	34.283	66.220	26.940
Minimum	1.334	0.222	0.246	0.408	0.788	0.321
Average	25.970	4.321	4.799	7.943	15.342	6.242
Standard deviation	24.287	4.041	4.488	7.428	14.348	5.837
SAR ( $\mu$ W/kg) due to Spectral Measurements around the 3G mobile Phones						
Incoming calls						
	Skin	Fat	Bone	Dura	CSF	Brain
Maximum	3.832	0.638	0.708	1.172	2.264	0.724
Minimum	0.200	0.033	0.037	0.061	0.118	0.038
Average	1.191	0.198	0.220	0.364	0.704	0.225
Standard deviation	1.024	0.170	0.189	0.313	0.605	0.193
Outgoing calls						
	Skin	Fat	Bone	Dura	CSF	Brain
Maximum	4.297	0.715	1.291	1.314	2.539	1.033
Minimum	0.073	0.012	0.022	0.022	0.043	0.017
Average	1.432	0.238	0.430	0.438	0.846	0.344
Standard deviation	1.236	0.206	0.371	0.378	0.730	0.297

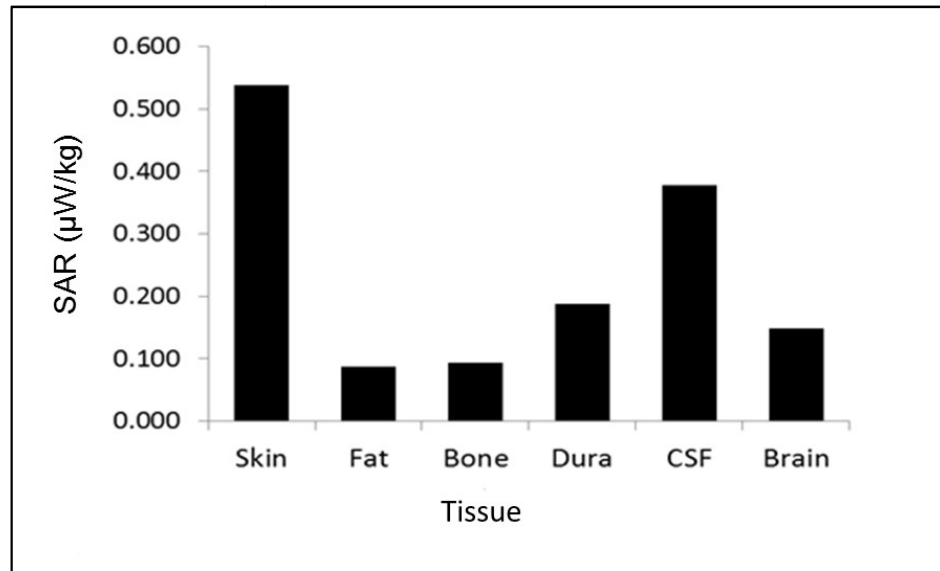


Figure 4.10: Distribution of SAR within the head tissues obtained from broadband measurements

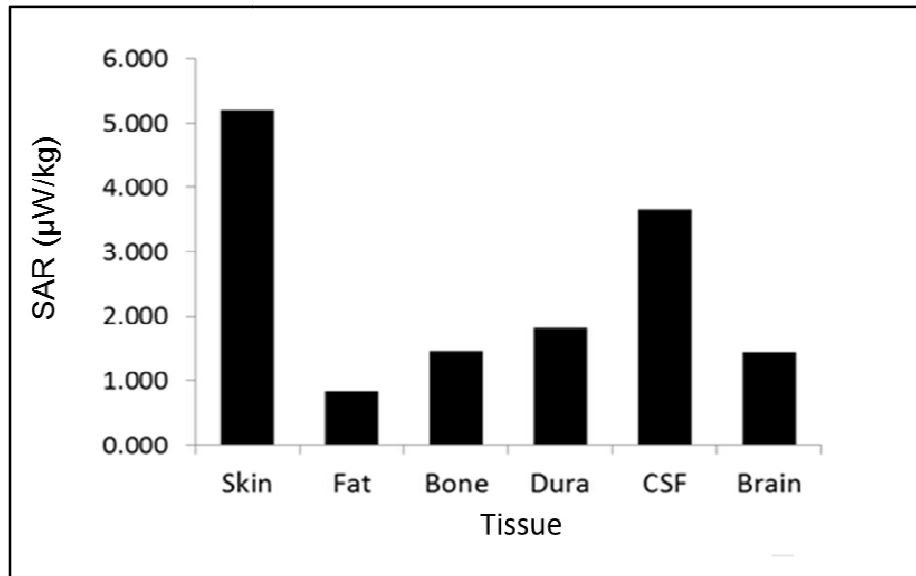


Figure 4.11: Distribution of electric field intensity within the head tissues obtained from spectral measurements

The results in Tables 4.12 and 4.13, and the illustration of the distribution of maximum SAR in the human head tissues in Figures 4.10 and 4.11, shows that the skin of the head absorbed more energy emitted in the use of a mobile phone than any other tissue. As observed in Tables 4.12 and 4.13, the maximum SAR in the brain for both spectral and broadband measurements around the 2G and 3G phones is about 28 and 24% of the maximum SAR in the skin, respectively. It can also be observed that more energy is absorbed in the brain during the use of the 2G mobile phones than in the use of the 3G mobile phones.

The energy absorbed in the brain due to BTS signals at the point of maximum power density from BTS masts in the cities of Lagos, Ibadan and Abuja, was calculated using the obtained sum of power densities of GSM 900, GSM 1800, CDMA-1900 and 3G-2100 signals in each city. The obtained resultant **E** and SAR in the brain due to each BTS signal band the cities are presented in Table 4.14. As observed in Table 4.14, the maximum SAR in the brain due to BTS signals is 17.00  $\mu\text{W}/\text{kg}$  from GSM 900 signals, 6.79  $\mu\text{W}/\text{kg}$  from GSM 900 signals and 73.14  $\mu\text{W}/\text{kg}$  from GSM 1800 signals in Lagos, Ibadan and Abuja, respectively.

#### **4.6 Risk of RF radiation Exposure in the three cities**

Radiofrequency (RF) signals between 900 and 2500 MHz was assessed in the cities of Lagos, Ibadan and Abuja and the results of this assessment are presented in this chapter. The energy absorbed in the tissues of the human head in the use of 60 common mobile phones in Nigeria and the values of **E** in this region were also obtained. The health implication of the obtained level of radiation exposure from the different BTS masts and mobile phones is discussed in this section.

As discussed in chapter two, the associated risk with RF radiation exposure from the numerous BTS antennas and mobile phone handsets to the generally public can be assessed by comparing its measured quantity against the recommended reference level.

Table 4.14: The ranges of the resultant **E** and SAR in the brain tissue due to BTS signals at the point of maximum intensities from BTS masts in each city

Electric field intensity in the Brain tissue <b>E</b> (mV/m)						
	Lagos		Ibadan		Abuja	
	Max	Min	Max	Min	Max	Min
CDMA(1900 MHz)	12.817	0.294	31.386	0.380	60.381	0.120
3G (2100 MHz)	39.228	0.111	46.749	0.111	104.117	1.864
GSM 900	194.401	2.045	122.891	1.413	244.342	1.980
GSM 1800	97.971	2.001	100.191	0.913	318.766	0.961
SAR in the Brain tissue ( $\mu$ W/kg)						
	Lagos		Ibadan		Abuja	
	Max	Min	Max	Min	Max	Min
CDMA(1900 MHz)	0.109	5.755E-02	0.655	8.020E-03	2.425	9.592E-03
3G (2100 MHz)	1.156	9.320E-03	1.642	9.592E-03	8.143	2.610E-02
GSM 900	16.997	1.881E-02	6.792	8.979E-02	26.852	1.763E-02
GSM 1800	6.384	2.664E-02	6.676	5.545E-02	73.139	6.143E-02



Measurements of RF radiation at the estimated distance of power density to some selected BTS masts in the three cities led to the identification of 9 prominent signal bands, which was categorised into non-BTS (mobile and broadcast satellite, radiosondes and radio navigation) and BTS signal bands. The obtained maximum spectral power density of satellite signals was 9.59, 4.74 and 8.18  $\mu\text{W}/\text{m}^2$  in Lagos, Ibadan and Abuja, respectively, while that of BTS signals was 447.56, 162.49 and 5411.26  $\mu\text{W}/\text{m}^2$  in Lagos, Ibadan and Abuja, respectively. The highest value of power density associated with both satellite and BTS signals in the cities is about 0.0002 and 0.12% of the ICNIRP minimum reference level of 4.5  $\text{W}/\text{m}^2$  for signals from 900 MHz, respectively.

The sum of power density of satellite and BTS signals was estimated. The maximum value of the sum of satellite signal from the selected BTS masts in each city was 24.17, 12.08 and 25.37  $\mu\text{W}/\text{m}^2$  in Lagos, Ibadan and Abuja, respectively, while the maximum value of the sum of BTS signals was 2546.91, 1594.91 and 7931.69  $\mu\text{W}/\text{m}^2$  in Lagos, Ibadan and Abuja, respectively. The highest value of power density associated with the sum all satellite and BTS signals in the cities is about 0.001 and 0.09%, respectively of the ICNIRP limit for signals between 900 and 1800 MHz.

The upper limit of broadband power density at each measurement spot was 27500, 8430 and 90900  $\mu\text{W}/\text{m}^2$  in Lagos, Ibadan and Abuja, respectively, with the highest value being about 0.91% of the ICNIRP limit of 10  $\text{W}/\text{m}^2$  for signals up to 300 GHz. Therefore, worst-case scenario of power density of the various RF sources within 900 MHz and 2500 MHz in each city is less than the ICNIRP recommended limits, showing that there is no risk of any health effect to the public in these cities.

The RF radiation emissions from some selected mobile phones were assessed by measuring the level of **E** in the near field region of the phones. The result of these measurements in chapter 5 showed that the maximum value of the total (broadband) **E** in the near field region of the 2G (1800 MHz) mobile phones was 76.52V/m, which exceeds the 58 V/m limit recommended for GSM 1800 by the ICNIRP. The obtained total **E** of 76.52V/m may raise a concern to whether the use of a 2G mobile phone is hazardous to human health, but this concern can only be factual if the energy absorbed

by the brain tissue due to the obtained  $E$  exceeds the recommend level of SAR by the ICNIRP. The maximum value of the total from the 3G (2100 MHz) mobile phones was 33.01 V/m and this value was about 54% of the 61 V/m limit recommended for 3G (2100 MHz) by the ICNIRP.

The maximum value of  $E$  from spectral measurements in the near field region of the selected 2G phones during an active call was 0.33 V/m and this value was about 0.57% of the 58 V/m recommended limit for 1800 MHz frequency. For the selected 3G phones, the maximum value of spectral  $E$  during an active call was 0.20 V/m and this is about 0.33% of the 61 V/m recommended limit for 3G (2100 MHz) by the ICNIRP respectively.

The maximum value of SAR in the brain from broadband and spectral measurements around 2G phones were 0.15 W/kg and 2.72  $\mu$ W/kg, respectively, while that of the 3G phones were 26.94 mW/kg and 1.03  $\mu$ W/kg, respectively. The highest value of SAR in the brain was about 8% of 2 W/kg limit set by ICNIRP. This is an indication that the exposure to the brain from the selected 2G and 3G mobile phones in this study is not harmful during the active use of the mobile phones.

The energy absorbed in the brain due to signal emissions from BTS masts in each city was estimated. The maximum value of SAR in the brain due to BTS signals was 17.00, 6.79 and 73.14  $\mu$ W/kg in the cities of Lagos, Ibadan and Abuja, respectively. The maximum value of SAR in Abuja is about 0.004% of the 2 W/kg recommended limit by the ICNIRP. This observation also confirms that there is no risk of any health effect on the public from the BTS masts.

## CHAPTER FIVE

### CONCLUSION

#### 5.1 Summary

The study of radiofrequency radiation exposure around 300 randomly selected BTS masts in the cities of Lagos, Ibadan and Abuja and in the near field region of 60 common mobile phones in Nigeria was carried out. Radiofrequency spectral measurements were made to determine the distance of maximum power density around BTS masts in each city and hence identify prominent signals between 900 MHz and 2500 MHz frequency band at estimated distance of maximum power density. The average distance of maximum power density around the BTS masts in Lagos, Ibadan and Abuja is  $183 \pm 58$  m,  $195 \pm 19$  m,  $190 \pm 63$ , respectively.

Nine prominent signals within this range frequency band were identified. Five of these signals were designated non-BTS (mobile and broadcast satellite, radiosondes and radio navigation) signals, within band 960-1700 MHz producing a maximum power density of  $9.6 \mu\text{W}/\text{m}^2$  at a point in Lagos. The remaining four (within 935-960 MHz and 1805-2290 MHz) were from BTS, with the band 935-960 MHz (GSM 900) producing the overall maximum power density of  $5411.3 \mu\text{W}/\text{m}^2$  in Abuja. The result of this study showed that the level of power density of non-BTS signals is significantly lower than that of BTS signals.

The worst-case scenario of power density at the point of maximum intensity of all signals from BTS masts in the three cities was  $2546.91$ ,  $1594.91$  and  $7931.69 \mu\text{W}/\text{m}^2$  in Lagos, Ibadan and Abuja, respectively. This value is about 23, 26 and 46% of the maximum broadband power density obtained at the point of maximum intensity from the BTS masts in Lagos, Ibadan and Abuja, respectively.

The level of radiation exposure from BTS masts in the city of Abuja is higher than that of Lagos and Ibadan. The maximum radiation power density in Lagos and Ibadan was about 30.25 % and 9.27 % of the maximum power density in Abuja on the average.

Electric field intensity measurements were made with the both the calibrated spectrum analyzer and the broadband meter in the near field region of the selected mobile phones in this study. The values of  $E$  obtained in the near field region of the selected mobile phones and the estimated fraction of  $E$  in the tissues of the head was used to estimate the exposure in the brain due to the RF radiation from the use of the mobile phones. The maximum values of SAR in the brain was 0.15 W/kg and 2.72  $\mu$ W/kg from broadband and spectral measurements around 2G phones, respectively, while that of 3G phones was 26.94 mW/kg and 1.03  $\mu$ W/kg, respectively.

The risk associated with RF radiation exposure from the numerous BTS antennas and mobile phone handsets to the general public was assessed by weighing the results of power density and SAR obtained in this study against a references or limit set by the ICNIRP. It was observed that the highest value of GSM 900, GSM 1800, CDMA-1900 and 3G-2100 signals in the cities of Lagos, Ibadan and Abuja were less 1 % of the reference levels or recommended limits for each frequency band. The value of maximum broadband power density in the three cities was found to be about 2 % of the 4.5  $\mu$ W/m<sup>2</sup> the ICNIRP limit.

The highest value of SAR in the brain due to RF emissions from mobile phones is about 8 % of the 2 W/kg limit set by ICNIRP. The maximum value of SAR in brain due to RF emissions from BTS is about 0.004 % of the 2 W/kg recommended limit by the ICNIRP. The worst-case scenario of RF exposure from the various RF sources within 900 MHz and 2500 MHz in each city, and the selected mobile phones are far less than the ICNIRP recommended limits. It can be concluded from this study that there is no risk of any health effect on the public from BTS mast and mobile phones in the three cities.

### **5.3 Contributions, Limitations and Suggestion for Further Studies**

This study has successfully identified the prominent signal bands within the frequency range of 900 – 2500 MHz, provided information on their level of power densities and their contributions total RF power density in the cities of Lagos, Ibadan and Abuja. Information on the exposure level due to RF radiation emitted from 60 brands of mobile phones in Nigeria was provided in this study. The amount of energy that may be absorbed in the human brain during the use of these phones was also provided in this study.

This study was carried in only in three major cities in Nigeria due to limited resources. More cities and BTS masts in various locations could be studied without necessarily being present at their location if technical parameters like GPS data, BTS antenna power, tilt angle and vertical beam width of the antennas in the various cities in Nigeria were readily available.

Despite this limitation, this study has provided the background for which assessment of RF exposure around BTS masts in all other cities in Nigeria can be made. Measurements of power densities of the various existing and newly emerging RF mobile communication radiation in each neighbourhood can be made at the established distance of maximum power density around each mast in the country. In addition, with the estimated fractions of incident power density in the head tissue, the level of RF exposure to the brain from the radiation emitted from newer brands of phone can be studied.

## REFERENCES

- Aaronia, 2011. SPECTRAN HF-6060 V4, HF-6080 V4 or HF-60100 V4 manual, . Aaronia AG [www.aaronia.de](http://www.aaronia.de), Euscheid.
- Abdalla, A. and Teoh, A., 2005. A multilayered model of human head irradiated by electromagnetic plane waves of 100 MHz - 300 GHz. *International Journal of Scientific Research*, 15: 1-7.
- Abdulrazzaq, S.A. and Aziz, J.S., 2013. SAR Simulation in Human Head Exposed to RF Signals and Safety Precautions *IJCSET*, 3(9): 334-340.
- Abuja fact, 2005. Top 5 cities to do business in Nigeria. Abuja is 2nd. [Abujafacts.ng](http://www.abujafacts.ng), <http://www.abujafacts.ng/top-5-cities-to-do-business-in-nigeria-abuja-is-2nd/>, Accessed 07/03/2016.
- ACGIH, 1996. Threshold Limit value for Chemical substance, physical agents and Biological exposure indices, American Conference of Government Industrial Hygienists, Cincinnati.
- Aderoju, O.M. et al., 2014. Space-Based Assessment of the Compliance of GSM Operators in Establishing Base Transceiver Station (Bts) In Nigeria Using Abuja Municipal Area Council as Case Study. *IOSR Journal of Environmental Science, Toxicology and Food Technology* 8(1): 46-57.
- Agilent, 2001. Fundamentals of RF and Microwave Power Measurements Classic application note on power measurements: Application Note 64-1C, Agilent Technologies, U.S.A.
- Ahaneku, M., A, Nzeako, A., A. and Udora, N., N., 2015. Investigation of Electromagnetic Radiations by GSM Base Stations in Nigeria for Compliance Testing. *Advances in Physics Theories and Applications*, 47: 10-17.
- Ahaneku, M.A. and Nzeako, A.N., 2012. GSM Base Station Radiation Level: A Case Study of University of Nigeria Environment. *International Journal of Scientific & Technology Research*, 1(8): 102 - 107.
- Ahlbom, A., Feychting, M., Hamnerius, Y. and Hillert, L., 2012. Radiofrequency electromagnetic fields and risk of disease and ill health: Research during the last ten year, Swedish Council for Working Life and Social Research (FAS), Stockholm.
- Ajetunmobi, A.E., 2014. Assessment of Radio Frequency Radiation in The Far- Field of Selected Mobile base Station in Ijebu-Ode, Ogun State, Nigeria. *International Journal of Scientific Research*, 3(9): 83-84.
- Akintonwa, A., Busari, A.A., Awodele, O. and Olayemi, S.O., 2009. The Hazard of Non-Ionizing Radiation of Telecommunication Mast in Urban Area of Lagos, Nigeria. *African Journal of Biomedical Research*, 12: 31-35.

- Akpolile, F.A., Akpolile, F.D. and Osalor, O.J., 2014. Radiofrequency Power Density Measurements of Telecommunication Masts around Some Selected Areas in Delta State. *Journal of Natural Sciences Research*, 4(15): 77-79.
- Al-Mously, S.I. and Yahya, R.I., 2010. Temperature Rise Computation in the Human Head Exposed to Different Mobile Phone Models. *Al- Mustansiriya J. Sci*, 21(4): 159 -178.
- Alenoghena, C.O., Emagbetere, J.O. and Aibinu, M.A., 2014. Development Of A Comprehensive City Structure Data Base For The Placement Of Base Stations: A Case Study Of Minna, Nigeria. *Covenant Journal of Informatics and Communication Technology*, 2(1): 46 - 56.
- Aminu, A., Tonga, D.A., Abubakar, Y.H. and Abdullahi, Z.H., 2014. Measurement of Electromagnetic Waves Radiated from Base Transceiver Stations (BTS) for Assessing Exposure Limit in Kaduna State. *The International Journal Of Engineering And Science (IJES)*, 3(8): 28-34.
- ANSI, 1982. American National Standards Institute. Safety Levels with respect to Human Exposure to Radio Frequency Electromagnetic Fields, 300 kHz to 100GHz Report ANSI C95-1982, The IEEE Inc, New York.
- ARPANSA, 2000. Levels of Radiofrequency Radiation from GSM Mobile Telephone Base Stations, AUSTRALIAN RADIATION PROTECTION AND NUCLEAR SAFETY AGENCY, Melbourne.
- Balanis, C.A., 2005. Antenna Theory Analysis and Design. John Wiley & Sons, Hoboken.
- Bernhardt, J.H., 1988. The establishment of frequency dependent limits for electric and magnetic fields and evaluation of indirect effect. *Radiat. Environ. Biophys.*, 27: 1-27.
- Biebuma, J.J. and Esekhaigbe, E., 2011. Assessment of Radiation Hazards from Mobile Phones and GSM Base Stations. *Journal of Innovative Research in Engineering and Science*, 2(1): 1-9.
- Boumphrey , S., 2010. World's Fastest Growing Cities are in Asia and Africa. *Euromonitor*, <http://blog.euromonitor.com/2010/03/special-report-worlds-fastest-growing-cities-are-in-asia-and-africa.html>, Accessed 07/03/2016.
- Briggs-Kamara, M.A., Funsho, B.I. and Tamunobereton-Ari, I., 2018. Assessment of Radiofrequency Exposure from Base Stations in Some Tertiary Institutions in Rivers State, Nigeria. *Dutse Journal of Pure and Applied Sciences*, 4(2): 188-200.
- Cember, H. and Johnson, T.E., 2009. Introduction to health physics. McGraw Hill, New York.

- Chaudhary, A. et al., 2016. Lightweight and Easily Foldable MCMB-MWCNTs Composite Paper with Exceptional Electromagnetic Interference Shielding. *ACS Appl. Mater. Interfaces*, 8(16): 10600–10608.
- Cooper, T.G., Mann, S.M., Khalid, M. and Blackwell, R.P., 2004. Exposure of the General Public to Radio Waves near Microcell and Picocell Base Stations for Mobile Telecommunications NRPB, CHILTON DIDCOT.
- Delisle, J., 2014. A Closer Look at RF Power Measurements, *RF Essentials*, [http://www.ab4oj.com/test/docs/rf\\_pwr\\_meas.pdf](http://www.ab4oj.com/test/docs/rf_pwr_meas.pdf) Accessed 17-01-2019.
- Durduran, S.S., Seyfi, L., Avci, C. and Ozan, A.M., 2013. Measurement of Electromagnetic Signal Strengths of Four GSM Base Stations at 900 MHz in a Pilot Region, *Proceedings of the World Congress on Engineering 2013*, London, U.K.
- Durney, C., Massoudi, H. and Iskander, M., 1986. Radiofrequency radiation dosimetry handbook, Report: USAFSAM-TR-85-73.
- Earsite, 2015. Earsite The Neurotology Research Center, <http://www.earsite.com/acoustic-neuroma-treatment>.
- Eberspächer, J., Vögel, H., Bettstetter, C. and Hartmann, C., 2009. *GSM – Architecture, Protocols and Services*. John Wiley & Sons Ltd, West Sussex.
- edirectsms, 2016. GSM phone numbers in Nigeria grouped by stateslocal government area, [www.edirectsms.com/index.php/ng-database](http://www.edirectsms.com/index.php/ng-database), Assessed 8-1-2016.
- Eger, H. and Neppe, F., 2009. Incidence of cancer adjacent to a mobile telephone basis station in Westphalia. *Umwelt medizin gesellschaft*, 22: 55-60.
- Enyinna, P.I. and Avwir, G.O., 2010. Characterization of the Radiofrequency Radiation Potential of Alakahia and Choba Communities, Nigeria. *Working and Living Environmental Protection*, 7(1): 25 - 31.
- ETSI, 1996a. Digital cellular telecommunications system (Phase 2+); Radio transmission and reception (GSM 05.05): GSM Technical Specifications, ETSI TC-SMG Version 5.0.0, European Telecommunications Standards Institute (ETSI) Valbonne, France.
- ETSI, 1996b. Digital cellular telecommunications system; Base Station Controller - Base Transceiver Station (BSC - BTS) interface; Interface principles (GSM 08.52), European Telecommunications Standards Institute (ETSI), Valbonne, France.
- ETSI, 1996c. Radio Network Planning Aspects: Technical report ETR 364 (GSM 03.30 version 5.0.0), European Technical Standards Institute (ETSI), Valbonne, France.
- ETSI, 2008. Universal Mobile Telecommunications System (UMTS); Base Station (BS) radio transmission and reception (FDD) (3GPP TS 25.104 version 6.17.0



Release 6), European Telecommunications Standards Institute, Antipolis, France.

- Farai, I.P., Ayinmode, B.O. and Onada, T.O., 2012. Estimation of Radio Frequency Power Density around Global System of Mobile Communication (GSM) Base Stations in Ibadan City, Nigeria. *Journal of Science Research*, 11: 167 - 170.
- Feldman, Y., Puzenko, A. and Ryabov, Y., 2005. *Dielectric Relaxation Phenomena in Complex Materials*. John Wiley & Sons, Inc., 1-125 pp.
- Frei, P. et al., 2009. A prediction model for personal radio frequency electromagnetic field exposure. *Science of the Total Environment*, 408: 102-108.
- Frei, P. et al., 2010. Classification of personal exposure to radio frequency electromagnetic fields (RF-EMF) for epidemiological research: Evaluation of different exposure assessment methods. *Environment International*, 36: 714-720.
- Gandhi, O.P., 1974. Polarization and frequency effects on whole animal absorption of RF energy. *Proc. IEEE Trans. Biomedical Engineering*, 62(8): 1171-1175.
- Gandhi, O.P. et al., 2012. Exposure Limits: The underestimation of absorbed cell phone radiation, especially in children. *Electromagnetic Biology and Medicine*, 31(1): 34-51.
- Gretel, M.P., Mickan, S., P and Abbott, D., 2006. Simulation of terahertz radiation in stratified media, *Proc. SPIE 6038, Photonics: Design, Technology, and Packaging II*, 60380M, doi:10.1117/12.638107.
- Haim, M. and Shimshon, L., 2002. *Basic RF Technic and Laboratory Manual*, Holon Institute of Technology, Holon, Israel.
- Hardell, L., Carlberg, M. and Hansson, M.K., 2005. Case-control study on cellular and cordless telephones and the risk for acoustic neuroma or meningioma in patients diagnosed 2000-2003. *Neuroepidemiology*, 25: 120–128.
- Harte, L., Kikta, L. and Richard, R., 2002. *3G Wireless Demystified*. McGowan-Hill, New York.
- Haumann, T., Munzenberg, U., Maes, W. and Sierck, P., 2002. HF-radiation levels of GSM cellular phone towers in residential areas, 2nd International Workshop on Biological effects of EMFS, Rhodes, Greece.
- Hayt, W.H. and Buck, J.A., 2012. *Engineering electromagnetics* McGraw-Hill, New York.
- Hutter, H.P., Moshammer, H., Waller, P. and Kundi, M., 2006. Subjective, Sleeping Problems, and Cognitive Performance in Subjects Living Near Mobile Phone Base Station. *Occup. Environ. Med.*, 63: 307-313.
- Hyland, G.J., 2000. The physics and biology of mobile telephony. *Lancet* 200, 356: 1833-1836.

- Hyland, G.J., 2003. How exposure to GSM and TETRA can adversely affect humans, [http://www.powerwatch.org.uk/news/20030701\\_hyland\\_basestations.pdf](http://www.powerwatch.org.uk/news/20030701_hyland_basestations.pdf).
- Ian, P., 2017. GSM Power Control and Power Class. Radio-electronics.com: [http://www.radio-electronics.com/info/cellulartelecomms/gsm\\_technical/power-control-classes-amplifier.php](http://www.radio-electronics.com/info/cellulartelecomms/gsm_technical/power-control-classes-amplifier.php). Assessed 27/5/2017.
- Ibitoye, Z.A. and Aweda, A.M., 2011. Assessment of radiofrequency power density distribution around GSM and broadcast antenna masts in Lagos City, Nigeria. *Nig Q J Hosp Med.* , 21(1): 35-40.
- ICNIRP, 1998. Guidelines for limiting exposure to time-varying Electric, Magnetic and Electromagnetic fields (up to 300 GHz). *Health physics*, 74(4): 494-522.
- IEEE, 2002. IEEE Recommended Practice for Measurements and Computations of Radio Frequency Electromagnetic Fields With Respect to Human Exposure to Such Fields, 100 kHz-300 GHz (R2008), Institute of Electrical and Electronic Engineers, New York, NY.
- Imaida, K. et al., 1998. Lack of promoting effects of the electromagnetic near-field used for cellular phones (929.2 MHz) on rat liver carcinogenesis in a medium-term liver bioassay. *Carcinogenesis* (19): 311-314.
- Ipatov, V., 2000. Spread Spectrum and CDMA. John Wiley & Sons, Ltd., New york.
- Isabona, J. and Ojuh, O.D., 2015. Experimental Assessment of Specific Absorption Rate Using Measured Electric Field Strength in Benson Idahosa University and Environs. *American Journal of Modern Physics*, 4(2): 92-96.
- Islam, M.R., Khalifa, O.O., Ali, L., Azl, i.A. and Zulkarnain, M., 2006. Radiation Measurement from Mobile Base Stations at a University Campus in Malaysia. *America Journal of Applied Sciences* 3: 1781-1784.
- Ismail, A., Norashida, M.D., Jamaludin, M.Z. and Balasubramaniam, N., 2010. Mobile phone base station radiation study for addressing public concern. *American J. of Engineering and Applied Science* 3(1): 117-120.
- ITIS, 2016. Database of Tissue Properties, The Foundation for Research on Information Technologies in Society (ITIS), Zurich, Switzerland. <https://www.itis.ethz.ch/virtual-population/tissue-properties/database/dielectric-properties/>. Assessed 2/11/2016.
- ITU, 2013. Recommendation ITU-T K.70 (2007) – Amendment 3: Mitigation techniques to limit human exposure to EMFs in the vicinity of radiocommunication stations, International Telecommunication Union, Geneva.
- Kopp, C., 2005. An introduction to Spread spectrum Technique. Dr. Carlo Kopp Industry Publications. [www.csse.mornash.edu.au](http://www.csse.mornash.edu.au). Assessed 17/10/2016.

- Kraus, J.D., 1988. Antennas. McGraw-Hill, New York.
- L'Annunziata, M. and Baradei, M., 2003. Handbook of Radioactivity Analysis. Academic Press, Cambridge.
- Linhares, A., Soares, A.J.M. and Terada, M.A.B., 2014. Determination of Measurement Points in Urban Environments for Assessment of Maximum Exposure to EMF Associated with a Base Station. International Journal of Antennas and Propagation, vol. 2014, Article ID 297082, 7 pages(doi:10.1155/2014/297082).
- Linhares, A., Terada, M.A.B. and Soares, A.J.M., 2013. Estimating the Location of Maximum Exposure to Electromagnetic Fields Associated with a Radiocommunication Station. Journal of Microwaves, Optoelectronics and Electromagnetic Application, 12(1): 141-157.
- Lo, Y.T. and Lee, S.W., 1993. The Antenna Hand Book, Volume 1: Fundamentals and Mathematical Techniques. Chapman & Hall, New York.
- Mamilus, A., Ahaneku, A. and Nzeako, N., 2012. GSM Base Station Radiation Level: A Case Study of University of Nigeria Environment. INTERNATIONAL JOURNAL OF SCIENTIFIC & TECHNOLOGY RESEARCH, 1(8): 102-107.
- Manjish, A., 2015. A Survey and Review of GSM Base Transceiver System Installation, Architecture and Uplink/Downlink. Journal of The International Association of Advanced Technology and Science, 16(1): 1-6.
- Mann, K. and Roschke, J., 1996. Effects of pulsed high frequency electromagnetic fields on human sleep. Neuropsychobiology, 33: 4-47.
- Maskarinec, G., Cooper, J. and Swygert, L., 1994. Investigation of increased incidence in childhood leukemia near radio towers in Hawaii: Preliminary observations. J. Environ. Pathol.Toxicol. and Oncol., 13: 33-37.
- Mason-Jones, K. and Cohen, B., 2012. Case Study: Lagos BRT-LITE. WWF-SA. [www.wwf.org.za/media\\_room/publications](http://www.wwf.org.za/media_room/publications), Assessed 10-3-2016.
- Mehta, A., 2011. Introduction to the Electromagnetic Spectrum and Spectroscopy, Pharmaxchange.info.
- Milligan, T.A., 2005. Modern antenna design. John Wiley & Sons inc., Hoboken, New Jersey.
- Mousa, A., 2011. Electromagnetic Radiation Measurements and Safety Issues of some Cellular Base Stations in Nablus Journal of Engineering Science and Technology Review, 4(1): 35-42.
- MTU, 2019. Absorption of EM radiation. Michigan Technological University, [http://pages.mtu.edu/~scarn/teaching/GE4250/absorption\\_lecture\\_slides.pdf](http://pages.mtu.edu/~scarn/teaching/GE4250/absorption_lecture_slides.pdf) Assessed 23-01-2019.

- NBS, 2018. Telecoms Data: Active Voice and Internet per State, Porting and Tariff Information: Telecoms Sector Data - Q4 2017, National Bureau of Statistics, Abuja.
- NCC, 2019. Industry Statistics, Nigerian Communications Commission (NCC), <https://www.ncc.gov.ng/stakeholder/statistics-reports/industry-overview#> Assessed 23-01-2019.
- NFMC, 2014. National Frequency Allocation Table, National Frequency Management Council of the Federal Republic of Nigeria, <http://www.ncc.gov.ng/technology/spectrum/frequency-allocation>, Accessed 07/02/2017.
- NPC, 2006. 2006 Population and Housing census of the Federal Republic of Nigeria 2006: Priority Tables, Volume II.
- NRPB, 1992. Electromagnetic Fields and the Risk of Cancer Report of an Advisory Group on Non-Ionizing Radiation, National Radiation Protection Board, Chilton, UK.
- Ojuh, O.D. and Isabona, J., 2015. Radio frequency EMF exposure Due To GSM Mobile Phones Base Stations: Measurements And Analysis In Nigerian Environment Nigerian Journal of Technology (NIJOTECH), 34(4): 809 – 814.
- Okonigene, R.E. and Yesufu, A.K., 2009. Radiation from GSM systems and the associated effects on human health. *Thammasat Int. J. Sc. Tech.*, 14(3): 56-63.
- Oladapo, O.O., Ishola, G.A., Ayokunnu, D.O. and Akerele, O.O., 2011. Analysis of Public Perceptions of Increased Radiofrequency Exposure from Mobile Phones in Southwestern Nigeria. *IJRRAS* 7(1): 54-56.
- Olorunfemi, E., Ojo, J., Aboyeji, O.S., Akeju, M. and Okezie, C., 2016. Determination of Electromagnetic Radiation levels from Cell Phones and GSM Masts in Ile-Ife, Southwest Nigeria. *Ife Journal of Science*, 18(4): 1041-1051.
- Olowu, D., 1992. Urban local government finance in Nigeria: The case of Lagos municipal area. *Public Administration and Development*, 12(1): 19-38.
- Oluwajobi, A.O., Falusi, O.A. and Oyedum, O.D., 2014. Estimation of the number of 900MHz GSM Antennae and the Field Intensities of their Ray Emissions in Minna Metropolis, Nigeria. *IJABR*, 6(2): 56 - 62.
- Pérez-vega, C., Zamanillo, J.M. and Herran, I.F., 2008. Measurement and Model of Non-Ionizing Radiation Levels in an urban environment, 8th WSEAS International Conference on SIMULATION, MODELLING and OPTIMIZATION (SMO '08), Santander Cantabria Spain.
- Ralph, M.I., 2012. Physical Hazards: Ionising Radiation. In HaSPA (Health and Safety Professionals Alliance), The Core Body of Knowledge for Generalist OHS Professionals. Tullamarine, VIC. Safety Institute of Australia.

- Ramo, S., Whinnery, J.R. and Van Duzer, T., 1994. *Fields and Waves in Communication Electronics*. John Wiley and Sons, New York.
- Rasaki, R., 1988. *Managing Metropolitan Lagos, Inaugural Programme of the Africa Leadership Forum*. The Africa Leadership Forum, Ota.
- RPII, 2013. *Sources of Ionising Radiation Fact Sheet, Radiological Protection Institute of Ireland Fact Sheet*, Dublin, Ireland.
- Sabbah, A.I., Dib, N.I. and Al-Nimr, M.A., 2011. Evaluation of specific absorption rate and temperature elevation in a multi-layered human head model exposed to radio frequency radiation using the finite-difference time domain method. *IET Microw. Antennas Propag.*, 5(9): 1073–1080.
- Samaras, R. and Kuster, N., 2000. Electromagnetic and heat transfer computations for non-ionizing radiation dosimetry. *Phys. Med. Biol.*, 45: 2233-2246.
- Sambo, Y.A., Héliot, F. and Imran, M.A., 2015. A Survey and Tutorial of Electromagnetic Radiation and Reduction in Mobile Communication Systems. *IEEE Communications Surveys & Tutorials*, 17(2): 790 - 802.
- Samra, H., 2008. *The Open BTS Project (Telecommunications industry)*.
- Satooshi, M., Katsuhiko, T. and Takehiko, H., 2002. Base transceiver Station for WCDMA. *Fujitsu Sci.Tech.J*, 38(1): 167-173.
- Savitz, D.A. and Loomis, D.P., 1995. Magnetic field exposure in relation to leukemia and brain cancer mortality among electric utility workers. *Am. J. Epidemiol.*, 141: 123-134.
- Schantz, H.G., 2003. *Introduction to Ultrawideband Antennas, Proceedings of the 2003 IEEE UWBST Conference*.
- Serway, R.A. and Jewett, J.W., 2010. *Physics for Scientists and Engineers with Modern Physics*. Brooks/Cole, Belmont.
- Seybold, J.S., 2005. *Introduction to RF propagation*. John Wiley & Sons, Hoboken.
- Shaw, G.W. and Croen, L.A., 1993. Human adverse reproductive outcomes and electromagnetic fields exposures: review of epidemiologic studies. *Environ. Health Persp*, 101: 107-119.
- Shurdi, O., Kamo, B. and Lala, A., 2010. *EMF Measurements in the Vicinity of Bts Cellular Stations of Vodafone Albania, BALWOIS, Ohrid, Republic of Macedonia*.
- Siwiak, K. and Bahreini, Y., 2007. *Radiowave Propagation and Antennas for Personal Communications*. Artech House, Norwood.
- Skolnik, M., 1962. *Introduction to Radar Systems*. McGraw-Hill, Inc., New York.
- Straw, R.D., 2007. *The ARRL Antenna Book*. ARRL, Newington.

- Stutzman, W.L. and Thiele, G.A., 2012. *Antenna Theory and Design*. John Wiley & Sons, Newyork.
- Tai, C.T. and Pereira, C.S., 1976. An Approximate Formula for Calculating the Directivity of an Antenna. *IEEE Trans. Antennas Propagat*, AP-24( 2): 235-236.
- Tomori, M.A., 2007. Ibadan metropolitan area and the challenges to sustainable development  
MACOS Consultancy,  
[www.http://macosconsultancy.com/Ibadan%20metropolitan.html](http://macosconsultancy.com/Ibadan%20metropolitan.html), Accessed 7-3-2016.
- Tpub, 2016. *Introduction to Communication theory*. Integrated Publishing, Inc. <http://www.tpub.com/neets/book17/74.htm>, Accessed 6/5/2016.
- Ulaby, F.T., Michielssen, E. and Ravaioli, U., 1994. *Fundamentals of Applied Electromagnetics*. Pearson, New York.
- Umar, S., Garba, N.N. and Zakari, Y.I., 2017. Assessment of Radio-frequency Radiation Exposure from selected Mobile Base Stations in Kaduna State, Nigeria. *Nigerian Journal of Scientific Research*, 16(2): 184-186.
- Ushie, P.O., Nwankwo, V.U.J., Ayinmode, B. and Osahun, O.D., 2013. Measurement and Analysis of Radiofrequency Radiation Exposure Level from Different Mobile Base Transceiver Stations in Ajaokuta and Environs, Nigeria. *IOSR Journal of Applied Physics* 3: 17 - 21.
- Wertheimer, N. and Leeper, E., 1979. Electrical wiring configurations and childhood cancer. *Am. J. Epidemiol*, 109: 273-284.
- WHO, 2010. *WHO Research Agenda for Radiofrequency Fields*. World Health Organization press, Geneva.
- Wolf, R. and Wolf, D., 2004. Increased incidence of cancer near a cell-phone transmitter station. *International journal of cancer prevention*, 1(2): 1-19.
- Wu, T. et al., 2013. A large-scale measurement of electromagnetic fields near GSM base stations in Guangxi, China for risk communication. *Radiat Prot Dosimetry*, 155(1): 25-3.
- Yee, K.S., 1966. Numerical Solution of Initial Boundary Value Problems Involving Maxwell's Equations in Isotropic Media. *IEEE Transaction on Antennas and Propagation*, 14(3): 302-307.
- Zeng, D.Z., 2008. *Knowledge, Technology, and Cluster-based Growth in Africa (WBI development studies)*. World Bank Publications, Geneva.
- Zhao, B. et al., 2016. Yolk-Shell Ni@SnO<sub>2</sub> Composites with a Designable Interspace To Improve the Electromagnetic Wave Absorption Properties. *ACS Appl. Mater. Interfaces*, 8(42): 28917-28925.

